CONTINGENCY MANAGEMENT IN POWER SYSTEMS AND DEMAND RESPONSE MARKET FOR ANCILLARY SERVICES IN SMART GRIDS WITH HIGH RENEWABLE ENERGY PENETRATION

A DISSERTATION SUBMITTED TO THE GRADUATE DIVISION OF THE UNIVERSITY OF HAWAI'I AT MANOA IN PARTIAL FULFILLMENT OF THE REQUIREMENTS FOR THE DEGREE OF DOCTOR OF PHILOSOPHY IN MECHANICAL ENGINEERING

NOVEMBER 2017

By

Mahdi Motalleb

Dissertation Committee:

Dr. Reza Ghorbani (ME, Chair)

Dr. Peter Berkelman (ME)

Dr. Richard Rocheleau (ME/HNEI)

Dr. Scott Miller (ME)

Dr. Matthias Fripp (EE)

This thesis is dedicated to my parents.

For their endless love, support and encouragement

Table of contents

Acknowledgments

First and foremost I sincerely would like to thank my advisor, Dr. Reza Ghorbani, for supporting my PhD studies and giving me opportunity to work in the field of renewable energy, energy market, and demand response in smart grids. I am also grateful for the very friendly and constructive atmosphere he has constantly been creating for our research group in Rebewable Energy Design Laboratory (REDLAB).

I would also like to thank Dr. Richard Rocheleau, Dr. Matthias Fripp, Dr. Scott Miller, Dr. Peter Berkelman, and Dr. Bardia Konh for their invaluable suggestions, discussions and efforts serving on my committee.

Furthermore, I would like to thank Dr. Mehrdad Nejhad, chair of the Department of Mechanical Engineering at University of Hawaii at Manoa, who has always been a great support for me and all other graduate students in the department. My sincere thanks also goes to Dr. Anuradha Annaswamy, Senior Research Scientist in the Department of Mechanical Engineering at MIT for offering me a research scholar opportunity in her group and leading me working on a research project in Active Adaptive Control Laboratory (AACLab) at MIT.

In addition, I would like to extend the gratitude to my friends and lab mates, Ehsan Reihani, Saeed Sepasi, Michael Angelo, Matsu Thornton, Freddie Wheeler, Shawyun Sariri, and John Branigan for their help and encouragement in times when I needed them the most. Special thanks to Greenpath Technologies Inc. for industry support. This dissertation is sponsored by United States National Science Foundation (NSF) under award number: 1310709.

Abstract

The modern power grid has seen a marked increase in renewable energy generation resources. The intermittent nature of these resources give rise to additional challenges in maintaining grid stability. To design a grid which is secure, a number of factors need to be considered. On a basic level, security is defined as the ability of a certain system configuration to continue to function and withstand a wide range of operating parameters, outside influences, or even subsystem failures. In the event of contingencies such loss of a generation unit, the entire system needs to be able to remain operating long enough for the grid operators to restore stability. Maintaining a balance of power is critical to the continued operation of the grid at these times.

Development and implementation of smart grid technologies offers advantages over traditional electric utilities. In these days, demand response programs have been developed to help traditional power market to provide different services such as contingency reserves specially with increasing penetrations of renewable energies.

Demand response is Voluntary (and compensated) load reduction used as a bulk system reliability resource. Demand-side provision is a good source of ancillary services, because the larger number of participants increases competition, lowers cost and leads to a better utilization of resources. The focus of this thesis is on demand response market in order to provide different ancillary services such as contingency reserves. This market framework is presented as an alternative to the traditional vertically-integrated market structure, which may be better suited for developing demand response and smart grid technologies.

List of tables

List of figures

List of abbreviations

Demand Response (DR)

Battery Energy Storage System (BESS)

Artificial Neural Networks (ANN)

Complex-Valued Neural Networks (CVNN)

Time Domain Power Flow (TDPF)

Economic Dispatch (ED)

Dynamic Programing (DP)

State of Charge (SOC)

Ancillary Services (AS)

Contingency Reserve (CR)

Independent System Operators (ISO)

Optimal Power Flow (OPF)

Demand Response Aggregators (DRA)

Generation Company (GENCO)

Water Heater (WH)

Electric Vehicle (EV)

Air Conditioner (AC)

Locational Marginal Price (LMP)

Incomplete-Information Game (*i*-game)

Complete-Information Game (*c*-game)

Demand Side Management (DSM)

Time-of-Use (TOU)

Decision-Making (DM)

Dynamic Economic Dispatch (DED)

Real-Time Pricing (RTP)

Networked Cournot Competition (NCC)

Networked Stackelberg Competition (NSC)

Distribution Companies (DISCOs)

Chapter 1

Introduction

Developments of renewable energy resources imposes many uncertainties and variabilities in power grids. One of the best approaches to mitigate these stochastic disturbances is thought the use of storage systems. Besides application of the storage devices such as mitigating the fluctuations in distribution side of the grid, the frequency can be controlled in contingencies using the appropriate storage. In chapter 2 of this thesis, a method has been proposed in order to find the optimal place(s) and capacity of the storage devices. Its objective function is to minimize costs and losses. For the goal of contingency management and frequency regulation, a sensitive analysis is performed using an artificial intelligence processing method. In the distribution side of the grid, the goal is peak load shaving and load curve smoothing.

The increased presence of variable renewable generation drives a greater need for authorities to procure more services for grid balance such as the reserves which are used to regulate the grid frequency in contingencies. In smart grids, demand side can participate alongside traditional supply-side resources to provide the necessary services. The available capacity of the generators can be used more efficiently for power production which they were designed for. It cuts operation

costs and reduces air pollution. As the ratio of inverter-based generation (such as solar generation) compared to conventional generation increases, the mechanical inertia used to stabilize frequency decreases. Chapter 3 provides a method to use demand for providing reserves to ensure system stability for a set of credible contingencies, while also satisfying economic and market goals.

During grid contingencies, frequency regulation is a primary concern. Historically, frequency regulation during contingency events has been the sole responsibility of the power utility. A practical method of using distributed demand scheduling is presented in chapter 4 to provide frequency regulation during contingency events. Chapter 4 discusses the implementation of a control system model for the use of distributed energy storage systems such as battery banks and electric Water Heaters (WHs) as sources of Demand Response (DR). An algorithm is presented in chapter 4 which handles the optimization of DR scheduling for normal operation and during contingency events.

Chapter 5 is primarily concerned with the construction of a theoretical model of the competition between aggregators for selling energy previously stored in an aggregation of storage devices (which the aggregator manages) given sufficient demand from other aggregators through game theory. Demand for power generated by the utility through combustion of fuel could be replaced, lowering emission of pollutants, when the energy used to charge the batteries is produced sustainably and traded on smaller scales. The model culminates in a game-theoretically justifiable decision making procedure for the sellers which may be used to predict and analyze the bids made for energy sale in the market. The methodology for applying the model is worked out in detail for a three-aggregator case where two players compete with each other for sale to a third. The goal is to find the optimal bidding strategy and Nash equilibrium of strategies for the seller aggregators.

In chapter 6, the proposed market in chapter 5 is cleared in each time interval of a day (for example hourly) using a repeated game-theoretic framework. In each time interval of a day, after clearing the market in a game, optimal bidding strategy has been determined for each aggregator in order to maximize the aggregators' payoffs. After finding the Nash equilibrium of strategies in each time interval, dispatch of the generators is updated based on the updated demand. It generates updated price signal for the next time interval. In other words, dynamic pricing has been considered in the proposed game-theoretic DR market framework. Effect of demand scheduling is considered simultaneously. The proposed method minimizes the emission, fuel, and operation costs and optimally schedules the generation in supply side. It also presents optimal prices during different periods i.e. valley, off-peak, and peak periods simultaneously. The customers in light of the utility's optimal price minimize theirs electricity costs and optimally schedule their power consumption in order to participate in the DR market and sell the energy stored in the storage devices.

In the classical Cournot competition model, each firm tries to maximize its own payoff by deciding an optimal strategy for determining the quantity of goods produced during each time period-–i.e. turn, of the game. In the typical application, all firms compete in the same market. In more recent economic models, firms compete across a number of markets simultaneously. In this situation, a networked competition model has been presented in chapter 7 which models the relationship between firms and markets. Chapter 7 describes a model of competition among aggregators (as firms) to sell energy (as a homogenous good) stored in an aggregation of residential battery energy storage systems in a networked environment where market constraints are effected and trades are generally facilitated through the actions of a market maker who's turn is sequentially

distinct from the other players. For each firm, the optimal bidding strategy and Nash equilibrium are obtained through analyses of in a game as mentioned in chapters 5 and 6. Criteria required for existence of uniqueness of a Nash equilibrium are presented, and efficiency of the game is also studied in chapter 7 demonstrating DR scheduling improves market efficiency.

Appendix A includes the details of arterial intelligence processes which have been used for data forecasting. Details of Developed hardware, devices, and micro-grid testbed in REDLab have been provided in Appendix B.

Chapter 2

Optimal Placement and Sizing of the Storage System

Abstract

Developments of renewable energy resources imposes many uncertainties and variabilities in power grids. One of the best approaches to mitigate these stochastic disturbances is thought the use of Battery Energy Storage System (BESS). Besides application of the BESS such as decreasing the disturbances in distribution system, the grid frequency can be controlled in contingencies using the appropriate storage in transmission network to compensate the power shortage. Thus, the optimal siting and sizing of the BESS is important to have the minimum costs and losses. This chapter describes a heuristic method to find the optimal location(s) and capacity of a multi-purpose BESS including transmission and distribution parts. In the transmission storage part, a sensitive analysis is performed using Complex-Valued Neural Networks (CVNN) and Time Domain Power Flow (TDPF) in order to detect the optimal BESS location(s). Additionally, running TDPF and Economic Dispatch (ED) leads to the optimal BESS size. In the distribution storage part, the optimal BESS size is calculated to perform distribution grid services such as peak load shaving and load curve smoothing. The proposed method has been applied to a real model (Maui island in Hawai'i -United States) to calculate the optimal results for both transmission and distribution sides.

Nomenclature

TDPF Formulation:

I_{Bus} Injected current to the buses (positive value in generation buses and negative in loads)

Y_{Bus} Admittance matrix of the grid

V_{Bus} Voltage vector of the buses

f, g Algebraic and differential equations to solve time domain problem

f_n A function dependent on the method of the integration

A_c^i A matrix dependent on the algebraic and state Jacobian matrices

x^{i+1}, y^{i+1} Calculated values of x and y in time $t = i+1$

ED Formulation:

$C(P_{GEN})$ Generation cost function ($/hr)

$C_{GEN,i}^{local}$ Generation cost of the i^{th} local generator ($/hr)

$C_{GEN,j}^{dist}$ Generation cost of the j^{th} distant generator ($/hr)

$C_{BESS,k}^{total}$ Total generation cost of the k^{th} BESS (located in the k^{th} sensitive bus) ($/hr)

$NGlocal$ Number of the local generators (located in the sensitive buses)

$NGdist$ Number of the generators located far from than the sensitive buses

$NBESS$ Number of the required BESS stations (is equal to the number of the sensitive buses)

$a_{local,i}$ The first coefficient of the quadratic cost function of the i^{th} local generator

$b_{local,i}$ The second coefficient of the quadratic cost function of the i^{th} local generator

$c_{local,i}$ The third coefficient of the quadratic cost function of the i^{th} local generator

$a_{dist,j}$ The first coefficient of the quadratic cost function of the j^{th} distant generator

$b_{dist,j}$ The second coefficient of the quadratic cost function of the j^{th} distant generator

$c_{dist,j}$ The third coefficient of the quadratic cost function of the j^{th} distant generator

$P_{GEN,i}^{local}$ Generated power of the i^{th} local generator (MW)

$P_{GEN,j}^{dist}$ Generated power of the j^{th} distant generator (MW)

$C_{j,l}^{trans}$ Power transmission cost between the j^{th} and l^{th} bus

$C_{BESS,k}^{st}$ Cost of storage unit in the k^{th} BESS ($/hr)

$C_{BESS,k}^{pcs}$ Cost of power conversion in the k^{th} BESS ($/hr)

$R_{j,l}$ Resistance between j^{th} and l^{th} bus (Ω)

$X_{j,l}$ Reactance between j^{th} and l^{th} bus (Ω)

$I_{j,l}$ Passing current from j^{th} to l^{th} bus (kA)

$P_{j,l}^{flow}$ Transmitted active power from j^{th} to l^{th} bus (MW)

$V_{j,l}$ Voltage difference between j^{th} and l^{th} bus (kV)

$C_{BESS,k}^{st,unit}$ Unit cost of the storage in the k^{th} BESS ($/MWhr)

$P_{BESS,k}$ Generated power of the k^{th} BESS (located in the k^{th} sensitive bus) (MW)

$C_{BESS,k}^{pcs,unit}$ Unit cost of the power conversion in the k^{th} BESS ($/MWhr)

$P_{GEN\,\min,i}^{local}$ The minimum allowed power generation of the i^{th} local generator (MW)

$P_{GEN\,\max,i}^{local}$ The maximum allowed power generation of the i^{th} local generator (MW)

$P_{GEN\,\min,j}^{dist}$ The minimum allowed power generation of the j^{th} distant generator (MW)

$P_{GEN\,\max,j}^{dist}$ The maximum allowed power generation of the j^{th} distant generator (MW)

$P_{req,m}$ The required power for the m^{th} sensitive bus to cope with the contingency (MW)

Peak Shaving/ Load Curve Smoothing:

$P_{bat}(t)$ Battery power flow at time t (kW)

$P_{cir}(t)$ Circuit power demand at time t (kW)

$SOC_{\min}$, $SOC_{\max}$ The minimum and maximum allowed state of charge of BESS

E_{tot} Total capacity of distribution part of BESS (kWh)

$E(t)$ Energy level of distribution part of BESS at time t (kWh)

Δt Optimization time interval (hr)

$P_{ref}(t)$ Reference power curve at time t (kW)

$P_L(t)$ Smoothing power line (kW)

t_k The k^{th} time step

2.1 Introduction

High penetration of renewable energy generation poses some challenges in the operation of power systems [1]. The main issue inherent with renewables is intermittency of power which will cause fluctuations in voltage and frequency of the power grid. BESS is one of the leading means to solve problems caused by these fluctuations. Applications of BESS have other benefits in the power grid such as frequency control, reserve providing, and flattening the load curve. The capacity and location of the BESS are important for cost-effectiveness of storage applications. Allocation of BESS in the inappropriate locations increase losses in the grid [2].

This chapter proposes a framework to optimize the location(s) and size of the BESS for two purposes including: decreasing the fluctuations from the renewable energy sources in the distribution side, and controlling the frequency under contingencies in the transmission side. The transmission BESS compensate for the power shortage in the abnormal conditions in order to help the grid to reliably cope with the contingencies with less impact on frequency. The distribution BESS mitigates the fluctuations caused by renewables and also shifts the load from peak to low load time. These multi-purpose optimizations increase the reliability of the power grid considering the issues of the transmission and distribution networks. The proposed method in this chapter solves a few problems of the transmission and distribution networks through calculation of optimal

two-purpose BESS.

2.1.1 Literature Review

The majority of published papers in the storage area only focus on operation related to the distribution network. There are less publications about optimal location(s) of the BESS in comparison with optimal sizing due to the complexity of the finding of the optimal locations [3, 4]. Thus, in many of the previous studies, it was posited that BESS is located near wind farms and large loads. The literature review can be divided into two categories: the first contains storage purposes while the second includes storage sizing and siting.

2.1.1.1 Storage Purposes

The majority of studies in the operation area are based on uncertainty and fluctuations related to distributed generations. Varkani et al. [5] modeled these uncertainties using Artificial Neural Networks (ANN) and stochastic programming. They discussed joint bidding design by a wind farm and a pumped hydro plant in the day-ahead and ancillary services markets. Forecasting electricity price [6] and wind generation are two good optimization parameters which Gonzalez et al. [7] used in their study for a pumped hydro storage plant. In their study, another approach for joint market participation was proposed by a wind power plant and a pumped hydro storage plant. Pandžić [8] proposed a method based on bilateral contracts and one day-ahead pricing in order to maximize the power plant profit considering the storage system, photovoltaic system, and a conventional generating unit. This model was for bilateral contracts and a day-ahead market. The conclusions were based on the importance of an accurate evaluation of the storage unit’s energy and power ratings.

Another stochastic model, based on real-time marketing, was proposed by Pandžić [9] for a similar power plant utilizing wind generation instead of photovoltaic system. Pandžić used a real-time market to balance the day-ahead market bids and the actual generation. Another scheduling method was proposed by Korpaas [10] based on Dynamic Programing (DP) in order to calculate the optimal electricity exchanges considering one transmission line constraints related to wind generation and storage. However, only one transmission line (between the storage and the rest of the transmission network) was considered. Simulation results show that energy storage enables the owners of the wind power plant to take advantage of variations in the spot price, therefore, increasing the value of wind power in the electricity market.

An optimal commitment policy considered conversion losses and energy prices in a grid which included wind farm and storage [11]. Zhou et al. [12] modeled a system, based on Markov decision prices and investigated wind farms, storage, and transmission systems. They proved that storage can increase the monetary value of the system. Cahndy et al. [13] performed optimal power flow on a power grid including the storage system and considered the integration of renewable energy resources. Therefore, this study was technical rather than economical. One economical study was done by Faghih et al. [14] with the goal of investigating optimal utilization of storage and the economic value of storage. They considered ramp-rate constraints and different electricity prices and they proved that optimal utilization of storage by consumers can induce price elasticity, particularly around the average price.

Nick et al. [15] performed an optimal day ahead scheduling of energy resources in active distribution networks. These resources included dispersed energy storage systems and volatile renewable embedded generators. Nick et al. proposed a convex formulation of optimal power flow

to compute the resources schedule. A multi-objective optimization was done by Steta [16] in order to obtain an optimal operation approach for a lossy energy storage system. They used a predictive control model based on a linearized version of an adiabatic compressed air energy storage plant.

2.1.1.2 Storage siting and sizing

Harsha and Dahleh completed an optimal storage analysis focused on a renewable generator that could support a part of local demand via storing excess generation [17]. Their objective function could find the optimal storage capacity in order to minimize the long-term average cost of demand not served by renewable generation. A similar study was done to find the optimal BESS sizing considering renewable energy resources and dynamic pricing [18]. Formulating the problem as a stochastic dynamic programing model helped the authors to minimize the long-term average cost of conventional generation, as well as the investment in storage, if any, while satisfying the demand. They proved that under fixed electricity prices, storage is profitable if the ratio of the amortized cost of storage to the price of electricity is less than 1/4.

A probabilistic reliability analyses was done by Zhang [19] in order to find the optimal size of the storage system that considered the transmission aspects. This study was also technical and did not focus on economical analysis. Dvijotham [20] used an algorithm to find the optimal locations of BESS in the grid. Their method was based on solving an optimization in order to find the minimum number of the optimal places considering the renewable energy forecasts. They used statistics describing usage patterns to reduce the number of storage devices. Denholm and Shioshans completed an analysis for co-locating a wing generation and storage system to decrease transmission costs. They also showed that using the BESS adjacent to wind generations is less

attractive than using them near the big loads if the storage device can take advantage of high-value ancillary or capacity services [21].

Arabali et al. [22] performed a cost analysis on a power grid in order to find the optimal placement of BESS using probabilistic optimal power flow. They used Particle Swarm Optimization (PSO) to minimize the sum of operation and congestion costs. A similar optimization method was used by Kerdphol in order to find optimal BESS with load shedding scheme when disconnection of the micro grid from the grid occurs [23]. The results proved that the optimal size of BESS-based PSO with load shedding scheme can achieve higher performance of frequency control compared to the optimal size of BESS-based analytic algorithm with load shedding scheme.

Li [24] presented a control strategy to improve the smoothing performance in a power system including wind farms, photovoltaic generations, and BESS. This method was based on decreasing the fluctuations of wind and photovoltaic generations and regulating battery State of Charge (SOC). Awad [25] proposed a method for the cost-effective improvement of reliability via the allocation of distributed storage units in the distribution systems. The purpose of their study was to optimize the installation cost of BESS with respect to reliability aspects of the grid.

Nick et al. [26] proposed a multi objective procedure in order to find optimal siting and sizing of distributed storage system to provide ancillary services. Their objective functions were voltage support and minimizing the network losses along with minimization of the energy cost from grid. In another study, optimal location of distributed storage system was found in [27] to minimize the

network voltage deviation. This study was based on formulation of a mixed-integer linear programing problem.

An optimal trade-off between technical and economical goals was performed in [28] to find the optimal allocation of dispersed energy storage system in active distribution networks. Their model of dispersed energy storage was able to support the network by both active and reactive power. In [29], a model predictive control strategy is used to smooth out wind power fluctuations thus making the wind power more dispatchable. In [29], authors showed that the control strategy is important to improve BESS performance for the mentioned application.

2.1.2 Contributions of the proposed heuristic method

The proposed methodology in this chapter focuses on distribution and transmission issues. This multi-purpose algorithm not only covers regular usages of the storage to smooth output power of renewable energy resources in the distribution network, but controls the frequency and provides power to cope with the contingencies in the transmission network. In abnormal situations of the grid, BESS compensates for power shortages in order to regulate the grid frequency. This study contains both technical and economical analysis. Using the proposed method is cost-efficient and the optimal storage can increase the grid reliability.

In this study, the problem is defined in the centralized system and utility operates the BESS along with conventional generators. In terms of the optimal location and capacity of the BESS in the transmission side, a wide variety of contingencies are analyzed in order to find the worst case scenario in a power grid. The applied contingencies are: losing wind or thermal generations and sudden or slow change in wind generations. The transmission BESS decreases the required reserve

capacity which is necessary to cope with the contingencies. On the distribution side, BESS is used to smooth the load curve and to remove fluctuations. This will decrease the reserve capacity allocated to deal with abrupt changes in the load. Peak shaving uses excess renewable energy generation in the low load time period and dumps back the stored energy in the peak load time. This helps to shift the renewable energy generation and replace the conventional unit power production. Peak shaving and load smoothing are investigated giving flexibility to the power system operator to manage the available reserve effectively in a timely manner.

Unit commitment problem is solved to find the optimal set of generators to meet the load demand. Moreover, in order to have the maximum benefit in power production under abnormal conditions, an ED has been performed to decide the optimal amount of power from generators and BESS.

2.2 Formulation and Definitions

The following subsections contain details about the tools used in the transmission part of BESS including: TDPF, CVNN, and ED.

2.2.1 TDPF Formulation

The power flow problem can mathematically be defined as:

$$[I_{Bus}] = [Y_{Bus}][V_{Bus}] \tag{2.1}$$

The active and reactive power flows ($\Delta P, \Delta Q$) can be calculated based on the change of voltage amplitudes and angles ($\Delta V, \Delta \theta$), which equation (2) shows that:

$$\begin{bmatrix} \Delta P \\ \Delta Q \end{bmatrix} = \begin{bmatrix} \frac{\partial P}{\partial \theta} & 0 \\ 0 & \frac{\partial Q}{\partial V} V \end{bmatrix} \begin{bmatrix} \Delta \theta \\ \frac{\Delta V}{V} \end{bmatrix} \tag{2.2}$$

Where the differential matrix is Jacobian. Newton-Raphson algorithm has been used to solve the power flow equations [30]. TDPF performs power flow during a time interval. In TDPF simulations, the grid's equipments have been modeled dynamically not statically. Time domain simulation includes solving the following problems for a typical time t and time step Δt :

$$f(x(t+\Delta t), y(t+\Delta t), f(t)) = 0 \tag{2.3}$$

$$g(x(t+\Delta t), y(t+\Delta t)) = 0 \tag{2.4}$$

Equations (2.3) and (2.4) are nonlinear and have been solved using Newton-Raphson method. This method repeatedly calculates the increments Δx^i and Δy^i of the state and algebraic variables and then updates the actual variables:

$$\begin{bmatrix} \Delta x^i \\ \Delta y^i \end{bmatrix} = -\left[A_c^i\right]^{-1} \begin{bmatrix} f_n^i \\ g^i \end{bmatrix} \tag{2.5}$$

$$x^{i+1} = x^i + \Delta x^i \tag{2.6}$$

$$y^{i+1} = y^i + \Delta y^i \tag{2.7}$$

The loop stops when the variable increment is less than a certain fixed tolerance or when the iteration number reaches its maximum value. There are two techniques to solve the TDPF

equations: Forward Euler Method and Trapezoidal Method. The first technique has been used in this study [31] [32].

By modeling the grid with TDPF, dynamic behaviors of the grid are analyzed and eigenvalues of dynamic system can be moved to ensure the grid stability. Additionally, the contingencies or disturbances can be easily applied to the model in order to analyze their effects on the grid. Therefore, appropriate strategies can be adopted to have the most optimized reaction to overcome the contingency or fault. In this study TDPF, is performed using PSAT toolbox in MATLAB [31].

2.2.2 CVNN Formulation

ANNs are widely used in energy systems applications [33, 34]. They can learn from the examples and perform forecasts in high speeds [35, 36]. The major difference between ANN and CVNN is the nature of using parameters. A real number is a subset of complex number, thus CVNN is an extension of ANN. CVNN is the complex form of ANN which is appropriate for the systems with the complex parameters such as power grid [37]. In this study, CVNN uses the load data of the grid in order to forecast the parameters in times ahead (either normal or atypical conditions ahead) [38]. Since, time plays a critical role in contingency management, it is more desirable to have a smaller system which produces the required results without dealing with computation burden. CVNN learns the power grid for different contingencies offline and creates a system which can easily and quickly find the contingency parameters.

In this chapter, a multi-stage learning process has been used by CVNN to forecast the voltage amplitudes and angles under contingencies. More details about the architecture of CVNN have been described in appendix A. Equation (2.2) has been used for two stages of learning: one stage

is learning through the active powers and voltage angles and another stage is learning through the reactive powers and voltage amplitudes.

Fig. 2.1 shows two stages of learning by CVNN. The parameters at the top and bottom of the arrows are related to the first and second learning stages, respectively. The input vectors of CVNN block (in time *t*) include two sections: the first input vector is the voltage amplitudes of last NL time series (including: $V_{t-1}, V_{t-2}, ..., V_{t-NL}$) and previous reactive power (Q_{t-1}), and the second input-vector is the voltage angles of last NL time series (including: $\theta_{t-1}, \theta_{t-2}, ..., \theta_{t-NL}$) and previous active power (P_{t-1}). The outputs of CVNN block are forecast of the voltage amplitudes and angles in time *t* (V_t, θ_t). NL is the minimum necessary number of previous parameters to learn the system well. All of the above parameters are defined for the whole buses.

Block diagram of Figure 2.2 indicates the complete steps of forecasting process using the proposed method which is a combination of CVNN and TDPF. The role of TDPF is to create the previous values of the voltage amplitudes and angles using the active and reactive powers of the grid. CVNN uses the previous values to learn the system and to forecast the voltage amplitudes and angles in time(s) ahead.

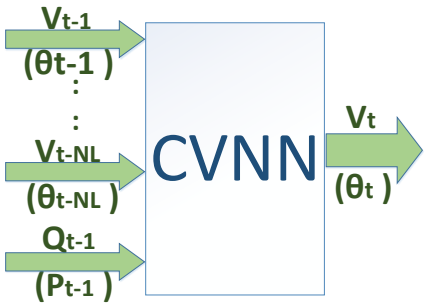

Figure 2.1: Two stages of learning by CVNN to forecast the voltage amplitudes and angles

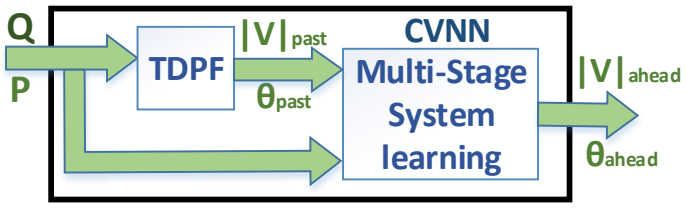

Figure 2.2: Combination of TDPF and CVNN to forecast the time-ahead parameters

2.2.3 ED Formulation

One of the purposes of combining the two previous tools (TDPF and CVNN) is to determine the optimal location(s) of BESS. These locations are sensitive buses of the grid. The other purpose is to calculate the power needed in order to cope with the contingencies and regulate the grid frequency. Next, it is necessary to calculate the optimal output of the generators and BESS to produce the required power economically. ED is the best tool to calculate how much power should be generated by each power source. For the proposed methodology, the generators of the grid are allocated into two groups: local generators (located in the sensitive buses) and distant generators (connected to the sensitive buses with transmission lines). The distant generators located far away from the sensitive buses. The objective function for the ED is a cost function with the following terms:

$$Minimize\ C(P_{GEN}) = \sum_{i=1}^{NGlocal} C_{GEN,i}^{local} + \sum_{j=1}^{NGdist} C_{GEN,j}^{dist} + \sum_{k=1}^{NBESS} C_{BESS,k}^{total} \tag{2.8}$$

Where;

$$C_{GEN,i}^{local} = a_{local,i} + b_{local,i}.P_{GEN,i}^{local} + c_{local,i}.(P_{GEN,i}^{local})^2 \tag{2.9}$$

$$C_{GEN,j}^{dist} = a_{dist,j} + b_{dist,j}.P_{GEN,j}^{dist} + c_{dist,j}.(P_{GEN,j}^{dist}) + \sum_{l=1}^{NBESS} C_{j,l}^{trans}{}^2 \tag{2.10}$$

$$C_{BESS,k}^{total} = C_{BESS,k}^{st} + C_{BESS,k}^{pcs} \tag{2.11}$$

$C_{j,l}^{trans}$ is a quadratic function of transmitted power:

$$Transmitted\ power = \sum_{l=1}^{NBESS} \left| R_{j,l} + jX_{j,l} \right| . I_{j,l}^{2} = \sum_{l=1}^{NBESS} \left| R_{j,l} + jX_{j,l} \right| . (\frac{P_{j,l}^{flow}}{V_{j,l}})^{2} \quad (2.12)$$

The components of the total cost of BESS are:

$$C_{BESS,k}^{st} = C_{BESS,k}^{st,unit} . P_{BESS,k} . (\frac{1}{\eta}) \quad (2.13)$$

$$C_{BESS,k}^{pcs} = C_{BESS,k}^{pcs,unit} . P_{BESS,k} \quad (2.14)$$

Where η is the inefficiency factor of the storage device [39]. The constraints of the optimization are:

$$P_{GEN\,\min,i}^{local} \le P_{GEN,i}^{local} \le P_{GEN\,\max,i}^{local} \quad (2.15)$$

$$P_{GEN\,\min,j}^{dist} \le P_{GEN,j}^{dist} \le P_{GEN\,\max,j}^{dist} \quad (2.16)$$

$$\sum_{i=1}^{NGlocal} P_{GEN,i}^{local} + \sum_{j=1}^{NGdist} P_{GEN,j}^{dist} + \sum_{k=1}^{NBESS} P_{BESS,k} = \sum_{m=1}^{NBESS} P_{req,m} \quad (2.17)$$

2.3 Methodology

The proposed method in this chapter includes economical and technical optimization of the capacity and location(s) of BESS in the power grid considering the issues of transmission and distribution networks. Figure 2.3 shows the whole steps of the methodology in two parts. The subsections below, 2.3.1 and 2.3.2, describe the proposed approach for the transmission and distribution parts, respectively.

2.3.1 Transmission part

The purpose of the transmission part (upper part of Figure 2.3) is to show how to determine the optimal place(s) and capacity of BESS to control the frequency and find the best reaction in the abnormal situations to successfully and reliably cope with the contingencies. The optimal results of the site(s) and size of the BESS minimizes the cost and power interruption. In this part, three powerful tools have been used: CVNN, TDPF, and ED which were described further in detail in section 2.2.

In the first step of the transmission part (forecasting step in Figure 2.3), a heuristic method is applied to the load data of the grid to forecast the voltage amplitudes and angles under different contingencies. This method is a combination of CVNN and TDPF. The second step is to compare the forecast values with actual data to ensure accuracy of forecasting (evaluation step in Figure 2.3). Next, a sensitive analysis is performed to detect the sensitive buses of the grid under a wide range of contingencies based on forecast results (sens. analysis step in Figure 2.3). Obviously, voltage amplitudes and angles of the buses change during the contingencies which lead to changes in the grid frequency. Therefore, the variations of the voltage amplitudes and angles are suitable indices in detecting the sensitive buses. Under contingencies, these buses have the highest variations in the mentioned parameters compared to other buses. Thus, adding the storage in these sensitive buses can optimally regulate the grid frequency. The optimal location(s) of the BESS are these sensitive busses which consider the effects of the whole range of the contingencies (including the worst case scenario).

In this study the applied contingencies are: losing wind or thermal generations and sudden or gradual change in wind generations. Generally, some of the sensitive buses are positioned close to

the wind generations. In the last step of the transmission part, the required power is calculated using TDPF. This power is the necessary active power which should be injected to the grid through the sensitive buses in order to control the frequency and compensate for power shortages in the worst case contingency. Running an ED determines how much power should be produced by each generator and BESS to have the minimum cost (calc. of req. power step in Figure 2.3). Combination of TDPF and ED calculates the optimal contribution of generators and BESS for power compensation in the transmission part.

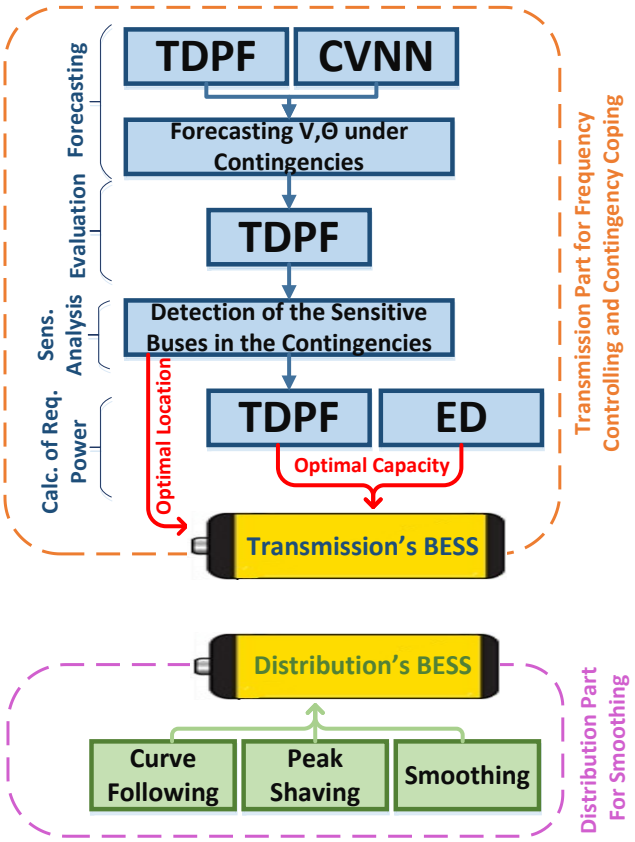

Figure 2.3: Algorithm of the proposed method including two parts

2.3.2 Distribution part

The purposes of the distribution BESS (lower part of Figure 2.3) are peak shaving and load curve smoothing. The following subsections provide more details.

2.3.2.1 Peak shaving

One of the important services in the distribution grid is peak load shaving [40]. Moving the required energy from the peaks of the load curve into the valleys assists the utility to reduce committed units and efficiently utilize renewable energy resources by using energy already stored in BESS to meet the demand. The underlying concept for peak load shaving is in the form of a quadratic programming method which flattens the load curve:

$$\sum_{t=1}^{N}\left(P_{bat}(t)+P_{cir}(t)\right)^{2} \tag{2.18}$$

Subject to BESS capacity constraints:

$$\frac{1}{\Delta t}[SOC_{\min}E_{tot}-E(t)]<P_{bat}(t) \tag{2.19}$$

$$\frac{1}{\Delta t}[SOC_{\max}E_{tot}-E(t)]>P_{bat}(t) \tag{2.20}$$

According to the following equation, energy of BESS is related to SOC:

$$E(t+1)=E(t)+P_{bat}(t)\Delta t \tag{2.21}$$

We can also force BESS to follow a reference load curve,

$$Minimize\ \sum_{t=1}^{N}\left(P_{bat}(t)+P_{cir}(t)-P_{ref}(t)\right)^{2} \tag{2.22}$$

2.3.2.2 Load Curve Smoothing

With growing penetration of distributed renewable generations such as rooftop photovoltaic resources, the variability in the aggregate load curve increases accordingly [41, 42]. Additional

reserve must be up and running to cope with the abrupt fluctuations in the load curve. BESS can mitigate the sharp variations in the power curve to save some time for rapid startup generators to pick up the load [43]. Smoothing out the load curve should keep the SOC constant to save energy for peak shaving purpose. BESS will remove fluctuations around a straight line rather than a horizontal line. The slope of this line is affected by the load forecast, SOC deviation from the desired point, and the startup time of available generators in the grid. The line connects the current load point and 20 minutes ahead forecast load point:

$$P_L(t) = \left(P_{bat}(t_k) + P_{cir}\left(t_k\right)\right) + m\left(t - t_k\right) \tag{2.23}$$

where the slope (m) is given by:

$$m = \frac{P_{cir}(t_{k+1}) - \left(P_{bat}(t_k) + P_{cir}\left(t_k\right)\right) + g\left(SOC\left(t_k\right)\right)}{t_{k+1} - t_k} \tag{2.24}$$

The last term in the slope compensates the SOC deviation from the desired point which is usually kept at the highest allowable limit kept for peak shaving service.

2.4 Case Study

The proposed approach in this chapter has been tested on a real world model of an island in the United States (island of Maui located in the state of Hawai'i). The island's grid includes 184 buses, 20 generators and two wind farms. Table 2.1 provides the generators' data, including coefficients of cost functions and generation constraints. These generators have the available capacity to produce power in the contingencies. This case study has been modeled using the real data of the grid's equipment, loads, and generators.

In the Maui grid, the wind generations have the highest priority to inject the power, according to the contract with the electric utility. This study has been modeled for simulation during times of peak-load with a reserve of 10% total capacity. In order to forecast the voltage amplitudes and angles in the abnormal conditions, different contingencies were applied to the grid model including: gradual and sudden change in wind generations and losing thermal generators. In this study, a wide range of scenarios have been considered in order to determine the worst case contingency of the grid.

Table 2.1: Cost coefficients and constraints of the available generators in the abnormal situation in Maui grid (with fuel cost of $12/MBtu) [44]

Cost=a+b*P+c*P^2				Pmin<P<Pmax	
Bus No.	a	b	c	Power Constraints	
				Pmin (MW)	Pmax (MW)
48	18.997	1.180	1.002	0	1.8
49	8.868	12.231	0.282	0	2.2
50	7.931	11.926	0.411	0	3.3
53	25.624	-2.922	1.477	0	2.8
140	14.680	6.588	0.052	0	2.2
181	24.598	3.762	0.289	0	2.5

2.5 Results

This section contains the results of transmission and distribution parts in order to find the optimal locations and capacity of the storage system.

2.5.1 Transmission part results

After ensuring the accuracy of the forecast parameters, a sensitive analysis is carried out (sen. analysis step in Fig. 2.3). In this step, a wide range of contingencies are applied to the grid and

their impact are considered to find the optimal location(s) of the BESS. Next, for finding the optimal capacity of BESS, the worst case contingency is considered. Fig. 2.4 shows load curve (MW) of Maui grid in one day.

Fig. 2.5 demonstrates the first set of scenarios, which is sudden change of both wind generations from their maximum output to zero in a short time (10 minutes). The second set of scenarios is change the wind generations, based on meteorological data of Maui, which has been shown in Fig 2.6. This figure demonstrates changes of the wind generations in one hour of a day. Losing the thermal generations in different times of day is the third set of scenarios, which Figure 2.7 represents it. Each color demonstrates one generator. The dashed red line represents the worst case contingency (losing the largest generation).

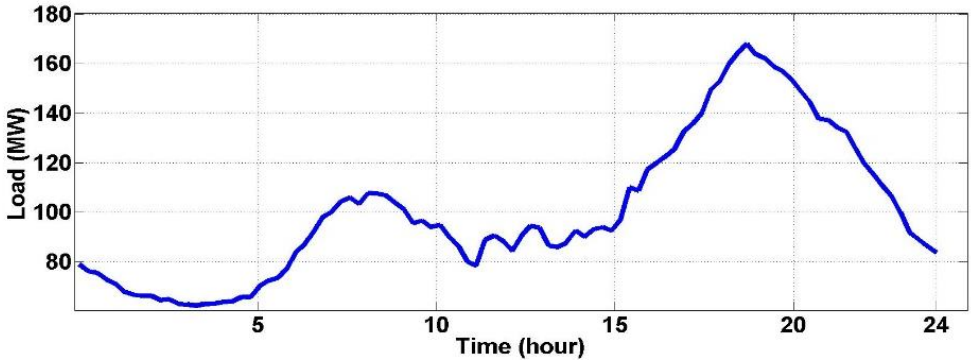

Figure 2.4: Load (MW) in one day of Maui [44]

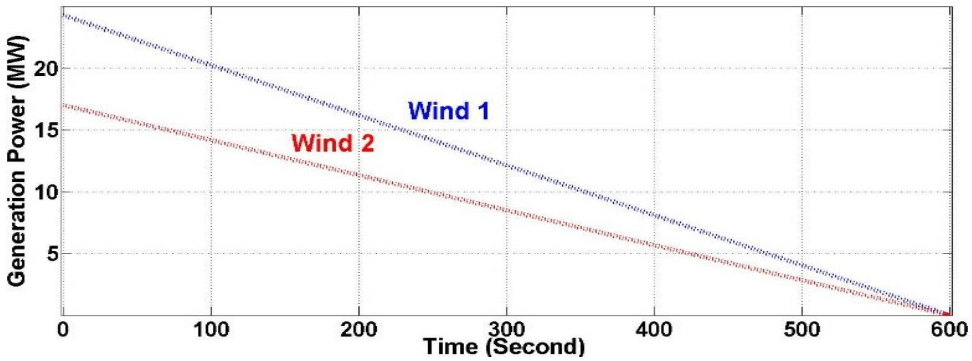

Figure 2.5. The first set of scenarios - Decreasing the wind outputs from maximum to zero

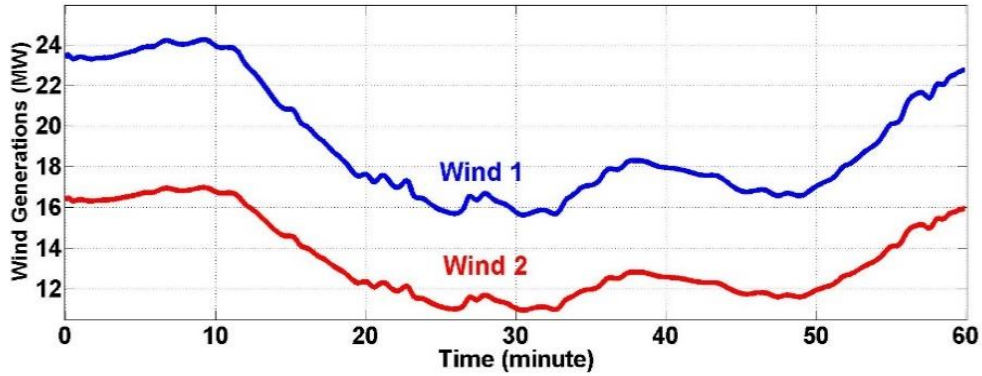

Figure 2.6. The second set of scenarios - Changing the wind generations in one hour of day [44]

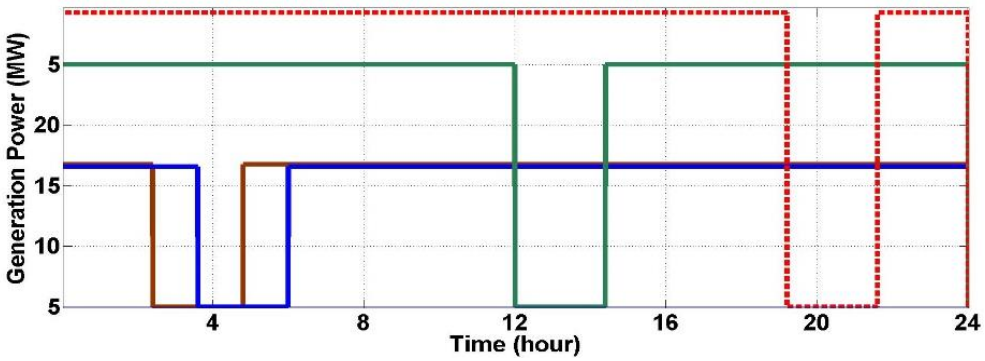

Figure 2.7. The third set of scenarios - losing the thermal generations in different times of day (including the worst case contingency)

Figure 2.8 shows the results of the sensitivity analysis during a wide range of contingencies to detect the sensitive buses as the optimal locations of the BESS. The sensitivity analysis shows bus numbers 166 and 180 have the maximum sensitivity in different contingencies. Therefore, these buses are the best places of the BESS (optimal locations of the BESS).

Bus 180 is a sensitive generation bus which is appropriate for the transmission BESS and bus 166 is a sensitive load bus which is appropriate for the distribution BESS. Using the storage system in these two buses not only regulates the frequency in the abnormal conditions but also compensates for the power shortage in the contingencies to have the minimum power interruption.

After finding the optimal locations of the BESS, the capacity of the transmission and distribution BESS should be calculated. In order to calculate the required active power in the transmission part (according to calc. of req. power step in Figure 2.3), the worst case scenario of contingency has been considered which is losing the biggest generation with 24.3 MW production. With running TDPF under the worst case contingency and using the equation (2.2), the required power can be calculated. This power should be injected (through the sensitive buses) into the grid to cope with the abnormal situations and regulate the frequency. In the worst case scenario of Maui grid, 15.73 MW power should be injected from through the sensitive buses to compensate for the power shortage.

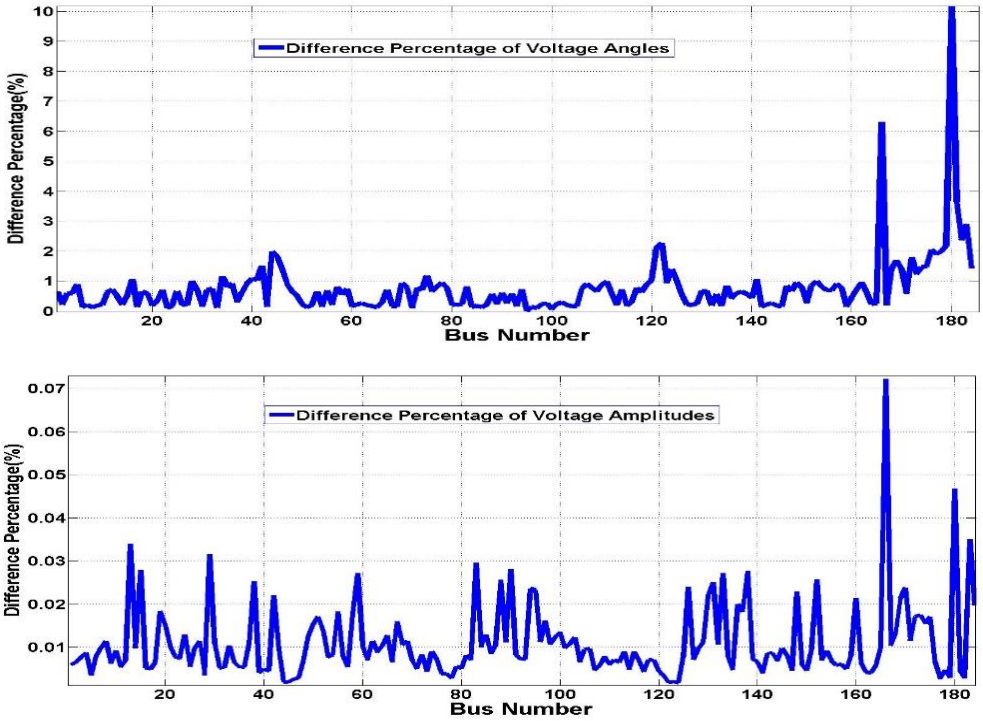

Figure 2.8: Sensitivity analysis results for the voltage amplitudes and angles in a wide range of contingencies

Table 2.2 shows data of transmission lines which connect the available generators of Maui to two sensitive buses. The transmission line impedance is Z=0.05+0.47j Ω /mile. Table 2.3 illustrates the results of ED for the both sensitive buses. The optimal output of power sources (including generators and BESS) have been calculated, at the lowest possible cost, subject to transmission and operational constraints.

Table 2.2: Transmission lines information for connecting the generators to two sensitive buses

	Transmission line distance (mile)	
From Bus No.	To the first sensitive bus (166)	To the second sensitive bus (180)
48	15	4.5
49	30	7.5
50	40	8
53	80	75
140	60	13
181	10	29

Table 2.3: ED results: optimal outputs of the available generators and BESS to cope with the worst case of contingency and regulate the frequency (in transmission part of BESS)

Power Source	Generation Power (MW) -based on ED results
Gen. bus #48	1.8
Gen. bus #49	2.2
Gen. bus #50	3.3
Gen. bus #53	2.8
Gen. bus #140	2.2
Gen. bus #181	2.5
BESS bus#180	**0.93**

The transmission BESS (for contingency management and frequency control) should be allocated in bus 180 (sensitive generation bus). Based on the results in table 2.3, the required power for the BESS is 0.93 MW. For having the maximum life and efficiency of the BESS, it is

recommended to use the BESS in the range between $SOC_{\min}$ and $SOC_{\max}$. For the given values of 0.2 and 0.8 for these parameters, respectively, the active power of the transmission part of the BESS is: $0.93MW * 1/(0.8-0.2) = 1.55MW$. Historical data for Maui Island shows that the maximum time for the contingency (especially losing the generation) is one hour. Thus, the energy of 1.55MWhr should be supplied by BESS to cope with the contingencies and regulate the frequency.

2.5.2 Distribution part results

The proposed method for the distribution part includes two techniques: peak shaving and load curve smoothing. In this section, the results of applying peak shaving technique are presented in Figs. 2.9 and 2.10. Next, the results of applying both techniques simultaneously are presented Figs. 2.11 and 2.12. Peak shaving is implemented on an actual distribution load curve shown in Fig. 2.9. Since there is less uncertainty in forecasting the load in the early morning and night, peak shaving performs well during time periods. A better load forecast around noon when photovoltaic generation comes online, will help to reach a flatter load curve.

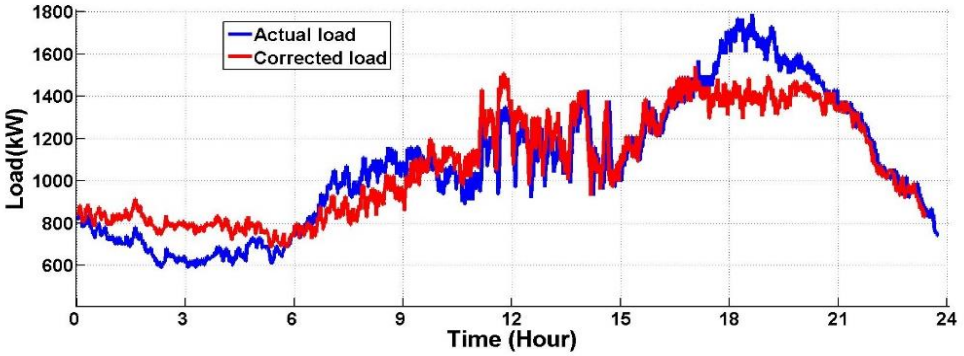

Figure 2.9: Peak shaving for the distribution grid

The SOC graph for the corresponding peak shaving purpose is shown in Fig. 2.10. The higher and lower SOC limits are assumed to be 0.8 and 0.2 respectively to increase the BESS lifetime. The SOC curve can be obtained from a reference power curve obtained from a combination of power system operation study and renewable generation forecast.

Load smoothing is performed on the same distribution load grid and the obtained results are depicted in Fig. 2.11. The original load has more fluctuation than the corrected load which needs higher spinning reserve to respond effectively to the imbalance of load and generation. Moreover, the corrected load is flatter than the original load which decreases the amount of generation form conventional generates in the peak time.

As a result, the cost of generation reduces and less fuels is burnt to meet the demand. The corresponding SOC change in Figure 2.12 shows that SOC does not alter significantly during smoothing period which occurs around noon. Peak shaving is also implemented in this figure with slight changes in $g(SOC)$. The advantage of this method over the previous one is that it benefits from the real time load information which make the forecast more accurate and SOC planning more reliable.

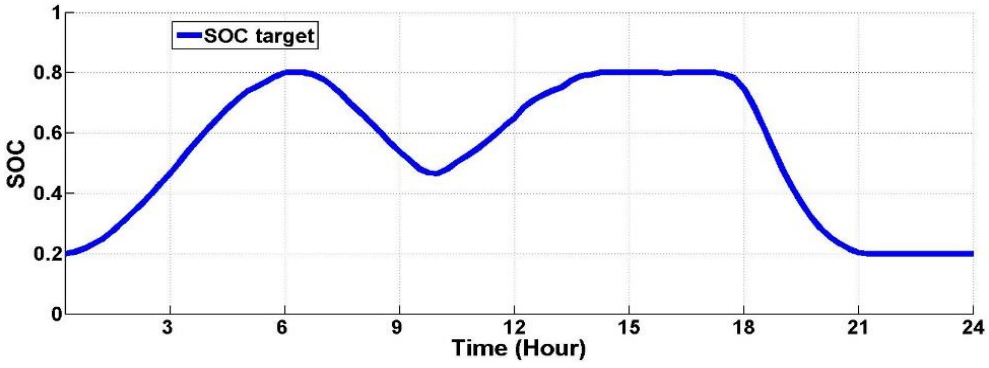

Figure 2.10: Target SOC obtained for peak shaving purpose

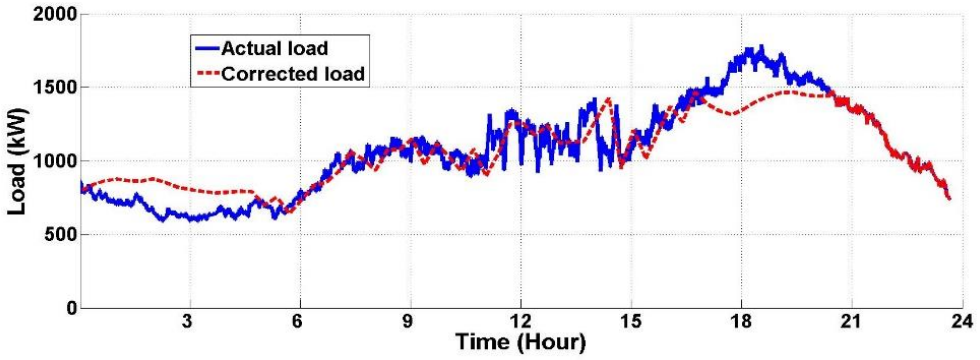

Figure 2.11: Simultaneous peak shaving and load smoothing for distribution grid with high intermittency

Figure 2.12: SOC variation for simultaneous peak shaving and load curve smoothing

Based on Fig. 2.11, calculation the integral of difference between the actual and corrected load in the peak load times leads to the required energy supplied by BESS. This integral will be about 700 kWh from 5-9 pm. In order to have the maximum life of the battery, it is better to utilize the BESS in the range between $SOC_{\min}(0.2)$ and $SOC_{\max}(0.8)$. Thus, the capacity of the distribution part of BESS will be: $0.7MWhr * 1/(0.8-0.2) = 1.17MWhr$.

Finally, for the Maui grid, the final results for the capacity of the multi-purpose BESS are: 1.55MWh for the transmission BESS (located in bus 180 as a generation bus in transmission system) and 1.17 MWh for the distribution BESS (located in bus 166 as a load bus in distribution system). The ratio of the transmission BESS to distribution is 1.32. By allocating the calculated

capacities of BESS in the obtained optimal locations of the grid, contingency management and frequency regulation goals can be reached on the transmission side. Moreover, peak shaving and load curve smoothing can be implemented on the distribution side. Fig. 2.13 shows the difference percentages of the voltage amplitudes and angles before contingency (normal conditions) and during contingency (using optimal BESS). This figure demonstrates the effectiveness of the proposed method to find the optimal locations and capacities of BESS to deal with the worst case contingency.

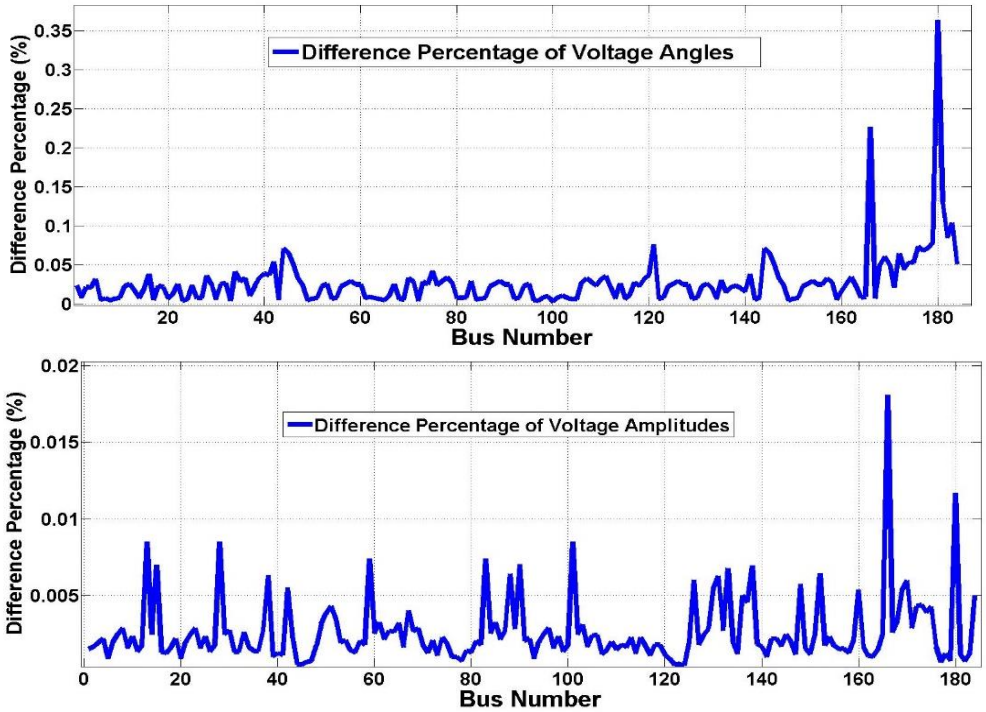

Figure 2.13. Difference percentages of the voltage amplitudes and angles before contingency (normal conditions) and during contingency (using optimal BESS)

2.6 Conclusions

A heuristic method was proposed in this chapter in order to find the optimal location(s) and capacity of a multi-purpose BESS in the power grid. One objective of the use of the BESS is related to the transmission side of the grid to cope with the contingencies and regulate the grid frequency

under abnormal conditions. In this objective, CVNN, TDPF, and ED programs are utilized to perform the optimizations. In the next objective, the BESS is used to manage the distribution system of the grid for peak shaving and load curve smoothing. The proposed heuristic method is applied on a real grid model to find the best location(s) and capacity of the BESS.

Chapter 3

A Nascent Market for Contingency Reserve Services using Demand Response

Abstract

The increased presence of variable renewable generation drives a greater need for authorities to procure more Ancillary Services (AS) for grid balance. One of these services is Contingency Reserve (CR), which is used to regulate the grid frequency in contingencies. Many Independent System Operators (ISOs) are structuring the rules of AS markets such that DR can participate alongside traditional supply-side resources. The available capacity of the generators can be used more efficiently for power production which they were designed for and not CR; cutting costs, and reducing pollution. As the ratio of inverter-based generation compared to conventional generation increases, the mechanical inertia used to stabilize frequency decreases. When coupled with the sensitivity of inverter-based generation to transient frequencies, the provision of AS from other sources than generators becomes increasingly important. This chapter provides a method to use AS for providing CR using DR to ensure system stability for a set of credible contingencies, while also satisfying economic and market goals. In the AS market, Optimal Power Flow (OPF) is used to find the optimal offers/bids and transient behavior of frequency is considered. The proposed model separates DR into two categories—faster and slower—based on the deviation from the normal frequency of grid power. In a standard numerical example, it has been shown that the proposed model can clear energy and AS' bids simultaneously while minimizing the total operating cost and satisfying transient frequency requirements.

3.1 Introduction

Security for grid power delivery and distribution systems can refer to many things. On a basic level, security is defined as the ability of a certain system configuration to continue to function and withstand a wide range of operating parameters, outside influences, or even subsystem failures [45, 46, 47]. To design a grid which is secure, a number of factors need to be considered. In the event of contingencies such as short circuits, large changes in load, or loss of transmission lines, the entire system needs to be able to remain operating long enough for the grid operators to restore stability. Maintaining a balance of power is critical to the continued operation of the grid at these times. In order to increase the capacity to maintain this balance of power, grid operators call upon what are known as AS to provide these changes in power to the grid quickly [45, 48, 49].

AS are typically products provided by a resource capability—generator reserve capacity, etc.—and are contracted to stand by for a request to deliver changes in power to balance grid conditions on very short notice [45, 50]. AS include regulation up, regulation down, spinning reserve, non-Spinning reserve and Volt/Var support (Reactive Power) [51, 52, 53, 54, 55, 56, 57]. AS are different from other power products in that they are purchased just so they might be available for an emergency. They are paid for whether utilized or not. Frequency responsive reserves are one type of AS and are services sufficient to cover the contingency of unplanned trips (or disconnect) of a large generator or transmission line to maintain system balance and recover frequency droops in line power signals. CRs are generally split between spinning and non-spinning reserves and are often based on the largest single hazard (generator or transmission capacity). Contingency events are big (many megawatt) and fast (within a few cycles) [58, 59, 60].

In order to plan the integration of AS, three questions should be answered: How much should be purchased? How should we prioritize the order in which resources are used? Who should pay for these services? There are two approaches for providing AS: compulsory provision by utility and the creation of market for AS vendors [61, 62]. Also, Battery storage can provide different services such as peak shaving, load smoothing and contingency management. These services can be offered in a vertical or deregulated market structure [63, 43]. Choosing the appropriate approach depends on the type of service and nature and history of the power system. Compulsory provision may provide more resources than needed and cause unnecessary investments.

One of the problems that can arise is that of ineffective use of generation capacity. Some generators are inherently more efficient than others. Running the most efficient generators at half of load capacity for CR becomes wasteful [45, 64]. The focus of this chapter is to describe the development and design of a spot market for vendors of AS and the application of this market in the effective implementation of DR as an AS. There are several advantages to the creation of a market for AS over compulsory provision. Grid operators purchase only the amount of service needed and only participants that find it profitable provide services. This provides for a system that becomes financially sound. The market serves to determine the true cost of AS and brings the overall cost of implementation down [45].

Grid operators are faced with the challenge of stabilizing transmission and distribution systems after system failures or other contingencies. From a system designer's viewpoint, it is desirable to maximize grid security. In a perfectly designed system, no component would ever be made to function outside its safe operating range, and would be able to continue to operate following subsystem failures or other grid contingencies long enough for an operator to restore the system.

The power system should remain stable following any of the common disturbances and that it should be able to continue operating in this new state long enough to give the operator time to restore the system to a normal state. OPF is a method which allows operators and designers to find the operating parameters for a given system which will minimize the overall cost.

DR is Voluntary (and compensated) load reduction used as a bulk system reliability resource. Demand-side provision is a good source of AS, because the larger number of participants increases competition, lowers cost and leads to a better utilization of resources. For example, reserve can be provided with interruptible loads rather than partially loaded thermal generating units. This is particularly important if the proportion of generation from renewable sources increases substantially [65, 66, 67, 68, 69, 70]. Generating units can then be used for producing electrical energy rather than as sources of CR [71]. Additionally, the demand side may be a more reliable supplier of some ancillary services than large generating units [72].

The probability that the demand side may fail to deliver a critical service on time is indeed smaller. This service would be provided by the combination of a large number of relatively small loads, all of which are much less likely to fail at the same time than a single large generating unit. Some consumers (for example, those who have large water pumping loads equipped with variable speed drives) might also be able to compete for a share of the AS market [73]. One of the shortfalls of the current state-of-the-art is that customers who place a higher value of security are not able to pay to receive higher security from the grid individually. Thus the system operator provides an average level of security to all customers and the cost of ancillary services is shared by all users on the basis of their consumption [45].

DR is one of the tools that helps to alleviate grid stress as a result of increases in renewable generation. The Federal Energy Regulatory Commission (FERC) has been passing rules in an attempt to level the playing field between traditional and alternative grid resources such as DR and mandating that fast acting resources be compensated for the additional security that their flexibility brings the grid. Conceptual studies have argued that DR is ideally suited to provide AS to the grid and limited field tests have examined their technical capability. The majority of DR literature focuses on its traditional uses such as emergency load relief, system peak management [74] and price responsive demand. The major differences between traditional applications of DR and DR for AS are the reduction of notification time, and the increased speed and accuracy of measurements. There are different algorithms for using DR to provide ancillary service like minimizing the amount of manipulated loads [75], and using an automated system architecture for DR [76].

Behrangrad et al. [77] investigated optimal reserve scheduling through DR to see what impact it would have on reducing pollution and emissions. The focus of the study was to minimize the social costs as related to providing energy, the purchase of AS, grid stability, and pollution. In [78], a model was proposed in which DR is utilized by using flexible bidding to create an active market for distributed AS. The goal of the model was to minimize the net system costs for the system states that may occur with reasonable probability in [79]. For the provision of system reserves, a smart agent system can be implement which can incorporate the outputs of stochastic market optimization problems. Using SA-Q learning algorithms, the proposed agent would continuously work to increase effectiveness in increasing the ratio between cost and benefit by adjusting how much system reserve to offer and at which time.

DR programs were proposed to provide AS and handle multiple contingencies in a power system using a constrained unit commitment problem [60]. Rezaei [80] also proposes a novel energy management system to coordinate and manage DR and distributed generation. In this method, a hierarchical frequency control structure uses microgrid components whose individual models are described in [81]. The components acted in concert to keep the frequency of the system within defined constraints. A linearized DR program had been proposed in order to seek active participation of consumers in the grid frequency management. Chen [82] used security constrained economic dispatch and security constrained unit commitment in order to analyze how demand response resources are appropriated during market clearing processes.

Gitizadeh and Aghaei [83] implemented corrected transient energy function and a linearized form of corrected transient energy margin as dynamic security index to consider the transient stability issues of power system. They considered the transient stability which might be decreased because of hitting security limits or increasing the contribution of risky participants. A framework proposed in [84] considered the dynamic security aspects of power systems in the scenario-based market operation. Two objective functions are optimized including: expected social welfare and expected CTEM. This multi-objective optimization clears the market of the joint energy and reserve auctions. In another study [85], another multi-objective optimization was proposed to clear the market of joint energy and reserve auctions ensuring system security. These objective functions were: generation costs and security indices.

In describing the method to implement DR as a source of AS for CR, a spot market model has been applied here. The transient limitations of frequency for making a competitive market between different Demand Response Aggregators (DRAs) are considered to provide AS for producing CR.

One of the characteristics of renewable energy inverter generation is that it is highly sensitive to the transient behaviors of the power system. If there is a large contingency, the frequency will drop, and the inverters will respond by shutting off; further decreasing available generation, and exacerbating the contingency. With a large enough presence of inverter-based generation, the effect of a system-wide failure could be catastrophic [86]. Thus, AS become even more important.

The method described in this chapter not only guarantees transient constraints of frequency in contingencies by supplying CR services by DR, but also can make profit for both Generation Company (GENCO) and DRAs. Additionally, the available capacity of the generators can be used more efficiently for power production which they were designed for and not CR; cutting costs, and reducing pollution. In this study, the probability of two nearly simultaneous independent faults or failures is generally assumed to be so small that such events do not deserve to be considered. As a model for the worst case of contingency, case *N-1* has been designed to simulate losing the biggest generator in the system. Section 3.2 describes the power control system used to regulate the system frequency. Section 3.3 represents the proposed methodology calculate CR cost and the creation of a market to allow the DRAs to participate in AS. Section 3.4 includes a standard case study (IEEE-24 bus model) and the results after applying the proposed method. Closing remarks can be found in section 3.5.

3.2 Power Grid Frequency Control

In calculating the cost of CR, it has been carefully considered the requirement of the power system to remain within the allowable range of frequency. During contingencies or faults (like the loss of a generator), the grid frequency drops. When we consider a generator, when there is an

imbalance between mechanical power and load, the frequency changes. Torque can either accelerate the rotating mass of the generator or be converted into electrical energy. In general, to maintain a constant angular velocity, of course the acceleration must be zero. In order for the acceleration to be zero, the mechanical torque input must be completely converted to electrical energy. Any imbalance would translate into angular acceleration of the rotating generator mass and therefore a change in electrical frequency. This dynamic relationship is modeled using the swing Equation (3.1). This model is usually representative of just one generator, but for the purposes of microgrid, the aggregate behavior of the system is able to be modeled by combining the individual components into an equivalent representation.

$$\frac{2H}{\omega_S}\frac{d^2\Delta\delta}{dt^2} + D\frac{d\Delta\delta}{dt} + P_S\Delta\delta = 0 \tag{3.1}$$

where *D* is damping torque which can be determined either from design data or by test and P_S is synchronization coefficient. δ is electrical power angle (electrical radian) and ω_S is electrical angular velocity. *H* is the per-unit inertia constant (second); related to the moment of inertia of the rotating masses within the system [87, 88].

In grids where there is a high penetration of renewable energy generation, the actual mass of physical rotating masses is decreased and therefore the moment of inertial is also decreased (reflected in the value of *H)* which causes the entire system to be more sensitive to imbalances and exacerbating frequency droop [89]. The value of H depends on the size and type of synchronous machine. Frequency changes much less in large interconnected systems with more rotating mass than in smaller isolated systems [88]. Figure 3.1 shows a block diagram of the method used to control generator speeds in response to changes in frequency.

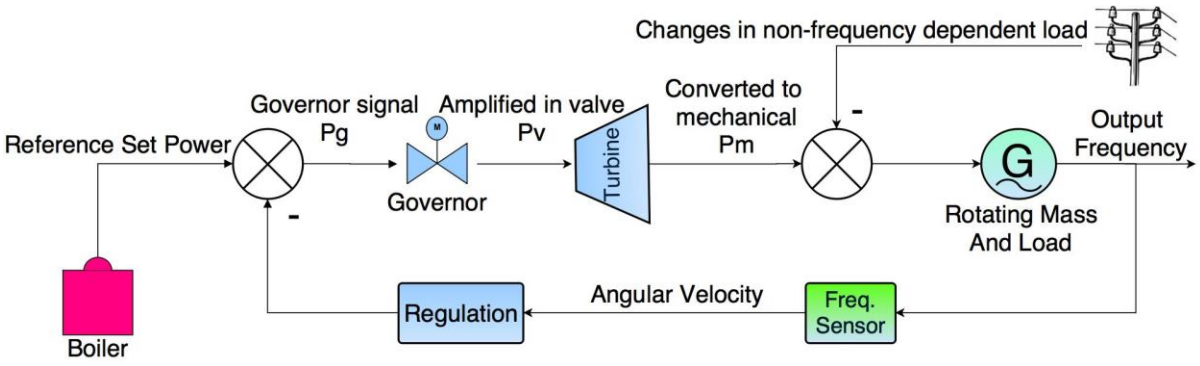

Figure 3.1: Block diagram of load frequency control

Changing of the load $\Delta P_L(s)$ has an effect on the change in output frequency $\Delta\Omega(s)$. The magnitude of the change in frequency compared to the change in load is can be expressed as shown in Equation (3.2):

$$\frac{\Delta\Omega(s)}{-\Delta P_L(s)} = \frac{(1+\tau_g s)(1+\tau_T s)}{(2Hs+D)(1+\tau_g s)(1+\tau_T s)+1/R} \tag{3.2}$$

Where τ_g and τ_T are the governor and turbine time constants, which determine the relative effect on frequency to changes in power. *D* is expressed as percent change in load divided by percent change in frequency (for frequency sensitive loads). *R* is droop or speed regulation (in percent). In a microgrid with an equivalent swing equation, it can be supposed that losing generation is equivalent to increasing the load. Thus transient and dynamic behaviors of the grid frequency can be analyzed using equation (3.2). Deviation of the steady state frequency can be obtained from Equation (3.3):

$$\Delta\omega_{ss} = (-\Delta P_L)\frac{1}{D+1/R} \tag{3.3}$$

If there are several generators with governor speed regulations $R_1, R_2, ..., R_n$, Equation (3.3) can be rewritten as:

$$\Delta\omega_{ss} = (-\Delta P_L)\frac{1}{D + 1/R_1 + 1/R_2 + ... + 1/R_n} \tag{3.4}$$

In the developing modern power grid there has been a steady increase in the presence of grid-tied photovoltaic inverter systems. These power generating systems are designed to shut down in response to grid input frequencies outside of the normal range as a safety feature. They come with electronics sensitive to signal frequency variation; designed to shut off under abnormal frequency conditions. In the case of a contingency event, where grid frequency is affected, there is risk of losing the power generated by these inverter systems. As this happens, the frequency of the system is further affected and system imbalances are exacerbated. Table 3.1 shows frequency settings of inverters in different ranges of transient frequencies based on IEEE 1547 standard [90].

Table 3.2: Standard inverter operating frequency ranges. IEEE 1547 *[90]*

IEEE Designation	OFR2	OFR1	NORH	NORL	UFR1	UFR2
Frequency Range(Hz)	>62	60.5-62	60-60.5	58.5-60	57-58.5	<57
Mode	Cease	Moment	Normal	Normal	Mand.	Trip
Ride Through (s)	-	300	Infinite	Infinite	300	-
Trip (s)	<=0.160	301	Infinite	Infinite	301	0.16

3.3 Methodology

The methods for calculating profits of the GENCO and DRAs as a result of participation in the AS market are explained in subsection 3.3.3 below. CR is purchased directly from DRAs as clients. In order to complete the calculations, it should be first determined the price at which the GENCO would offer to purchase the amount of CR which would be sufficient to maintain security

(subsection 3.3.1), independently of DR. This price is determined through OPF. The OPF constraints can be updated based on the availability of frequency regulation resources such generating units, interruptible load as well as DR. Therefore, OPF is executed to find the optimal allocation of each unit and also find the cost curve of procuring DR. Subsection 3.1.2 models the DRAs role in the market and describes their required functionality.

3.3.1 CR cost of GENCO using OPF

The first stage of the proposed method is to find the cost which GENCO must pay to maintain provisional AS (in particular CR) considering transient limitations of the frequency. The initial cost of CR is theoretically maximized sufficiently to correct the single worst case contingency event (*N-1*) - i.e. failure of the highest capacity generator. Considering IEEE 1547 standard [90], the key transient parameters of the frequency are: undershoot, undershoot time, and settling time.

Figure 3.2 illustrates the overall concept of the method. The system begins to act at the start of a contingency event. For illustrative purposes, worst-case-scenario event has been assumed (*N-1* or the loss of the largest generator in the plant). In order to prevent failsafe systems from shutting off distributed generation of inverters, mitigation of frequency droop below 57 Hz must be provided by traditional means of spinning reserve in order to bring the grid back to 57 Hz within the allotted 0.16s. It is at this point that we introduce the system for providing the rest of the rest of the AS required for frequency recovery through DR. First the amount of DR required is calculated and a cost curve is generated for this amount of AS for the GENCO using OPF. The GENCO then sends out an offer to the DRAs to purchase DR for AS. There are two distinct price curves, one is for faster DR to recover frequencies from 57-58.5 Hz and slower DR to recover

from 58.5-60 Hz. Faster DR is valued at a higher rate. At this point, the market is open for DRAs to bid to fill the GENCO offers. The market is cleared with the purchase of DR as AS until either the entire amount of DR is used, the contingency is over, or the bids from the DRAs exceed the offer from GENCO.

Bi-directional communication is maintained between DR resources and the aggregator through means of existing network infrastructures. The GENCO cost curve algorithm (Figure 3.3) and GENCO market algorithm (Figure 3.4) show the details of how this method is applied to obtain the remaining AS through DR. The purchase of AS from the DR market is optimized through these methods to minimize the costs of operation and maximize social welfare.

Figure 3.3 shows the algorithm for determining CR cost curve for GENCO. In the event of an *N-1* contingency, the transient parameters of frequency and new inertia are calculated. If the overshoot is less than 3 Hz, IEEE standards leave 300s to clear the fault. If it is greater than 3Hz, IEEE standards leave 0.16s to clear the fault. If the fault is not cleared during this period, the inverter-based generators are tripped off. DR is not fast enough to increase the frequency to 57Hz during 0.16s thereby maintaining functionality independently. GENCO controls the only generating capabilities able to recover the grid frequency to at least 57Hz within the time frame required; once the quick response of the generator reserve brings the frequency back to 57Hz. DRAs may compete to provide AS to increase the grid frequency back to 60Hz from there. Thus, GENCO and DR each contribute to the total increase in frequency.

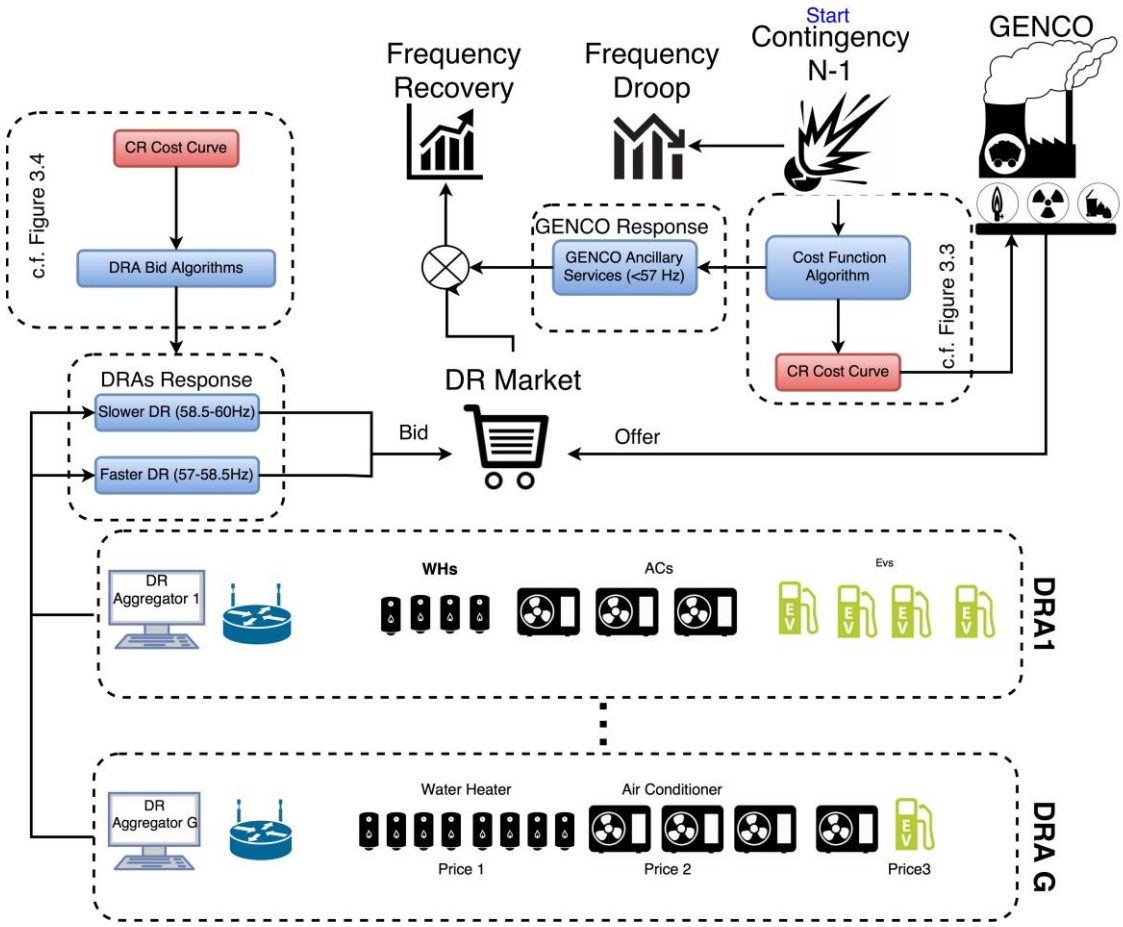

Figure 3.2: DR market implementation for open trading of AS

After determining the GENCO and DR's contributions, an OPF is performed for the GENCO in order to find the new available capacities of generators after providing the necessary AS contribution. The remaining AS for CR should be supplied by DR from the nascent market. The starting point of CR cost curve is the point at which the grid frequency is recovered to at least 57Hz- i.e. the cost of the GENCO's initial CR requisite. Clearly, if frequency remains above 57Hz after the *N-1* contingency event, the CR cost includes only non-emergency reserve which can be supplied by DR.

Given the initial point of the cost curve, the remaining values may be found by partitioning the range of frequencies which DR is responsible to regulate over. Let the range (57-60 Hz) be split into *M* sections (equal or unequal sections). In each section, equation (2) calculates required power (ΔP) which should be supplied by GENCO to increase the frequency as much as Δf. In each section, with increasing power, the inertial constant (*H*) changes. The calculated CR cost in each section is equal to the marginal cost of the cheapest available generator at that moment which is calculated by running OPF in each section.

Based on the IEEE standard (Table 3.1), if the frequency of the grid is between 57 and 58.5 Hz, the required power must be supplied within a timeframe of less than 300 seconds or the inverter-based generation that is sensitive to frequency will trip off in response. The last point of the curve (point *M*) is the only one where optimal grid frequency conditions may be realized. Finally, plotting the CR cost as a function of frequency, while respecting the constraints produces the CR cost curve.

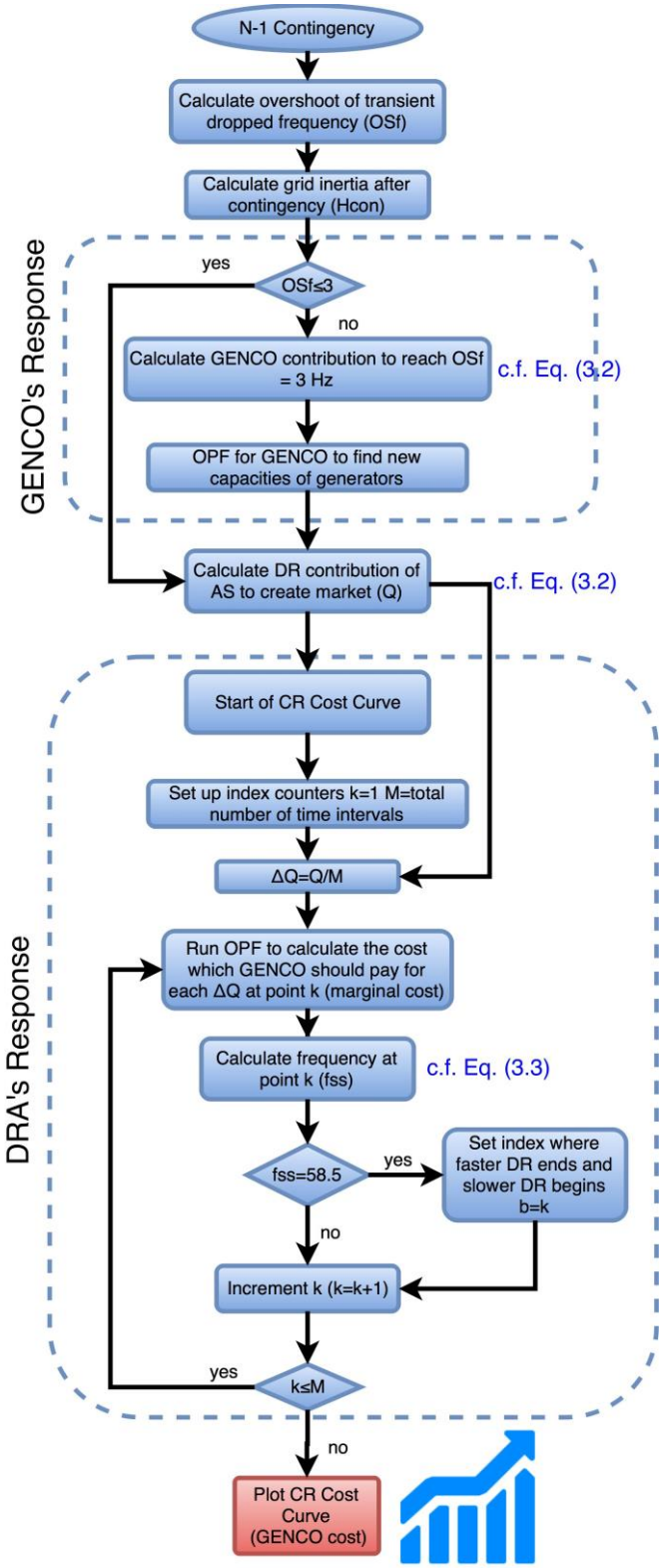

Figure 3.3: GENCO's CR cost curve algorithm for using in the market

3.3.2 Forming DR market

The CR cost curve constructed previously outputs GENCO's offer price for CR generation. In order to utilize DR to provide counter bids for provided services, a market has been constructed for trading DR directly as a source of AS, it is assumed that *G* aggregators, each holding contracts with an unspecified number of buildings, participate in the market directly providing DR from its own pooled resources. Figure 3.2 illustrates the participation on both sides of the market.

Figure 3.4 represents the GENCO market algorithm which is the method by which the market is cleared in a manner which works toward maximizing profit for all participants and system efficiency. Remember that in the GENCO cost curve algorithm, the total range of frequency recovery is divided into *M* sections. In the GENCO market algorithm, the index starts at *k=0* and goes up to index *M* using the calculated price for each section of frequency recovery as a condition by which we base decisions. Recall that *b* was the point at which the divisions of frequency recovery were split between faster and slower DR price schemes. All sections below 58.5 Hz fall into the faster category while those greater than 58.5 Hz fall into the slower and less valuable category. While *k* is less than *b*, the Faster Demand Response Algorithm (FDRA) is used to determine the DRA bid.

If this bid price is below the cost of the GENCO to provide AS through spinning reserve, the GENCO will purchase the DR from the DRA, if it is greater, the GENCO will provide its own AS. Each section of frequency recovery is handled by incrementing *k* for every step. Once *k* is greater than *b*, the Slower Demand Response Algorithm (SDRA) is used to determine the DRA bid. Once the algorithm has cleared each of *M* sections, the entire range of frequency recovery has been

accounted for. The market parameters are output and profit for DRAs and GENCO are tabulated with the amount of AS traded in the market.

Based on IEEE 1547 standard, AS for CR sufficient to recover grid frequency from 57-58.5Hz should be supplied less than 300 seconds after the contingency event to prevent inverter safety shut off and exacerbation of frequency instability. Each DRA divides its resources into two distinct classes depending on time required to deploy. DRAs can manage and categorize loads of houses based on the contracts, consumers' desired levels of comfort, and essential shading levels. Thus, a given DRA suggests two programs in the market: a Faster Demand Response Program (FDRP) and a Slower Demand Response Program (SDRP).

Dependent on the priority levels of the loads, the faster demand response loads will include those which are less time critical and can be shed first. For example, WHs can be the first priority loads to be shed and refrigerators can be considered as time critical and shed last; with values also reflected in bid price. This effect can be visualized in the step nature of the bid price in the graphs illustrated in Figure 3.8 in the test case and simulation. The algorithm depicted in Figure 3.4 shows the steps of the second stage of the proposed method. FDRPs try to increase the grid frequency from 57 to 58.5Hz and SDRPs continue to increase the frequency thereafter to 60Hz, with *G* aggregators that bid prices for FDRP: $F_1^{DR,fast}, F_2^{DR,fast}, ..., F_G^{DR,fast}$ and for SDRP: $F_1^{DR,slow}, F_2^{DR,slow}, ..., F_G^{DR,slow}$ ($/MW).

In the faster demand response zone, at each point of the cost curve, the market price of AS for CR ($price_{fast}^{CR}$) is the minimum of the bids by DRAs if it is less than the GENCO cost for CR:

$$price_{fast}^{CR} = \min\{C^{CR}, F_1^{DR,fast}, F_2^{DR,fast}, ..., F_G^{DR,fast}\} \quad (3.5)$$

$$\text{s.t.} \quad \sum_{k=1}^{b} \Delta q_{k,g}^{DR,fast} . \alpha_{k,g}^{fast} \le q_{g,\max}^{DR,fast} \qquad g = 1,2,...,G \quad (3.6)$$

$$\sum_{k=1}^{b} \sum_{g=1}^{G} \Delta q_{k,g}^{DR,fast} . \alpha_{k,g}^{fast} = q_{fast}^{DR} \quad (3.7)$$

Similarly, in the slower demand response zone, the market price of AS for DR ($price_{slow}^{CR}$) is:

$$price_{slow}^{CR} = \min\{C^{CR}, F_1^{DR,slow}, F_2^{DR,slow}, ..., F_G^{DR,slow}\} \quad (3.8)$$

$$\text{s.t.} \quad \sum_{k=b+1}^{M} \Delta q_{k,g}^{DR,slow} . \alpha_{k,g}^{slow} \le q_{g,\max}^{DR,slow} \qquad g = 1,2,...,G \quad (3.9)$$

$$\sum_{k=b+1}^{M} \sum_{g=1}^{G} \Delta q_{k,g}^{DR,slow} . \alpha_{k,g}^{slow} = q_{slow}^{DR} \quad (3.10)$$

$$\text{and} \quad q_{fast}^{DR} + q_{slow}^{DR} = q^{DR} \quad (3.11)$$

where C^{CR} is the price offer by GENCO as the cost offer CR (\$/MW). $\Delta q_{k,g}^{DR,fast}$ ($\Delta q_{k,g}^{DR,slow}$) is the energy quantity provided by the g^{th} aggregator in the k^{th} section of the CR cost curve partition (MW). $q_{g,\max}^{DR,fast}$ ($q_{g,\max}^{DR,slow}$) are the maximum capacities of the g^{th} aggregator in the FDRP and the SDRP (MW). $\alpha_{k,g}^{fast}$ ($\alpha_{k,g}^{slow}$) is a participation factor of the g^{th} aggregator in the k^{th} section of the CR cost curve partition. If it participates, its number is 1 and if it doesn't participate, its number is 0. Equations (3.5) and (3.8) present that the market price is the minimum of the offered process by DRAs and utility cost for faster and slower demand response programs, respectively. Conditions provided in equations (3.6) and (3.9) guarantee the available DR resources in the DRAs (based on the collected data from communication devices). Equalities in equations (3.7) and (3.10) guarantee that all the required DR can be provided by aggregators to regulate the frequency (if there are enough DR resources available).

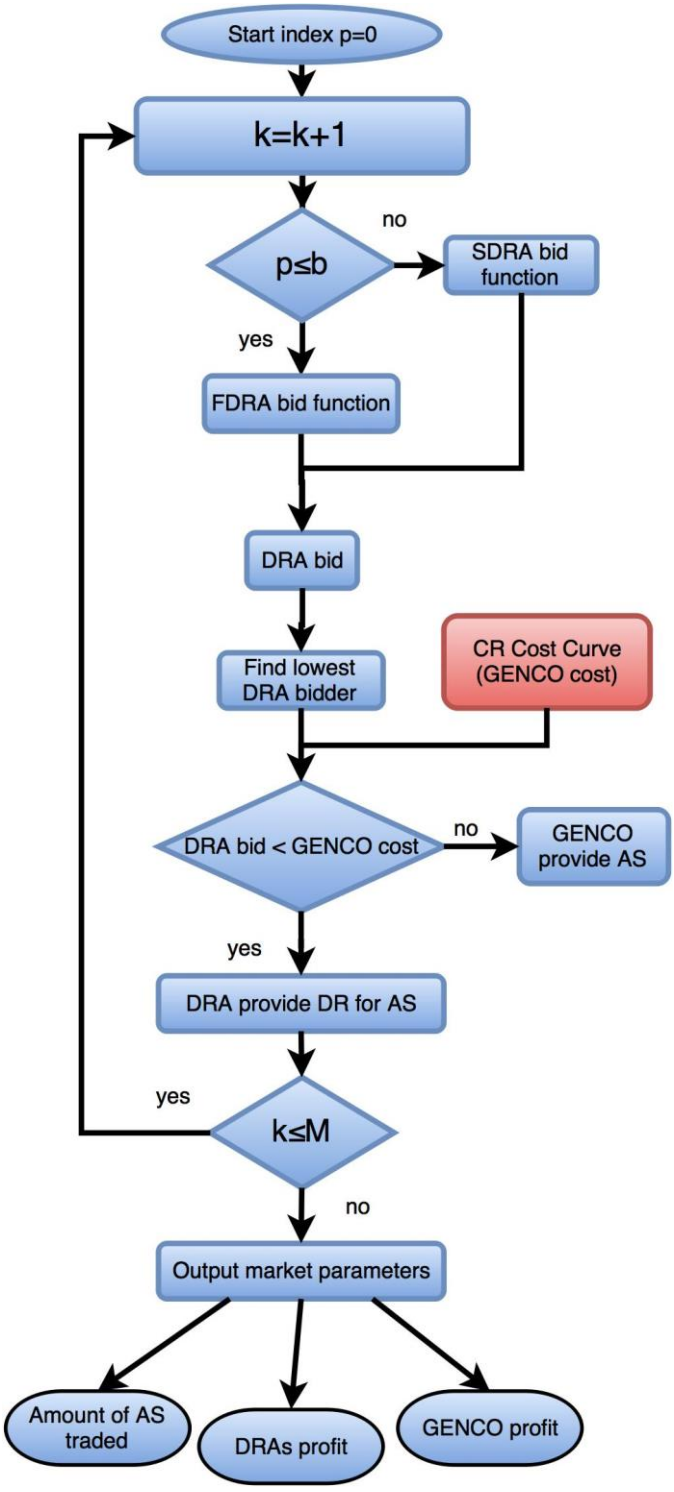

Figure 3.4: Market algorithm, determination for purchase of DR for AS to maximize profit and efficiency

Constraints (3.6) and (3.9) require that the total energy provided by the g^{th} aggregator that is distributed over multiple intervals does not exceed its total capacity. q^{DR} is the total energy quantity required of AS for CR which is to be supplied by DR (MW)- i.e. the sum of the total energy quantities to be supplied by DR through FDRP and SDRP: $q_{slow}^{DR}$and q_{fast}^{DR}. The b^{th} section in the partition of the CR cost curve is the boundary separating faster and slower demand response zones. *M* is the number of sections in the partition of the CR cost curve.

In competition between the aggregators, the winner will be that which bids the minimum price if it has sufficient capacity available to participate in the AS market, otherwise it is be replaced by the next cheapest DRA.

3.3.3 Calculations of profit

The DR devices availability is determined by the measurements across the distribution grid. An example of such devices are grid interactive WHs which send the temperature and status of water heater and can be remotely controlled via utility or third part aggregator [91, 92, 93]. After deciding which aggregator(s) should participate for different parts of cost curve, the GENCO profit can be obtained from the following equations:

$$PR_{genco}^{fast} = \sum_{k=1}^{b} \Delta q_k .(C^{CR}(q_k)) - \sum_{k=1}^{b}\sum_{g=1}^{G} \alpha_{k,g}^{fast} .\Delta q_k .F_g{}^{DR,fast}(q_k)) \tag{3.12}$$

$$PR_{genco}^{slow} = \sum_{k=b+1}^{M} \Delta q_k .(C^{CR}(q_k)) - \sum_{k=b+1}^{M}\sum_{g=1}^{G} \alpha_{k,g}^{slow} .\Delta q_k .F_g{}^{DR,slow}(q_k)) \tag{3.13}$$

PR_{genco}^{fast} and PR_{genco}^{slow} are the profits of GENCO in FDRP and SDRP, respectively ($). Parameter of $C^{CR}(q_k)$ is the CR cost corresponding to quantity of q_k. Parameter of Δq_k is the shaded load by aggregators between k^{th} and $(k+1)^{th}$ section of CR cost curve. ($\Delta q_k = q_{k+1} - q_k$). The first terms of equations (3.12) and (3.13) are CR cost in GENCO side ($) and the second terms are the money that GENCO pays to aggregators for AS ($). The total profit of GENCO is:

$$PR_{genco}^{tot} = PR_{genco}^{fast} + PR_{genco}^{slow} \tag{3.14}$$

The profit corresponding to DRAs can be obtained from the following equations.

$$PR_{DRA,g}^{fast} = \sum_{k=1}^{b} \alpha_{k,g}^{fast} . \Delta q_k . F_g^{DR,fast}(q_k)) \tag{3.15}$$

$$PR_{DRA,g}^{slow} = \sum_{k=b+1}^{M} \alpha_{k,g}^{slow} . \Delta q_k . F_g^{DR,slow}(q_k)) \tag{3.16}$$

where $PR_{DRA,g}^{fast}$ and $PR_{DRA,g}^{slow}$ are the profits of g^{th} aggregator in FDRP and SDRP, respectively ($). The total profit of g^{th} aggregator is:

$$PR_{DRA,g}^{tot} = PR_{DRA,g}^{fast} + PR_{DRA,g}^{slow} \tag{3.17}$$

3.4 Test Case and Simulation Results

A standard cast study (IEEE 24-bus model) was chosen and the proposed method was applied to it in order to demonstrate the provision of AS for CR using DR. Fig. 3.5 shows the schematic of IEEE-24 bus model with the locations of generators, loads, and DRAs. Data of the generation units are available in table 3.2. The objective function (3.5) minimizes the total

generation cost where the cost for each generator's real power output is given by a second order polynomial term $Cost^{gen}(P_g) = \sum_{i=1}^{N} \eta.P_{g,i}^2 + \beta.P_{g,i} + \gamma$ where N is the number of generators and P_g is the generated active power. The cost coefficients (η, β, γ) are selected from the MATPOWER package [94]. The parameters related to control loop model of the grid are: τ_g =0.2s, τ_T =0.5s, D =0.8, R =0.05 per unit, H =5s.

And the open-loop transfer function will be:

$$\frac{\Delta\Omega(s)}{-\Delta P_L(s)} = \frac{0.1s^2 + 0.7s + 1}{s^3 + 7.08s^2 + 10.56s + 20.8} \tag{3.18}$$

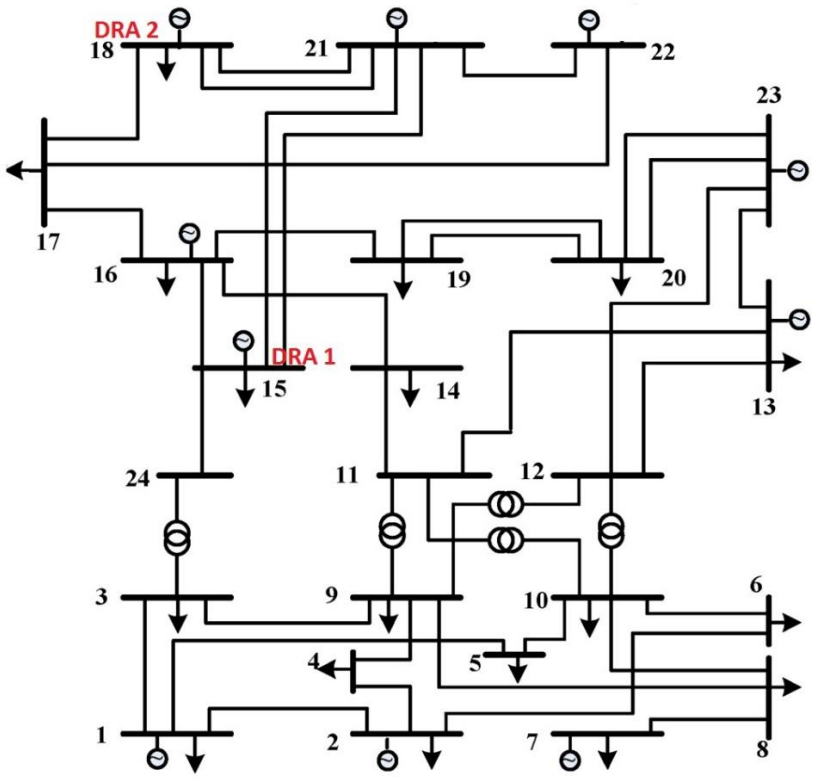

Figure 3.5: IEEE-24 bus model with the locations of generators, loads, and DRAs

Table 3.2: Technical data for generation units of IEEE 24-bus standard model

Node No.	Real power output: P_g *(MW)*	P_{max} *(MW)*	P_{min} *(MW)*	$Cost^{gen}(P_g) = \eta.P_g^2 + \beta.P_g + \gamma$		
				η	β	γ
1	2 x 10	20	16	0.3300	75.0000	400.6849
1	2 x 76	76	15.2	0.0141	16.0811	212.3076
2	2 x 10	20	16	0.3300	75.0000	400.6849
2	2 x 76	76	15.2	0.0141	16.0811	212.3076
7	3 x 80	87	25	0.0527	43.6615	781.5210
13	3 x 95.1	170	69	0.0072	48.5804	832.7575
15	5 x 12	12	2.4	0.3284	56.5640	86.3852
15	155	155	54.3	0.0083	12.3883	382.2391
16	155	155	54.3	0.0083	12.3883	382.2391
18	340	340	100	0.0002	4.4231	395.3749
21	340	340	100	0.0002	4.4231	395.3749
22	6 x 50	50	10	0	0.0010	0.0010
23	2 x 155	155	54.3	0.0083	12.3883	382.2391
23	350	350	140	0.0049	11.8495	665.1094

The *N-1* contingency includes loss of the largest generator with capacity of 350 MW located in bus 23. Based on the algorithm of Fig. 3.3, the first step is to calculate the GENCO and DR's contribution in AS for CR and to find the starting point of CR cost curve. In the mentioned case study GENCO and DR's contribution are 282.9 and 67.1 MW, respectively. Fig. 3.6 shows the transient frequency at the starting point of the CR cost curve before using the market for AS which the overshoot is less than 3Hz. After the emergency CR (282.9 MW) had been supplied by GENCO to restore the grid frequency above 57 Hz, algorithms of Fig. 3.3 and 3.4 were performed to determine how DR could then be used to affect the remaining CR.

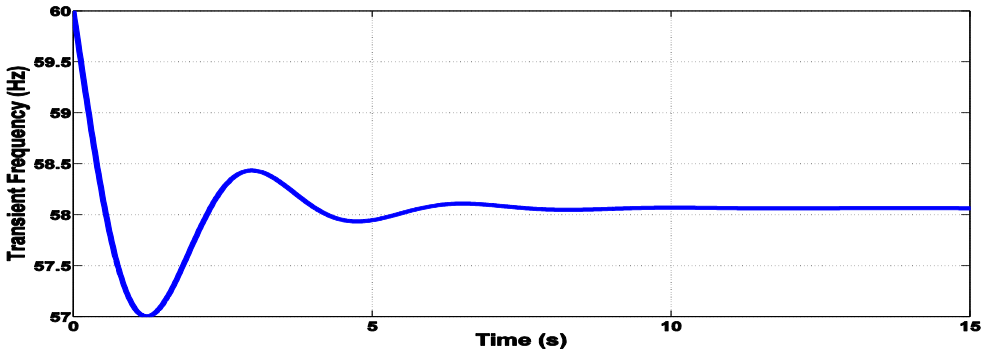

Figure 3.6: Transient frequency at the starting point of the CR cost curve

Based on the DR's contribution for AS, the market should be formed only for 67.1 MW. After emergency CR was applied to bring grid frequency above 57Hz, this marked the starting point of the CR cost curve at which the new available capacities of the generators were obtained, from which the points of the CR curve were determined using OPF. Fig. 3.7 shows the cost of CR which GENCO should pay as an AS.

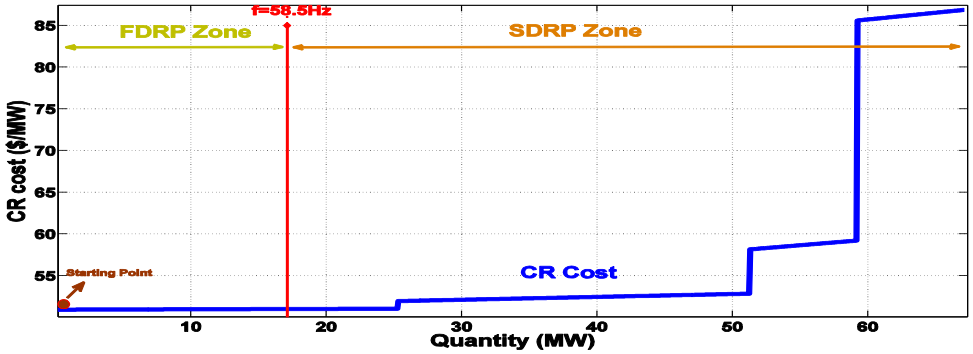

Figure 3.7: Cost of CR which GENCO should pay as an AS

The red vertical line shows the border between the zones that should be supplied by FDRP and SDRP, based on the IEEE 1547 standard. It means that 17.11 MW of the load should be shaded in FDRP less than 300 seconds after the contingency. In this case study, it is supposed that there are two aggregators in buses 15 and 18 with demand of 317 and 333 MW, respectively. The availability of the DR sources are obtained using communication devices based on the data measurement in houses [92]. Each of which have both a FDRP and SDRP for their covered house

loads. Fig. 3.8 demonstrates the bid price for DR by two aggregators in FDRP and SDRP, respectively. Fig. 3.9 shows the participation factor of DRAs in FDRP and SDRP. These results show the competition between these two aggregators and contribution of them in order to provide AS for CR in the market. Fig. 3.10 shows the aggregate quantity of the shed load by DRAs.

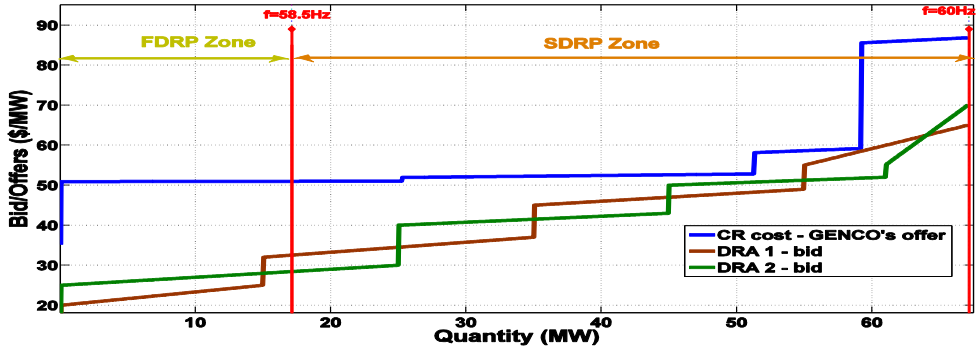

Figure 3.8: Bid price for DR by two aggregators in FDRP and SDRP

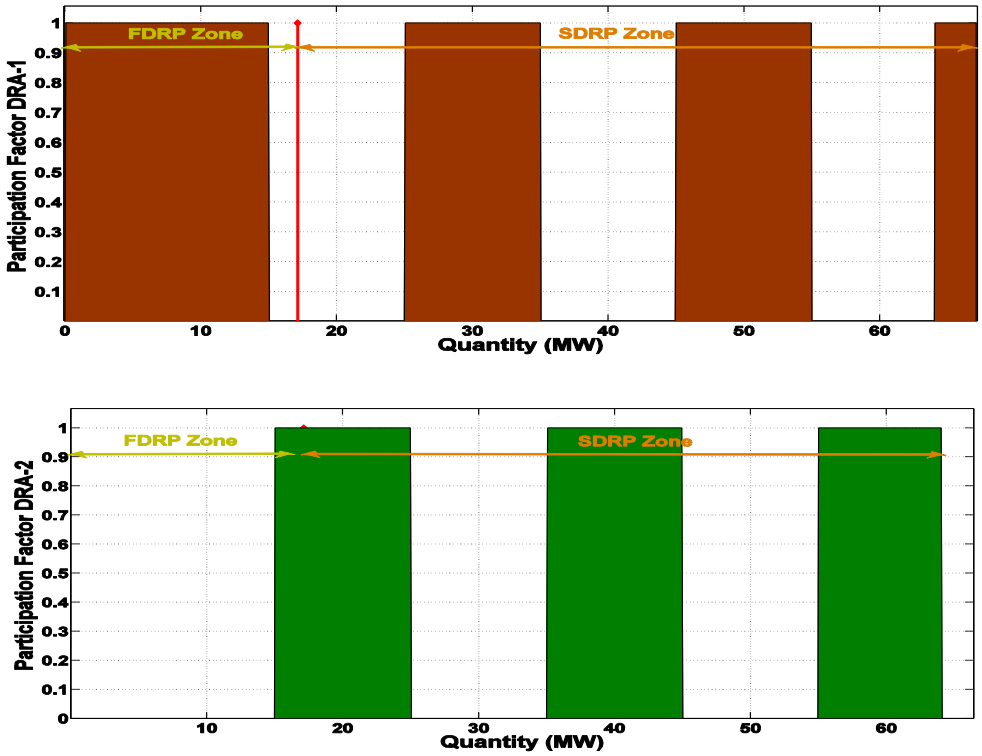

Figure 3.9: Participation factor of DRAs in both FDRP and SDRP

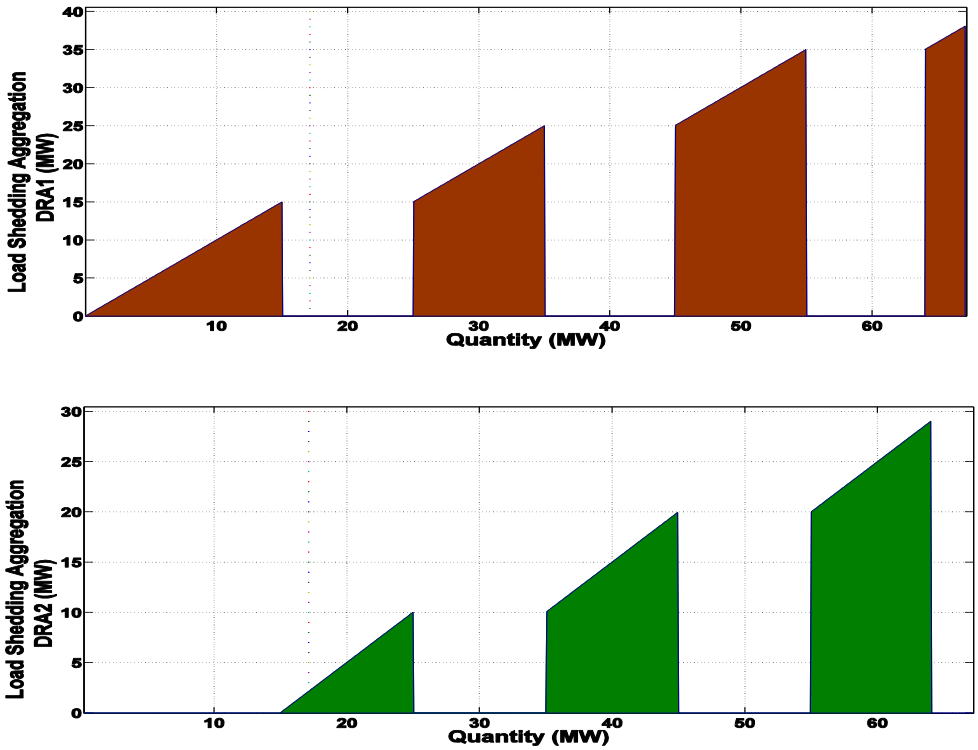

Figure 3.10: Aggregate quantity load shed by DRAs

The contribution of the DRAs for load shedding are 38.08 and 29.02 MW for the first and second DRAs, respectively. The profit of GENCO and DRAs are

$PR_{genco}^{tot} = \$1225, PR_{DRA,1}^{tot} = \$1372, PR_{DRA,2}^{tot} = \$1200.$

3.5 Conclusions

In this chapter, a method was proposed to determine the value for DR to provide AS especially for CR using a market model. The method minimizes the cost of AS provided by DR, maximizes social welfare, and maintains grid stability by mitigating frequency transients to an operating range within industry standards. The IEEE 24-bus model was used to demonstrate the application of the method in the event of the loss of the largest generator in the system. Simulated results showed the cost differential of frequency droop mitigation using DR compared to conventional generation for

AS using the proposed market model. The model included multiple aggregators competing for faster and slower DR programs.

The proposed method is intended for use in grid systems which are experiencing or would have an increased ratio of renewable generation and frequency sensitive technologies, such as inverters, that may be prone to tripping during a contingency event. The reduction in system inertia during a contingency event requires alternative economically viable solutions to provide AS and spinning reserve. The simulations in this work clearly show that the proposed methods for providing AS through DR has a basis for being both economically viable and ensuring system security for credible contingencies.

Chapter 4

Proving Frequency Regulation Reserve Services using Demand Response Scheduling

Abstract

During power grid contingencies, frequency regulation is a primary concern. Historically, frequency regulation during contingency events has been the sole responsibility of the power utility. A practical method of using distributed DR scheduling is presented to provide frequency regulation during contingency events. This chapter discusses the implementation of a control system model for the use of distributed energy storage systems such as battery banks and electric WHs as sources of DR. An algorithm is presented here which handles the optimization of DR scheduling for normal operation and during contingency events. Dynamic Programming (DP) has been used as an optimization tool. A price signal is developed using OPF calculations to determine the Locational Marginal Price (LMP) of electricity, while sensor data for water usage is also collected. Using these inputs to DP, the optimal control signals are given as output. A market model has been assumed in which distributed DR resources are sold as a commodity on the open market and profits from DRAs as brokers of distributed DR resources can be calculated. In considering control decisions for regulation of transient changes in frequency, IEEE standard 1547 has been used in order to prevent the safety shut-off of inverter-based generation and further exacerbation of frequency droop. This method is applied to IEEE case 118 as a demonstration of the method in practice.

4.1 Introduction

The modern power grid has seen a marked increase in renewable energy generation resources. The intermittent nature of these resources give rise to additional challenges in maintaining grid stability. To design a grid which is secure, a number of factors need to be considered. On a basic level, security is defined as the ability of a certain system configuration to continue to function and withstand a wide range of operating parameters, outside influences, or even subsystem failures. One of these security aspects is related to grid frequency which is very important for inverter-based generations [90, 81]. In the event of contingencies such as short circuits, large changes in load, or loss of transmission lines, the entire system needs to be able to remain operating long enough for the grid operators to restore stability. Maintaining a balance of power is critical to the continued operation of the grid at these times.

In order to increase the capacity to maintain this balance of power, grid operators call upon what are known as AS to provide these changes in power to the grid quickly. CR is one type of AS which is generally split between spinning and non-spinning reserves and are often based on the largest single hazard (generator or transmission capacity). Contingency events are big (many megawatts) and fast (within a few cycles) [95]. As mentioned in chapter 3, DR resources can provide different types of AS [96, 97] or can be used for power resources scheduling [98]. Different types of DR resources that participate in DR programs include industrial [66] and residential [99, 100, 101] equipment.

Different types of DR resources have been utilized in order to provide various AS such as: using active electric vehicles (EVs) to provide spinning reserves [53], using battery systems to provide primary control reserves [102], utilizing battery storage systems to provide multi-ancillary

services including refrigeration appliances (as dynamic demands) to provide primary frequency regulation through an advanced stochastic control frequency regulation and peak-shaving functions [103], using DR through pump scheduling to provide balancing services [101], and using domestic algorithm [104]. The use of DR as a source of AS is a strategy to recover the frequency after the contingencies [105, 80]. An approach was proposed in [106] which all types of loads can participate in DR programs. This approach considered energy and reserve scheduling, simultaneously. In that study, the energy and reserve scheduling were proposed for day-ahead and real-time.

In terms of using DR for voltage stabilization, an approach was presented in [107] for real-time voltage control which uses an emergency DR program that aims at maintaining voltage profile in an acceptable range with minimum cost. This approach is active in emergency conditions where, in real time, the voltages in some nodes leave their permissible ranges. There have been highlights in literature about demonstration projects showing much promise for WHs and battery storage systems as suitable candidates for AS [108]. Energy storage capacity—thermal in the case of WHs and chemical in the case of batteries—allow these systems to delay or anticipate energy consumption. The implementation of suitable optimization and scheduling strategies for these resources becomes a key factor in the successful deployment of these systems as sources of AS. Electric WHs represent a significant source of energy consumption on the modern grid and have the capacity for energy storage in the form of heat. An important characteristic of these resources is that they tend to cycle on and off randomly [109]. The idea is to use these resources by adding another measure of control to when and how these resources present their loads to the grid.

By having the resources work in concert, we are able to optimize and utilize these resources to function as AS providers. For instance, human consumption of thermal energy in the form of hot water comprises 40-60% of the monthly domestic electricity bill in Hawaii. In [110], potential of DRs in Hawaii has been studied in balancing supply and demand on an hourly basis. General Electric, in collaboration with the Hawaii Natural Energy Institute, did a recent study on AS in Hawaii [111]. This study shows that energy storage and DR should be allowed to provide a significant portion of spinning reserve for frequency recovery and mitigation.

Grid-interactive WHs provide many additional benefits to power grids which are increasing generation by renewables. Control over the timing of these loads can be optimized to enhance power quality and regulate grid frequency. By mitigating the harmful effects of the intermittent nature of renewable generation, greater penetrations can be achieved [112]. Wind farms are able to be utilized during windy low-demand periods. Arbitrage value is added by enabling participants to buy and store low-cost energy and sell demand reduction when energy prices are high. Transmission, distribution, and substation upgrades are able to be deferred by reducing peak demands, and a new resource for spinning reserve is added to supplement existing systems and enable the use of only the most efficient generators.

The management of DR is considered to be an important factor in the optimization of power systems. Increases in the proportion of renewable energy generation in power systems strain the flexibility of available systems. The use of DRAs as AS providers has become an important strategy for increasing stability. DRA is the entity which aggregates all the bids of DR contributions from houses that have signed up for this service. This entity then will participate in the DR market with the available amount of DR resources. Once the market is cleared and each

DRA's contribution is determined, DRAs perform an internal optimization to distribute the specified amount of DR among the houses. ISOs and even some governing bodies have incorporated new programs in order to support the participation of consumer side demand flexibility aggregators in order to meet the needs of the modern power grid. As a result, we expect to see the implementation of DR for AS from large populations of small residential loads very soon.

In order to bring these changes, smarter control systems and management approaches must be devised and implemented on a wide scale. With the advent of widespread and reliable communications infrastructure, the interaction of smart appliance networks can be realized and the multitude of devices can act in concert to facilitate the appropriate responses. The bidirectional flow of information and power between utility and customer enables the use of DR components to facilitate crucial services such as peak load shaving, load smoothing, and spinning reserve frequency regulation. With a wide variety of responsive loads at both the utility and residential levels, the pool of resources increases with each step taken toward greater control. When implemented effectively, DR elements can help to improve market efficiency and operational reliability [113].

Models have been shown where DR is used to procure reserve using a short term stochastic security constrained unit commitment [114]. The optimal scheduling of residential appliances and battery storage in consideration of operational and planning constraints has been investigated in [99], where utility goals are considered and integrated into an objective function in order to enhance the approach. In [115], consumer inconvenience is introduced and considered in market-based models. DR can be categorized by price-based and incentive-based types [116].

Different pricing schemes allow flexibility to provide customers with rates which more accurately reflect the price of electricity based on cost of generation and distribution. Price-based DR reacts to fluctuations in real-time prices of electricity to provide the optimum response. Incentive-based DR programs pay the customers to reduce their loads at times requested by the program sponsor. Although the methods are distinct, it would be an interesting question to pose whether qualities and features of both systems may be combined into a hybrid-system with benefits from both sides. Price signaling is based on several factors such as cost of reserve procurement, reliability studies, operational planning, and load forecasting [41].

Different types of energy storage can be used as DR. These can include thermal storage present in WHs or Air Conditioners (ACs), or chemical storage such as that found in electrochemical cells. Grid-interactive WHs are able to be controlled by utilities or aggregators in order to perform several grid services such as DR, grid stabilization, and peak load shaving. In experiments conducted in [117], we see that large tank heat pump WHs and electric resistance WHs can be significant sources of DR. The heat-pump type of WH was shown to be at least 10% more available for DR on average while the electric resistance WHs provided a greater degree of dynamic response and power flow when utilized. Data analysis of results and historical data allow for the definition of an improved price signal which considers the attitude of consumers in combination with financial incentives.

Distributed equipment connected to the grid that is capable of participating in DR can be programmed to process received sensor information and react autonomously based on user-defined policies [118]. Sometimes, these distributed devices are referred to as smart agents. These agents communicate and interact with each other to achieve an optimum aggregate response [118, 119].

Multi agent systems have been successfully applied to several different power grids [120]. The smart agents respond to sensor data and signals in a way that maximizes profit. The actual sensor data and price signals can be used as direct indicators of current grid conditions. In acting to maximize profits, the smart agents naturally stabilize grid conditions and optimize efficiency. This concept can also be described as power matching [120], which can be a major benefit to power grids with a large presence of intermittent renewable energy generation. Specific price signals can be used to generate a schedule for the switching of home appliances to maximize cost savings [121].

Several different algorithms have been proposed by researchers to generate schedules for controllable resources [122, 123] and vary in objective and input, for example: scheduling wind resources and energy storage [124] and a combination of schedules for generators and DR resources [125]. A robust optimization scheduling framework was proposed in [126] which derives optimal unit commitment decisions in systems with high penetration of wind power. This framework incorporated DR programs and bulk energy storage for co-optimized energy schemas in reserve markets. In prior research, several methods to optimize control over DR resources have been proposed [127, 128, 129, 130]. These include direct control and scheduling based on load requirements; market approaches where price signals between competing DR vendors and utility consumers are determining factors; methods of DP and machine learning for predictive algorithms; or static and dynamic security-constrained optimal power flow driven control algorithms. Each of these methods is representative of a distinct and separate approach when presented individually. The innovation which has been proposed in this chapter is to combine these methods and apply dynamic security-constrained optimal power flow, DP, and predictive algorithms to a market-

based approach. Prior work has presented portions of these methods in detail. In this chapter, a method has been presented to tie this work together in order to provide greater consideration for interrelated factors simultaneously such as customer comfort levels, market conditions, and security constraints on the power grid.

The optimization of load commitments is discussed in [131]. The sale of DR reduces the cost of electricity for participants and optimization maximizes the effect of these savings. Special attention is given to the optimization of WHs and battery systems, both of which contribute the majority of demand in household systems. An integrated control system for distributed DR was presented in [132], which is able to shift load appropriately to stabilize the grid throughout the day while also minimizing customer and GENCO costs. The GENCO consists of one or more generation units which meet the load demand. It should be mentioned that a reliable communication network between appliances and DR resource control devices is necessary for the implementation of the proposed algorithm.

A multi-objective energy management system was proposed in [133] which optimizes micro-grid performance for the short term in the presence of renewable energy sources for wind and solar energy generation with a randomized natural behavior. They present DR schedules that were created by considering the optimization and maximal profit for providers. A novel air conditioning system was presented in [134] with proactive demand control for daily load shifting and real-time power balance in the developing smart grid. Its purpose is to effectively use the DR potentials of buildings. Control systems strategies were developed in [135] to provide both immediate and stepped demand reduction through the strategic shutdown of chiller systems. The primary objective of this control strategy is to restrain the building's indoor temperature and maintain as

much indoor comfort as possible even throughout a DR event. This research presented an interesting investigation into the alternation potential for buildings which involve both active and passive cold storages which support DR of buildings connected to smart grids.

This chapter has several contributions in the area of procuring CR from conventional and distributed resources. First of all, generation units, as well as the operation of DR resources, have been optimized to cope with contingencies in order to avoid mass tripping of frequency-sensitive inverter-based generation based on the IEEE 1547 interconnection standard. DRAs compete with each other in an AS market to provide frequency regulation services in a pool market. Electrical data is collected via smart meters. The structure of these meters is presented in this chapter. The configuration of meter interconnection and the data storage infrastructure, which analyze big distributed data, are explained. Once the price signal is available, either before, during or after a contingency, DRAs optimize their resources to satisfy the designated frequency regulation service using DP. DP guarantees the global optimum point for the optimization problem. Since the scale of the problem at the house level is pretty small, DP can be easily utilized to find the optimal point without sacrificing the speed of computation. Therefore, in our case study, DP proves to be a better approach for optimal operation points of DR resources.

In this chapter, LMP has been used for price-sensitive scheduling of DR resources. LMP represents the lowest cost of supplying the next increment of electrical demand at a specific location or node on the power grid. This value takes into account both supply (generation/import) bids and demand (load/export) offers while also considering the physical aspects of the transmission system including transmission and other operational constraints. This system is designed to achieve two economic objectives simultaneously:

- Minimize the cost of generating enough electricity to meet the load; using the lowest cost generators possible given a certain set of constraints.
- Produce an instantaneous price of electricity at every point in the system which will be able to give the instantaneous cost of serving one unit of load at each location.

In this chapter, battery and WH's energy models have been explored and a strategy has been presented to optimize their operation given a signal price. These resources can be scheduled optimally to operate in the normal conditions and provide frequency regulating reserve under contingencies. The price signal is decomposed into contributing signals and each signal is given to a storage device to come up with the optimal operating points. In section II, we discuss how the models presented regulate frequency and the control systems, signals, and equations involved. Section 4.2 is devoted to the discussion of DP and its application to scheduling. Price signal and water consumption are the inputs and the output is a scheduling program. Section 4.3 discusses the practical application of how the proposed strategy works in a complete algorithm that handles non-contingency and contingency scheduling of DR resources. In section 4.4, the practical application of the proposed method has been demonstrated to the IEEE case 118-bus model. In section 4.5, the results are discussed. Conclusions are drawn in section 4.6.

4.2 Dynamic Programming (DP)

DP is a planning tool which addresses the decision-making of an agent in a stochastic environment. Each agent finds the best course of actions not only by using present environment information but also by considering future stages. This tradeoff relieves the problem from myopic

attainments among a set of interactive actions and presents an efficient sacrifice between immediate and future costs. The transition probability from state i to state j, denoted by p_{ij}, solely depends on the current state i and the taken action u which is a Markov property:

$$p_{ij} = f(i,u) \tag{4.1}$$

A discrete time dynamic system is defined as:

$$x_{k+1} = f_k(x_k, u_k, \omega_k), \quad k = 0,1,...,N-1 \tag{4.2}$$

The state x_k goes to state x_{k+1} following the action $u_k \in U(x_k)$ with probability $\omega_k \in P(\cdot|x_k, u_k)$. The class of control laws make up an admissible set of policies $\pi = \{\mu_0, ..., \mu_{N-1}\}$, where μ_k maps state x_k into control laws $u_k = \mu_k(x_k)$. The admissible set of control laws differ from state to state. For example, in the case of WHs, when the temperature is at its maximum point, the switch-on action is not an eligible state since it will take the temperature above the comfort range. The state transition is probabilistic in general, meaning the next state depends on other factors rather than the control variable. Again, in the case of WHs, switching on the heater will produce the next temperature state according to the hot water draw probability. Another example is battery storage where the charge/discharge command determines the next SOC in a deterministic manner. For every initial set of conditions $J_0(1),..., J_0(n)$, the sequence $J_k(i)$ proceeds backward in time from period $N-1$ to period 0, generated by the iteration:

$$J_{k+1}(i) = \min_{u_k \in U(i)} \left\{ g(i,u) + \sum_{j=1}^{n} p_{ij}(u) J_k(j) \right\} \tag{4.3}$$

Therefore, the cost of each state is calculated at all time steps in the optimization time horizon. In other words, $J_k(i)$ gives the optimal cost starting from state i of a k stage problem, with cost per stage given by g and a special cost-free termination state.

DR resources are considered agents in a stochastic/deterministic environment. Optimal operation points are obtained using DP. In the next part, a model of these resources are explained and the required parameters to formulate the optimization problem in the DP framework are presented.

4.2.1 Modeling of storage devices

4.2.1.1 Battery

Batteries are used as a storage for transferring energy from the grid at different time intervals. Since there is little control over the generation of electrical energy from renewable resources, storage is employed to add flexibility to the dispatch of electrical power. The equations governing the operation of a battery are the same for utility scale and small units and are given by:

$$E_{t+1} = E_t + P_t \Delta t \tag{4.4}$$

$$SOC_{t+1} = SOC_t + \frac{P_t \Delta t}{E_{tot}} \tag{4.5}$$

The power flow at each time step is constrained by the nominal power and SOC constraints:

$$P_t < \min\left\{\frac{\left(SOC_{\max} E_{tot} - E_t\right)}{\Delta t}, P_{nom}\right\} \tag{4.6}$$

$$P_t > \max\left\{\frac{\left(SOC_{\min} E_{tot} - E_t\right)}{\Delta t}, -P_{nom}\right\} \tag{4.7}$$

In the above relations, SOC_t, P_t, and E_t denote state of charge, power flow, and energy of battery at time *t*. Nominal power and capacity of battery are represented by P_{nom} and E_{tot}, respectively.

Δt is time interval. The state propagation is calculated by (4.5) using the given commands and the set of allowable actions at each state is limited by (4.6) and (4.7). The immediate cost $g(i,u)$ depends on the electricity cost at time *t*. After the values of all states are calculated for all time stages, the optimal SOC trajectory (SOC_{opt}) is found by following the optimal action from the state in the last stage with the minimum cost.

$$SOC_{opt}(N) = \arg\min J_N(j) \quad j = 1,2,..,n \tag{4.8}$$

$$SOC_{opt}(t-1) = SOC_{opt}(t) + \frac{P_{opt}(t)\Delta t}{E_{tot}} \tag{4.9}$$

Where P_{opt} is the optimal power of the battery.

4.2.1.2 Water Heater (WH)

The WH is modeled as a single heating element which heats up a nominal mass of water in the tank shown in Fig. 4.1 [136].

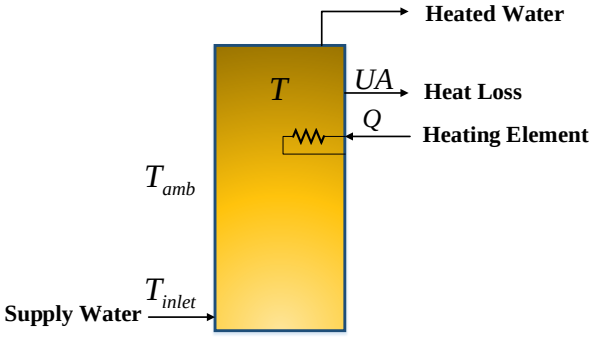

Figure 4.1: WH model as a single heating element *[136]*

The water temperature changes according to the heat applied via the thermal element:

$$M.SH_W.\frac{dT}{dt} = UA.(T_{amb} - T) + Q \tag{4.10}$$

M is mass of water in the tank (*lb*), SH_W is the specific heat of water ($BTU/lb/°F$), and *T* is temperature of the water in the tank ($°F$). Parameter t shows the time (hours), *UA* shows the standby heat loss coefficient times the area of the storage tank ($BTU/°F/hr$), and Q is rate of heat input to the tank from the heater (BTU/hr). Q is zero when the heater is off. T_{amb} is ambient temperature.

When water is drawn from the outlet, the same volume of inlet water with temperature of T_{inlet} refills the tank and the final temperature (T_{new}) is given by:

$$T_{new} = \frac{T_{curr}.M_{curr} + T_{inlet}.M_{inlet}}{M_{curr} + M_{inlet}} \tag{4.11}$$

The probabilistic nature of state changes arises from stochastic hot water draw. The new state, T_{new}, is calculated to find the next state transition for cases of hot and cold water mixing. Once all the state values for all the time stages are obtained, the optimal trajectory is found by following the optimal action at each time step moving backwards. The following equations present the optimal state at final and other time stages.

$$T_{opt,N} = \arg\min J_N(j) \quad j = 1,2,...,n \tag{4.12}$$

$$T_{opt}(t-1) = \sum_{j \in T_{opt}(t)} p\left(j, u_{opt}(t)\right) T_{opt}(t) \quad t \neq N \tag{4.13}$$

Parameters $T_{opt,N}$ and $T_{opt}(t-1)$ are the optimal temperature values at the final time stage and at $t-1$, respectively.

Therefore, in this study, the DP scheduling block acts like a block with two inputs (price signal and hot water usage) and one output (scheduled program for WHs and batteries). The temperature

states are obtained in equations (4.12) and (4.13). The calculations have been performed through MATLAB programing. The states are coded in m-file and the objective function is calculated at each state considering the constraints imposed at each state.

4.3 Methodology

Fig. 4.2 shows a general schematic of the proposed method on how end-users of electricity can participate in DR programs in contingency situations in order to regulate the frequency. During normal operations, the GENCO provides a price signal which, in combination with data from water usage, is input into DP and outputs a schedule for DR resources. This schedule is processed into individual control signals and sent to the devices throughout the power grid. In a major contingency, when the grid frequency drops below 57 Hz, all available DR resources shut off instantly to mitigate frequency droop as quickly as possible. For a minor contingency, the DRAs determine how much load needs to be shed in order to recover the frequency. In both contingency events, a modified contingency price signal is provided for DP and resources are scheduled accordingly.

The amount of frequency drop is relevant to the amount of power loss during contingency. The presented method not only works for the most common contingency criteria, which is *N-1*, but also is valid for other contingency criteria such as *N-2* and above. The reason is that the amount of power is calculated which is required to compensate for the frequency deviation. The power required for frequency regulation can come from either one or more generating units.

More details of the proposed method have been provided in the algorithm of Fig. 4.3. The scheduling algorithm begins with local frequency measurement at each of the individual

aggregator nodes. If the frequency is above 59.5 Hz, it is considered to be within the tolerance of normal range. During normal conditions, the non-contingency price signal and water consumption rates are used as inputs for DP, as described in section 4.2 above. Different price signals for non-contingency and contingency can be visualized in Fig. 4.4 below in section 4.5.

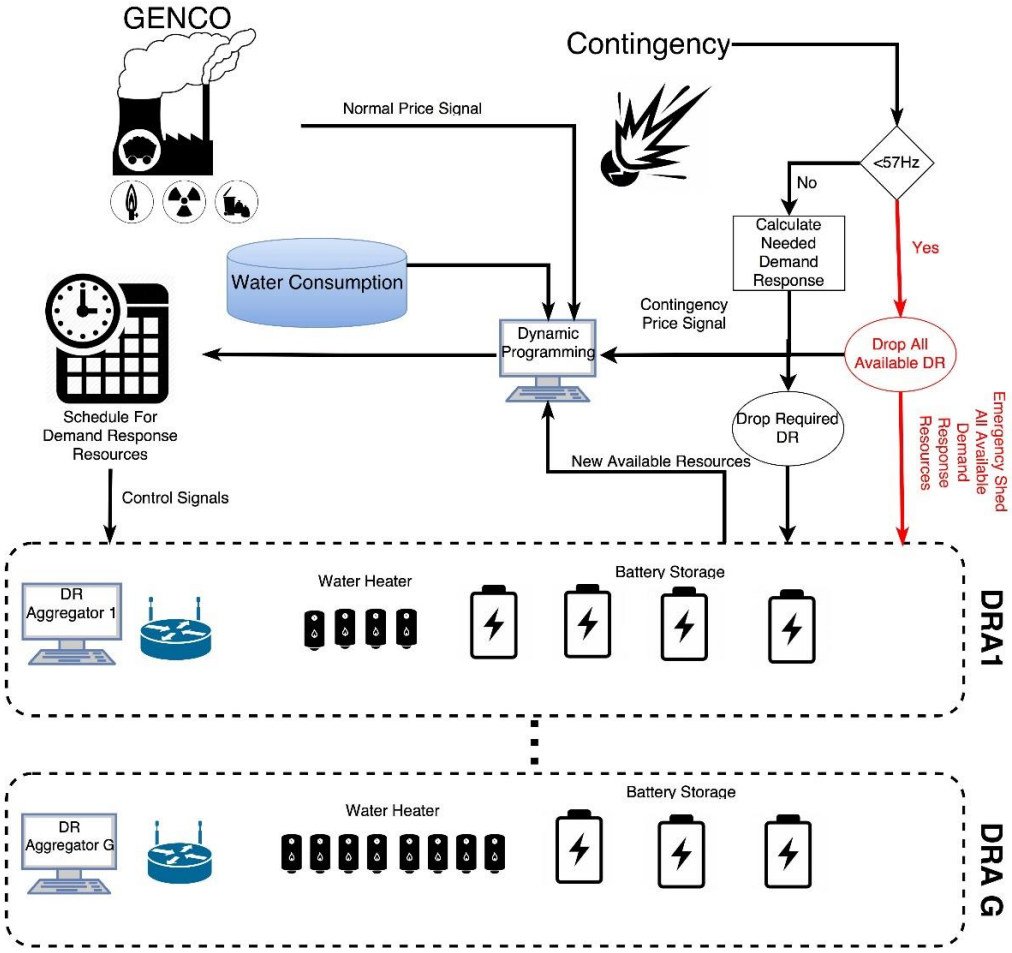

Figure 4.2: Proposed scheduling method overview

In fig. 4.4, the distinction is obvious between contingency and non-contingency price signals during the interval between 18:30 and 19:45 p.m. The output from DP gives us an optimized schedule for WHs and battery storage systems. Aggregators' profit for the sale of DR to the GENCO can be calculated based on price signal and demand scheduling for loads. The results can

be seen in section 4.5, where we see that the different scheduling outputs depend upon whether there was a contingency event or not.

During a contingency event, the measured frequency drops below 59.5 Hz. Contingency events are grouped into two major categories: major and minor contingencies. A major contingency occurs when grid frequencies drop below 57 Hz. This is considered the major threshold. Inverter-based generation from renewable energy sources are set by industry safety standards to switch off at these frequencies and can possibly exacerbate the contingency and lead to further frequency droop (based on Table 3.1).

It is, therefore, desirable to implement mitigation strategies as quickly as possible during these events. The control sequence for major contingency events is designed to react as quickly as possible and sheds all available controllable loads immediately. Calculations are then performed to determine how much power is required (P_{req}) to recover the frequency back within its operating range (using equation 3.4). Each aggregator sends data about how much load was shed to the GENCO. The GENCO then performs OPF calculations and is responsible for recovering the rest of the frequency using conventional spinning reserve and AS.

A minor contingency event occurs when a frequency of between 57 and 59.5 Hz is detected. During this type of contingency, there is more time available (300 seconds based on the IEEE 1547 standard) to calculate an optimum response. First, the amount of power necessary to recover the frequency is calculated. DRAs throughout the network communicate and work collectively to determine the total amount of DR available between all nodes. If the amount of DR required to recover the frequency is more than the amount available, then all available resources are

immediately switched off and the GENCO then handles the remaining frequency recovery. If there are more resources than are required, then the first available resources spread between all aggregators are switched until the sufficient amount of load is shed.

The frequency measurement is then updated. Until the contingency has cleared, DR resources are cycled to maintain social welfare. Previously unavailable and non-participating DR resources are switched out with the initially utilized resources as they become available for use. In this way, inconvenience and discomfort are minimized for individuals as the burden is distributed among all resources. Green arrows of the flowchart in Fig. 4.3 are related to switching the devices during the contingency. Once the contingency has cleared, DR resources are scheduled based on the new price curve. Once resource scheduling has been established, the profits for each aggregator are calculated.

4.4 Case Study

As a standard case study, the IEEE 118-bus model has been simulated in this chapter. The technical data of the buses, branches, and generators are available in MATPOWER's library [94]. This case study has 54 generators. The worst case contingency is the loss of the largest generator (located in 69^{th} bus with capacity of 516.4 MW). Table 4.1 shows the information of some of the larger DRAs, including location, capacity, and number of houses. In this case study, it has been supposed that each house has a WHs with a capacity of 10 kW and that half of the houses are equipped with batteries that have a capacity of 5 kW. It has been supposed that 60% of the residential house loads are related to thermostatic storage loads such as WHs.

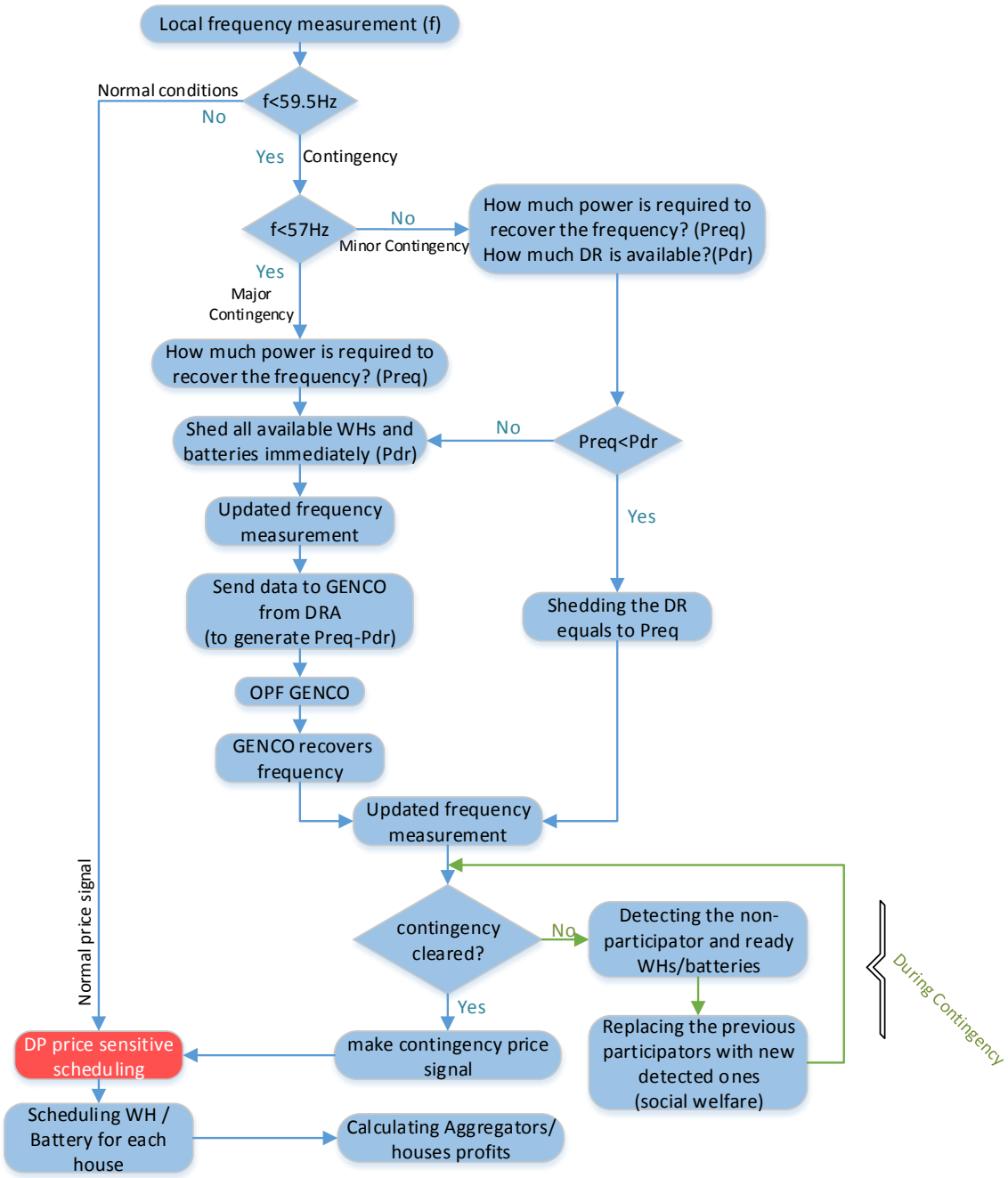

Figure 4.3: Scheduling algorithm

Table 4.1: Some of large DR aggregators' data of the IEEE 118-bus model

DRA location (bus #)	Total load (MW)	Number of houses	WHs	Storages	Other devices
11	65.79	3432	3432*10kW	1716*5kW	3432*6.67kW
15	84.59	4413	4413*10kW	2206*5kW	4413*6.67kW
27	66.73	3482	3482*10kW	1741*5kW	3482*6.67kW
54	106.21	5541	5541*10kW	2770*5kW	5541*6.67kW
59	260.33	13582	13582*10kW	6791*5kW	13582*6.67kW
80	122.18	6370	6370*10kW	3180*5kW	6370*6.67kW
90	153.20	8000	8000*10kW	4000*5kW	8000*6.67kW
116	172.94	9020	9020*10kW	4510*5kW	9020*6.67kW

The parameters related to the control loop model of the grid are: τ_g =0.2sec, τ_T =0.5sec, D=0.8, R=0.05 per unit, H=5sec and the open-loop transfer function will be:

$$\frac{\Delta\Omega(s)}{-\Delta P_L(s)} = \frac{0.1s^2 + 0.7s + 1}{s^3 + 7.08s^2 + 10.56s + 20.8} \tag{4.14}$$

4.5 Results and Discussion

In the mentioned case study, after losing the largest generation, the frequency drops more than 3 Hz and a major contingency takes place based on the algorithm of Fig. 4.3. Therefore, all of the available DR are shaded by the control signal of DRAs immediately, and the frequency rises a little bit. Next, the GENCO recovers the frequency completely using spinning reserve. It has been assumed that the whole available DR resources are 206 MW (20% of the demand in DRAs), which are ready to shed immediately after contingency according to the communication between houses and DRAs. The amount of ready DR resources is obtained using the communication device, which

has been explained in Appendix B of this thesis which is based on Internet-of-Things (IoT). Thus, the GENCO's contribution will be to provide 310.4 MW to recover the frequency completely.

Based on the algorithm in Fig. 4.3, a major contingency has been occurred, thus, DRAs have to shed all of their ready DR resources to regulate the frequency. In this case, it has been assumed that the contingency takes 1.25 hours from 6:30 p.m. to 7:45 p.m. Fig. 4.4 shows both price signals (LMPs) for normal conditions and the worst case contingency in the location of the largest load (bus 59). During the contingency, DRAs can participate to make a balance between supply and demand to regulate the frequency. It not only prevents the activation of the less efficient and more expensive generators but also makes profits for participating DRAs.

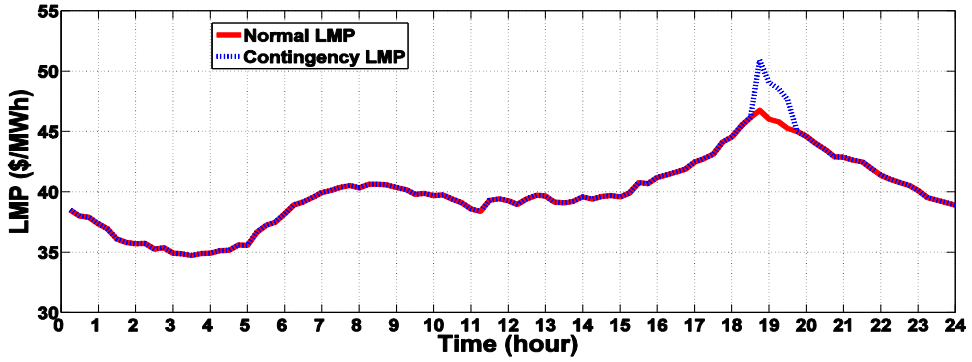

Figure 4.4: LMP signal for both normal and contingency conditions at bus 59 of case study

Using the algorithm in Fig. 4.3 and the DP scheduling block (section 4.2), residential batteries and WHs are scheduled based on the contingency price signal. Fig. 4.5 shows the scheduling of batteries for each house connected to the 59th bus, which is ready to participate in the DR program. This figure demonstrates the SOC of the battery during a period of 24 hours. In this case study, the nominal capacity of the battery is 5 kW.

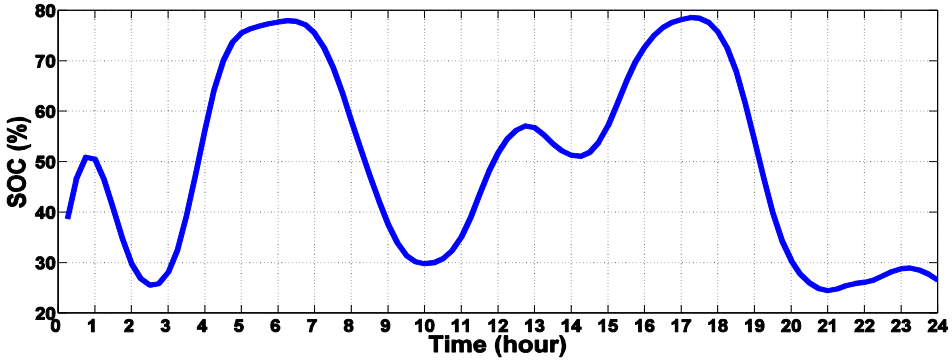

Figure 4.5: Changing of the SOC in the batteries at load bus 59 of the case study in contingency

Fig. 4.6 shows the charging and discharging of the battery in each house of the 59th bus using DP. Clearly, during the contingency or expensive electricity times, the battery discharges and does not receive any energy from the grid. Scheduling results for each house's WH (at bus 59) are presented here for two different seasons: summer with an inlet temperature of 85°*F* and winter with an inlet temperature of 75°*F*. The allowed range of the water temperature is between 120 and 140 °*F*. Fig. 4.7 shows the average usage of hot water in each house connected to bus 59 during one day, which is one of the inputs of the DP scheduling block.

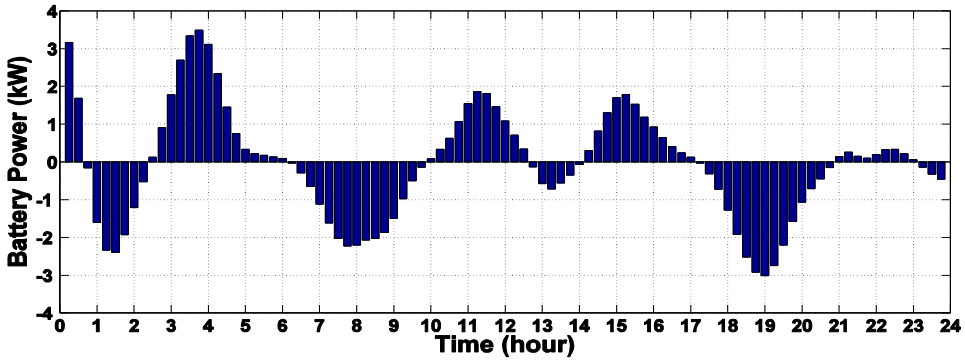

Figure 4.6: Charging and discharging of each house's battery at load bus 59 of the case study in contingency

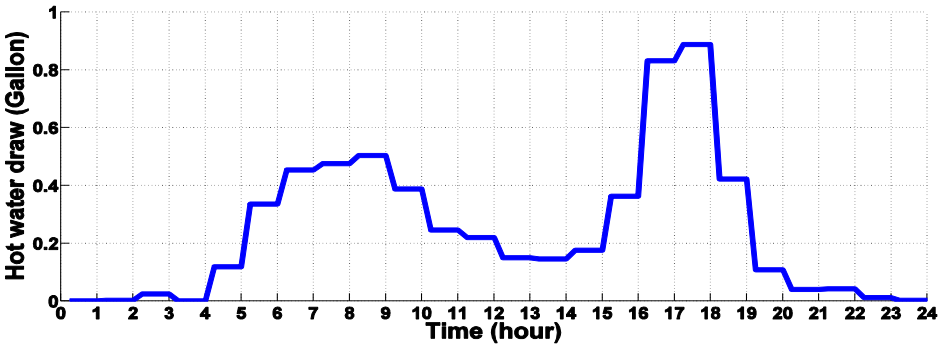

Figure 4.7: Average usage of hot water in each house at bus 59 of the case study during one day

Figs. 4.8 and 4.9 show the water temperature during summer days and winter days based on hot water consumption and WH schedules.

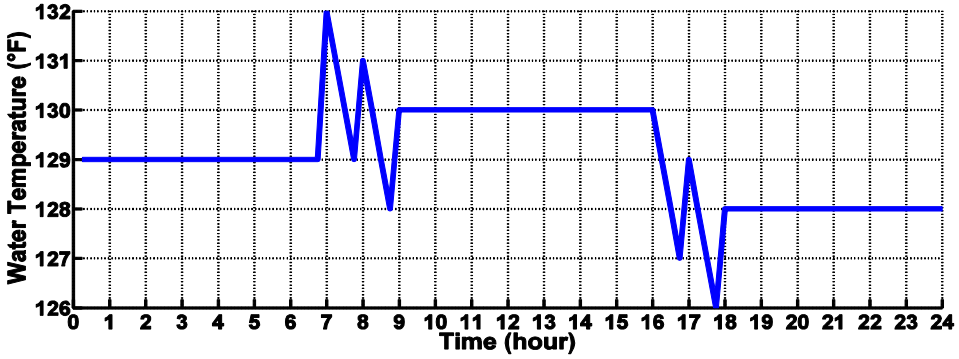

Figure 4.8: Water temperature of each house at bus 59 of the case study during summer days (85 °*F*)

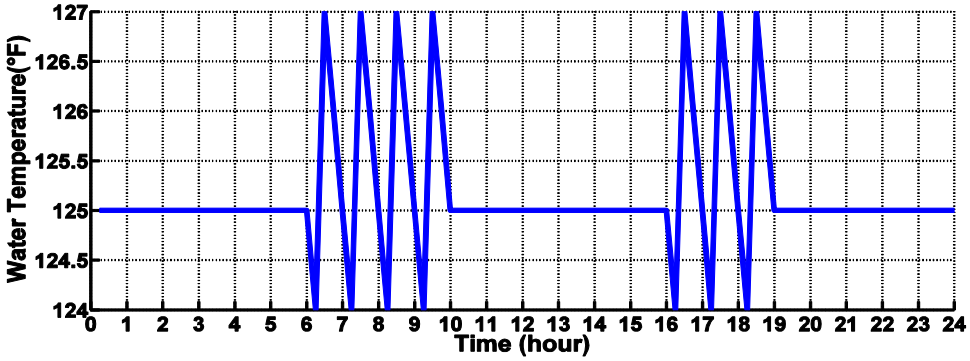

Figure 4.9: Water temperature of each house at bus 59 of the case study during winter days (75 °*F*)

Figs. 4.10 and 4.11 show the scheduling program for each house's WH during the summer and winter days, respectively. The participation of the available WHs have been considered to regulate the frequency after the worst case of contingency in the case study. In this situation, the contingency price signal (LMP) has been used as the input of the DP scheduling block rather than the normal price signal.

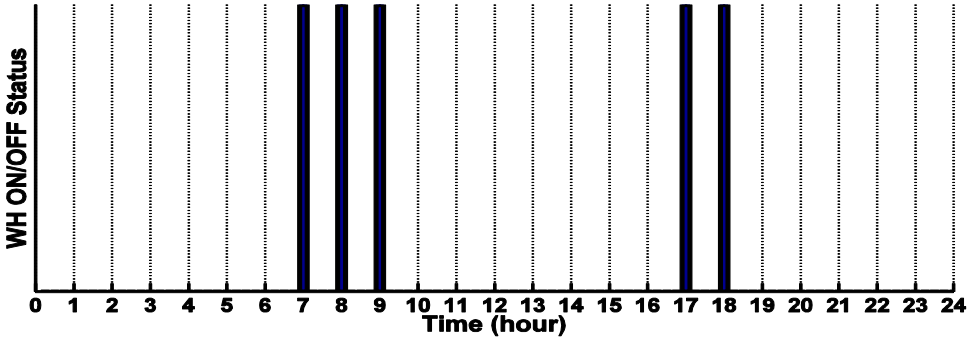

Figure 4.10: Scheduling program of WHs at bus 59 of the case study during summer days (85 °*F*)

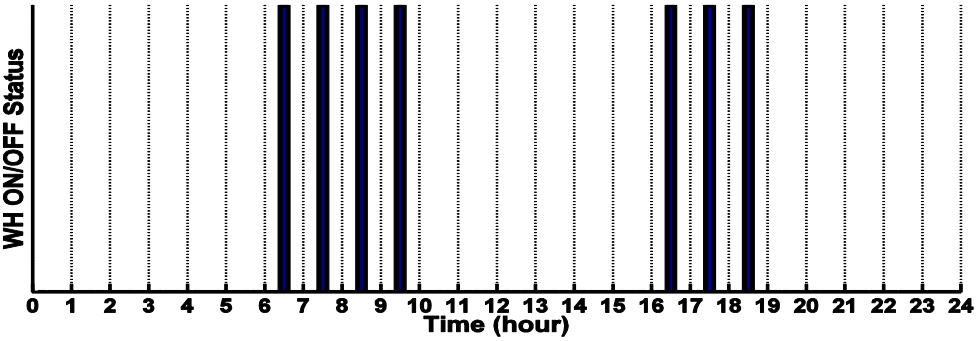

Figure 4.11: Scheduling program of WHs at bus 59 of the case study during winter days (75 °*F*)

The above figures show the most optimized time intervals, in which the WHs connected to the 59th bus of the case study should be turned on during 5 and 7 intervals in the summer and winter, respectively. These optimized scheduling programs not only satisfy the condition of maintaining social welfare by keeping the water temperature within a given range [120°*F*, 140°*F*], but they also allow the WHs to optimize their usage times to shift them into time

intervals when electricity is cheaper (based on time-of-use pricing). It allows the majority of the WHs to participate in DR to regulate the frequency in contingencies. In order to calculate the profits of the participating DR resources, the area under the contingency LMP curve in Fig. 4.4 is calculated. During contingency and the absence of DR participation, the cost spent to regulate the frequency by the GENCO ($C_{reg}^{no,DR}$) is:

$$C_{reg}^{no,DR} = A_{LMP} \times P_{lost} \tag{4.15}$$

A_{LMP} is the area under the contingency LMP curve in Fig. 4.4 ($/MW), and P_{lost} is the lost power in contingency (MW). In this case study, $A_{LMP} = 60.45$ and $P_{lost} = 516.4$. Without the presence of DR, the GENCO should pay $\$31{,}216$ to regulate the frequency due to the contingency. Since the DRAs' contribution is 206 MW in the case study, the GENCO pays $(516.4 - 206) \times 60.45 = \$18{,}764$ and would also burn less fuel with the added contribution to system efficiency from DR. On the other side, a portion of profit $(206 \times 60.45) = \$12{,}453$ is divided between the DRAs (or houses) based on their contribution in shedding their loads in providing CR services to regulate the frequency.

Loss of the largest generator (located in the 69th bus with a capacity of 516.4 MW) is a major contingency which has been described with detailed results. Two different contingencies have been analyzed here including: losing a small generation like a distributed generation located in the 54th bus with a capacity of 48 MW (as a minor contingency) and losing two large generators simultaneously (as a major contingency). These large generation units are located in the 10th and 66th buses with capacities of 450 and 392 MW, respectively. It has been assumed that these two mentioned contingencies took place at the same time as the first contingency (6:30-7:45 p.m.) and

that the availability of the DR resources is 20% of the DRAs' connected loads, as shown in Table 4.1.

In the minor contingency, the required power for recovering the frequency (P_{req}) is 48 MW, which is much less than the available DR resources (206 MW). Therefore, there is no need for the GENCO to inject power to the grid. A portion of the ready DR resources (based on the priority) sheds the loads immediately after detecting the frequency drop to participate in the frequency regulating AS market. The normal and contingency LMP of this contingency at the location of the largest load (59th bus) are shown in Fig. 4.12. Scheduling of residential storages and WHs follow the same approach as described and will be the same as Figs. 4.6, 4.10, and 4.11. In this contingency, $A_{LMP} = 57.81$ and $P_{lost} = 48$. Without the presence of DR, the GENCO should pay \$2,775 to regulate the frequency fluctuation stemming from the contingency. Since enough DR resources are available to shed the loads, the GENCO can save money without any extra payment in comparison with the normal situation. A portion of this profit (\$2,775) is divided between the residential participants.

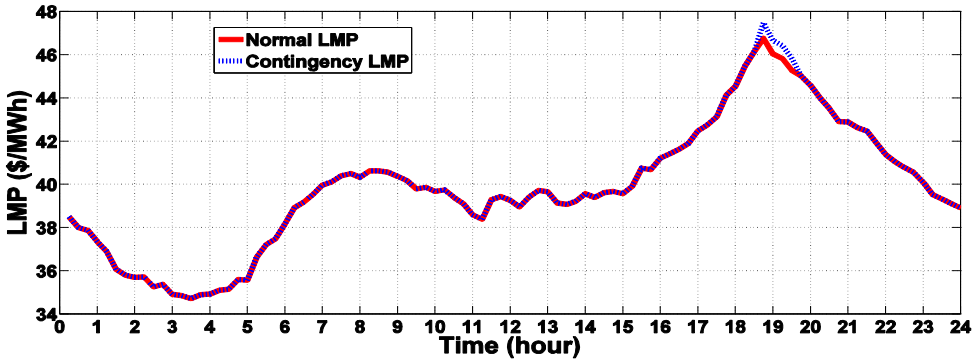

Figure 4.12: LMP signal for normal and contingency conditions at bus 59 of the case study – the 2nd contingency (loss of one small generation)

In the case of two contingencies occurring simultaneously, the required power for recovering the frequency (P_{req}) is 842 MW, which is more than the 206 MW of available DR resources (major contingency). Both the GENCO and DR resources participate in the frequency regulating AS market. The normal and contingency LMP of this contingency at the location of the largest load (59^{th} bus) are shown in Fig.4.13. Based on the shown contingency LMP, storages and WHs are scheduled similarly to Figs. 4.6, 4.10, and 4.11. In this contingency, $A_{LMP} = 63.13$ and $P_{lost} = 842$. Without the presence of DR, the GENCO should pay $\$53{,}155$ to regulate the frequency. Since the DRAs' contribution is 206 MW in the case study, the GENCO pays $(842 - 206) \times 63.13 = \$40{,}151$ and would also burn less fuel with the added contribution to system efficiency from DR. On the other side, a portion of profit $(206 \times 63.13) = \$13{,}005$ is divided between the DRAs (or houses) based on their contribution in load shedding in providing CR services to regulate the frequency.

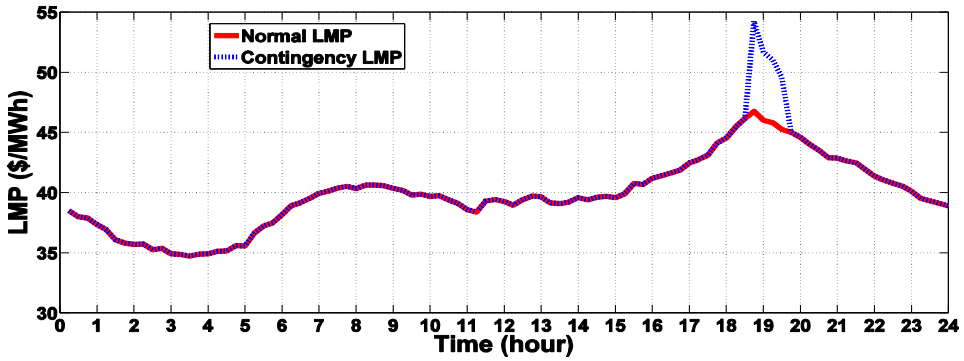

Figure 4.13: LMP signal for normal and contingency conditions at bus 59 of the case study – the 3rd contingency (loss of two large generations)

4.6 Conclusions

Use of DR has been a good strategy in providing AS in the power grid. One of these services is CR. Any fault in the grid, like a loss of a generator, transmission lines, etc. requires immediate

response by the utility to mitigate harmful consequences. Using DR for this purpose not only can compensate for the power shortages during contingencies and decrease the amount of spinning reserve needed by the utility but participants of the DR program can also make profit based on their contribution. On the other hand, using DR resources in contingencies helps the utility to turn off low efficiency generators to decrease pollution and save money.

Since a high percentage of energy demands include storages (such as batteries and WHs) and also because of the nature of these devices (having delays), which are appropriate to use in lieu of reserves, a model was proposed in this chapter to schedule these devices by using DP in an effort to regulate the grid frequency under contingencies. Based on the increasing presence of inverter-based generations, the transient behavior of grid frequency is extremely important to control in order to avoid tripping the safety mechanisms of the inverters and exacerbating the instability problems. These dynamic issues are considered in this study based on IEEE standard 1547.

Chapter 5

Game-Theoretic Model of Demand Response Aggregator Competition for Selling Stored Energy in Storage Devices

Abstract

This chapter is primarily concerned with the construction of a theoretical model of the competition between DRAs for selling energy previously stored in an aggregation of storage devices (which the aggregator manages) given sufficient demand from other aggregators through an incomplete-information game (*i*-game). The model culminates in a game-theoretically justifiable decision making procedure for the sellers which may be used to predict and analyze the bids made for energy sale in the market. The methodology for applying the model is worked out in detail for a three-aggregator case where two players compete with each other for sale to a third. Relevant numerical data for the competition is taken from a real case study which took place on the island of Maui, Hawaii. This market framework is presented as an alternative to the traditional vertically-integrated market structure, which may be better suited for developing DR and smart grid technologies. Two non-cooperative games have been considered with different market conditions: one competition with no limitation, and one a Stackelberg competition subject to limitations on transaction price and size, each separately with and without inclusion of demand scheduling (the focus is on significant load-bearing thermostatic storage devices such as WHs, though the principles should be applied generally). Determining the optimal bidding strategies follow the same procedure, and the equilibrium bidding strategies of all others are determined by each player in each case and demonstrates the wide applicability of our methods in each case. Demand scheduling offers greater payoff for aggregators who implement it, compared with those who do not. Addition of transaction price and power quantity regulations to the market lowers payoffs for all aggregators participating in the market relative to competition with no limitation.

Nomenclature

C_h^{bat} discharging cost of battery in house *h*

ΔE_h discharging energy of battery in house *h*

ΔP_h discarding power of battery in house *h*

t time interval for updating load data

C_h^{grid} charging cost of battery in house *h*

$C_h^{C\&M}$ capital/maintenance costs of battery

C_i cost function of aggregator *i*

P_i aggregated stored power in aggregator *i*

(a_i, B) coefficients of cost function (players' types)

λ_i marginal cost of aggregator *i*

λ_{0i} marginal cost of electricity at P_{0i}

m_i slope of bid curve (players' strategies)

R_i payoff of player *i*

ϕ spot market price

T_i transaction power for aggregator *i*

R_{seller} seller aggregator's payoff

R_{buyer} buyer aggregator's payoff

t_A^m , t_B^n types *m* and *n* in players *A* and *B*

π_{mn} probability distribution of *A*'s type *m* and *B*'s type *n*

ε_S players' strategy

EP_A^m, EP_B^n expected payoffs of players *A* and *B*

$\eta_A^m(n), \eta_B^n(m)$ conditional probabilities of players *A* and *B*

H_A^m , H_B^n conditional payoffs of players *A* and *B*

s_A^m, s_B^n strategies of players *A* and *B*

Ψ_A^f , Ψ_B^f probability distributions of players in scenario *f*

WH_{off} , WH_{on} on/off status of water heaters

$elec_{ch}$, $elec_{\exp}$ price status of grid electricity (cheap, expensive)

ϕ_T transaction price

P_A , P_B stored power in aggregators *A* and *B* for selling

L_C power purchased by aggregator *C*

5.1 Introduction

Development of smart grid technologies offers substantial advantages (for all parties involved) over traditional vertically integrated electric utilities [137, 138, 97]. Demand Side Management (DSM) programs have been developed to use the available energy resources more efficiently without installing new generation and transmission infrastructure. In many of the deployed DSM programs (e.g., in [139, 140, 141]), the main focus has been on interactions between the utility company and end users. Due to the recent advancements in smart grid technologies especially in terms of two-directional communication between utility and end-users [142, 143, 144], the interactions between users do not have to be manual, but can be automatic through two-way digital communication.

In this chapter, a market framework has been developed based on game-theoretical concepts where DRAs compete with each other to sell energy stored in consumers' storage devices. Our model determines the optimal bidding decision for each DRA to maximize its own payoff despite incomplete information in the game and significant variations in prevalent market conditions.

Game theory has been used in power system markets to interpret a participant's behavior in deregulated environments and to allocate costs among pool participants [145]. Two different hybrid algorithms were presented in [146, 147] for the generation expansion planning problem for a pool-based electric market where the modified-game-theoretic algorithms were divided into two programing levels: master and slave. A static computational game theoretic model has also been developed in [148] to investigate the impacts of competition on the wholesale price of electricity, the demand for electricity, the profits of firms, and levels of various polluting emissions. The most common electricity bidding mechanisms in electricity auction markets were analyzed using

signaling game theory [149] and also a Swarm platform was used to develop a simulation model based for multiple agents.

The role of sustainable energy volatility was investigated in the context of market participant's competitive expansion planning problem in [150]. An incomplete information non-cooperative game-theoretic method where each GENCO perceives strategies of other market participants was applied to make decisions about strategic generation capacity expansion. A practical program was proposed in [151] for charging scheduling of plug-in hybrid EVs based on game theory, aiming at optimizing customers charging cost. In another research work, a game approach was presented in [152] to formulate the charging problem of plug-in hybrid EVs to jointly optimize the cost of the utility company and payoff of the customers.

There are other applications of game theory in literature for energy and power markets. For instance, developing a dynamic game-theoretic model in [153] in natural gas and electricity markets, prospering a next-generation retail electricity market in [154] with high penetration of distributed residential electricity suppliers, and presenting a game-theoretic framework in [155] for economic operations of future residential distribution systems.

Game theory is an appropriate mathematical tool to solve many of the problems in DSM [156]. Several game-theoretical DR programs have been proposed with different objectives such as: determining the optimal hourly incentive to be offered to customers who sign up for load curtailment [157, 158], managing the demand in smart energy hubs [156, 159, 160], adjusting demand to meet supply, as well as smoothing the aggregated load in the system [161], and evaluating the impact of the response capability of smart-home consumers on promoting further

distributed PV penetration [162]. An optimal time-of-use (TOU) pricing with an evolutionary game-theoretic perspective was proposed in [163] for urban gas markets where a power structure DR program was employed to simulate user demand response.

An energy management technique was proposed in [164] for electricity and natural gas networks based on integrated DSM which hubs were formulated as a non-cooperative game. Game theory has also been used to improve strategies of Decision-Making (DM) in energy markets [165, 166]. Basically, Game theory is the formal study of DM under competitive conditions where choices potentially affect the interests of the other players [167, 168, 169]. For example, a game theoretic modeling approach was performed in [170] to develop financial transmission rights bidding strategies for power suppliers assuming that they have adequately forecast locational marginal prices. The game theoretic model considered multiple participants as well as network contingencies.

In another work, an evolutionary imperfect-information game approach was proposed in [171] to analyze bidding strategies in electricity markets with price-elastic demand. The research work presented in [172] characterized the impact of long-term plans on short-term maintenance decisions of GENCOs by applying the Cournot model, which has been used for strategic generation dispatch of generating units in electricity markets. Authors of [173] studied electricity users' long-term load scheduling problem and modeled the changes of the price information and load demand as a Markov decision process. Markov perfect equilibrium of a fully observable stochastic game with incomplete information was used in [173] to approximate the users' optimal scheduling policy.

Different types of games have been utilized for analysis of different types of problems in energy and power market. Games' types are categorized by number of players involved, symmetry of the game, and whether or not, cooperation among players is allowed. In the literature for power markets, the different game models used include: cooperative [174, 175, 176, 177], non-cooperative [162, 178, 179, 180], Stackelberg [181, 182, 183], multi-leader-follower [181], Forchheimer (one leader) [184], and Bertrand games (all players are leaders) [184]. Beside the these application, game theory has been used in diverse, and other related fields such as: analysis of EV charging station construction [185], charging method for plugged in hybrid EVs [186], analysis of power grid vulnerability [187], performance evaluation of thermal power plants [188], analysis of effects of higher domestic gas prices in Russia on the European gas market [189], and interactive energy management of networked microgrid-based active distribution systems [190].

Several research game theory has been utilized to develop market frameworks for managing demand and benefit customers at demand side [191, 155, 154, 138]. Game theory was utilized in [144] to formulate an energy consumption scheduling program where the players were the users and the strategies were the daily schedules of the residential appliances and loads. In the proposed DSM strategy in [144], each user applies its best response strategy to the total load and tariffs in the power distribution system.

A distributed game was proposed in [192] where energy is traded between multiple smart grid users. Sellers make profit by selling their surplus of energy stored in storage devices such as EV batteries. A distributed DSM method was presented in [179] intended for end users with load prediction capabilities, who possibly employ dispatchable energy generation and storage devices. These users participate in the day-ahead market and are interested in deriving the bidding,

production, and storage strategies that jointly minimize their expected monetary expense. A non-cooperative game was proposed in [180] to model a smart grid environment with a high penetration of residential storage devices. In [180], by using an appropriate electricity price structure, the electricity supplier influences residential electricity consumption.

In this chapter, a DR market framework has been developed based on game-theoretic considerations. In this market, the commodity is the aggregated energy stored in consumers' batteries. End-users of electricity charge their batteries when the electricity is cheap and sell it back to the grid (or other consumers) when the electricity is more expensive. There are four basic concepts in game theory including: players, nodes, moves, and payoffs. In the proposed market framework, the players are DRAs and each node belongs to one DRA. The possible moves of the game are the players' decisions–i.e.: any of the options chosen by a given DRA. A player's strategy will determine the action the player will take at each stage of the game. In the proposed market structure, strategies are different biddings of DRAs. The payoff to each player (DRA) is the difference between monetary gain upon selling its stored energy and the cost of storing that energy.

A comprehensive quadratic cost function has been proposed in this chapter for discharging the energy stored in batteries. In this study, a situation has been considered where players are not aware of other players' moves as it is close to the situation that would prevail in actual competition. Therefore, our proposed method models an *i*-game. Two different varieties of non-cooperative game are considered here: simple competition with no constraint; and competition with enforced market regulatory limitations on transaction size and price which we model as a Stackelberg game.

In these non-cooperative games, each aggregator can make a bidding decision (through an unregulated or regulated game) in order to maximize its own payoff. Therefore, a non-cooperative game accurately reflects the competition between the sellers. In the first game, DRAs compete to sell the energy stored in the batteries without any limitation or constraints on transaction size or price; but in the Stackelberg variety of competition we consider an additional player, the game leader (organized by the utility), which may move in such a way that other players transactions are not allowed to take place if the size and price do not fall within certain preset boundaries [193]. In each game, two different DR programs are considered: non-scheduled demand and price-sensitive scheduling of WHs (or all thermostatic storage devices). DP has been used for price-sensitive scheduling [137].

The novelty of the proposed method in this chapter is that we consider competition between DRAs to sell energy stored in the residential storage systems thereby allowing independent energy producers, and anyone capable of storing energy with the desire to sell it to participate in the market through participation in a DRA program. An *i*-game model has been proposed to find the optimal bidding strategy of each DRA with the objective of maximizing players' expected payoffs. In order to calculate the payoff of a given DRA (as a player of the game), the cost function of the player is required which this cost function has been proposed in this chapter. Each DRA's cost function depends directly on the discharging cost of the battery storage systems it manages.

Clearly, considering a game that each player knows the information of other players (complete-information game, *c*-game) is unrealistic. Therefore, another advantage of this work is that we have considered a more realistic model of competition- an *i*-game which is necessary for the more

variable, larger scale competition we envision between DRAs. In addition the effect of price-based demand scheduling has been analyzed on the players' payoffs.

Section 5.2 explains some principles of game theory's application to energy markets. Proposed players' cost function, bidding process, and players' payoff function are covered in section 5.2. Section 5.3 describes the proposed game-theoretic market framework including four types of non-cooperative games. In addition, effect of price-based demand scheduling has been explained in section 5.3. The presented market framework has been applied to a case study and its results have been provided in section 5.4. Finally, conclusions are presented in section 5.5.

5.2 Principles and Definitions of Game Theory in Power Market

At the beginning of this section, the fundamental principles and definitions of the game theory have been described that are required to analyze a power market. The following subsections cover: a proposed function we will use to model the aggregator's cost, the bidding process of DRAs, and the payoff function for DRAs.

5.2.1 Game theory in power market

In game theory, beliefs are formulated against risky alternatives in order to maximize the expected revenue (payoff values) for aggregators. In the real competition, each player (DRA) remains unaware of the detailed data of other players (for instance data of strategies and payoffs). Probability theory gives an expected value of the payoff given the probability of events and Bay's law is used to revise beliefs given new information. For our purposes, the objective of the game-theoretic analysis is to find a reliable DM procedure for determining bidding strategy in any

circumstance which will give the greatest payoff regardless of the strategy chosen by opponents (which is not necessarily know before decisions are made) [194, 195].

Fig. 5.1 illustrates a power market where some of the aggregators acting as buyers and others acting as sellers submit their bids to a center and this center sets a market spot price between aggregators. The center is an ISO.

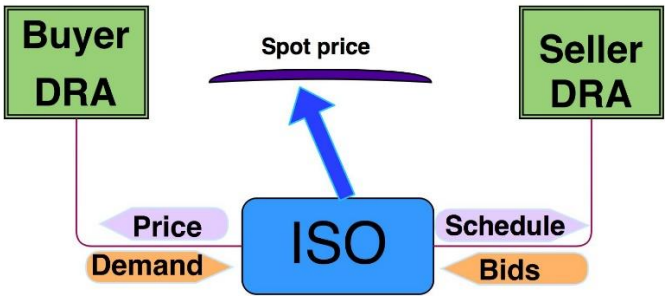

Figure 5.1: General structure of a power market including buyer DRAs, seller DRAs, and ISO

DRAs participate in the market to sell their available stored energy which is not consumed in powering local loads. In a power transaction game, aggregators' transactions are modeled as a game of strategies to maximize their payoffs. Two types of non-cooperative games are considered in this chapter: without a leader and with a leader (Stackelberg game). The first type of game takes place when each player (DRA) is interested to maximize its own payoff and there is no limitation for transaction quantity and price. In the Stackelberg game variety considered (in order to more closely represent real market conditions) competition between DRAs is similar with the exception that there is an additional player serving as the market leader (ISO or utility) endowed with the ability to limit market price and power transferred. The market leader neither buys nor sells directly, but may move to control other players' transactions in terms of transacted powers and price to ensure transactions are in the permissible ranges [196].

5.2.2 Aggregator cost function

This subsection shows how DRA's cost function can be presented with a quadratic function. Since the only energy resource available for sale by a given DRA is the aggregation of stored energy in residential batteries, the aggregator cost function is the battery cost function (cost of discharging the battery). For the battery, the function we chose is a variant of the widely used logarithmic barrier function, used as a penalty function in interior point methods [197, 198]:

$$C_h^{bat}(\Delta E_h) = -a_h \log(1 - \frac{\Delta E_h}{B}) \tag{5.1}$$

where C_h^{bat} is cost of the battery in house h as a function of stored energy. a_h is a pricing coefficient and depends on the electricity price which house h pays to the utility. Clearly a_h has higher values when the electricity is expensive during peak-hours. ΔE_h is the total load (kWh), and B is a parameter that has been used to give cost values very close to the values given by a quadratic one, it also serves as the maximum typical value for $|\Delta E_h|$ which means $\Delta E_h / B < 1$. The relation between the presented cost function (equation 5.1) and the quadratic one can be understood from its Taylor expansion. The Taylor series expansion is:

$$C_h^{bat}(\Delta E_h) = -a_h \log(1 - \frac{\Delta E_h}{B}) \approx -a_h(-\frac{\Delta E_h}{B} - \frac{{\Delta E_h}^2}{2B^2}) = \frac{a_h \Delta E_h}{B} + \frac{a_h {\Delta E_h}^2}{2B^2} \tag{5.2}$$

The above quadratic cost function of the battery can be rewritten as a function of power (ΔP_h):

$$C_h^{bat}(\Delta P_h) = \frac{a_h(t.\Delta P_h)}{B} + \frac{a_h(t.\Delta P_h)^2}{2B^2} \tag{5.3}$$

where t is the time interval for updating load data (hour). In our study, updates in load data are able to be resolved every 15 minutes with the measurement devices used ($t = 0.25$). We treat the

load for the interim 15 minutes between updates as a constant.

The way each house can use to calculate its own cost function's coefficients is explained here. In order to obtain the coefficients a_h and *B*, two factors should be considered: the electricity price of the grid (for charging the battery) and the capital and maintenance costs of the battery. Thus, the cost of the battery of house *h* for charging the power by an amount ΔP_h is:

$$C_h^{bat}(\Delta P_h) = C_h^{grid}(\Delta P_h) + C_h^{C\&M}(\Delta P_h) \tag{5.4}$$

where $C_h^{grid}(\Delta P_h)$ is the cost which house *h* pays to the utility to charge its own battery with the power of ΔP_h and $C_h^{C\&M}(\Delta P_h)$ is the contribution of capital and maintenance costs of the battery of house *h* for the power of ΔP_h. Clearly, charging cost of the battery includes two factors: grid's electricity price for charging the battery and capital and maintenance costs of the battery. Therefore, the whole cost which house *h* pays for charging its battery with the power of ΔP_h is shown in equation (5.4). Since both terms of equation (5.4) are known, a_h and *B* are obtained by equalizing equations (5.3) and (5.4).

If different houses of each aggregator have the same size of batteries and also have the same behaviors for charging their batteries (charging the batteries when electricity is cheap and discharge when the electricity is expensive either for feeding local loads or sale), discharging cost function of each aggregator has a quadratic form as well as individual houses:

$$C_i(P_i) = v_i P_i + u_i P_i^2 \tag{5.5}$$

where C_i is the cost function of aggregator *i* for selling the stored power of P_i (in kW), and the coefficients of u_i and v_i are:

$$v_i = \frac{a_i.t}{B} \tag{5.6}$$

$$u_i = \frac{a_i.t^2}{2B^2} \tag{5.7}$$

where $a_i = (1/N_h)\sum_{h=1}^{N_h} a_h$. In the proposed method in this chapter, the goal is to sell the aggregated energy stored in the residential batteries to other aggregators. Therefore, the cost coefficients u_i and v_i are obtained from the above equations for aggregator *i* with number of houses N_h.

5.2.3 Bidding process of DRAs

This section explains how DRAs bid their price for selling the stored energy in the batteries, based on the cost function defined in section 5.2.2. Using equation (5.5), the marginal cost of aggregator *i* is:

$$\lambda_i = \frac{dC_i}{dP_i} = v_i + 2u_i P_i \tag{5.8}$$

Since marginal cost is a linear function of stored power in the batteries, the simplest model of aggregator bids is also a linear function of stored power:

$$\lambda_i = \lambda_{0i} + m_i P_i \tag{5.9}$$

where λ_i is the bid price per unit of power at discharging power level P_i, λ_{0i} is the marginal cost of electricity at P_{0i}, and m_i is the slope of the bid curve. The market coordinator (ISO) receives sale bids from the DRAs given by equation (5.9) and matches the lowest bid with the buyer aggregators.

Fig. 5.2 shows bidding curve of aggregator *i* based on equation (5.9). In this figure, the aggregator intends to increase the battery discharging beyond P_{0i} if the spot market price is greater

than λ_{0i}. Here, T_i is the net power interchanged; if T_i is positive (negative), the aggregator is selling power to (buying power from) the other aggregators, $-P_{0i} \le T_i \le P_{\max,i} - P_{0i}$. The maximum stored power in the aggregated storages of DRA i is $P_{\max,i}$, the minimum of the local load of DRA i which should be fed by local batteries is P_{0i} (can be established as one of the governing policies of aggregator *i)*.

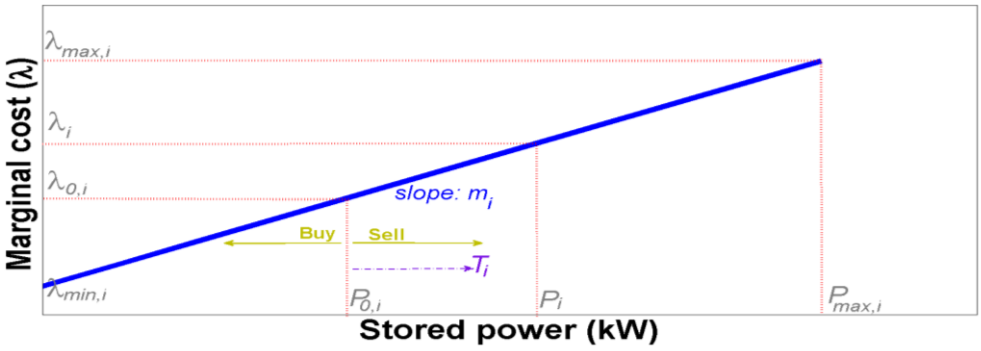

Figure 5.2: Aggregator *i*'s bidding curve

5.2.4 Aggregator payoff function

The mathematical formulation of the payoff function for each DRA in the game-theoretic framework is described below. For a given spot market price, ϕ, payoff of aggregator *i*, R_i, is:

$$R_i = -\Delta C_i + \phi T_i \tag{5.10}$$

ΔC_i is the difference between the discharging cost of the batteries in aggregator before and after power transactions, and T_i is the net power transacted. From the definition of the payoff function in equation (5.10), each aggregator tries to maximize its own payoff in a non-cooperative game:

$$maximize \sum_{k \in K} R_{ij}^k(\phi_{ij}, T_{ij}); \quad \text{where:} \qquad R_{ij}^k(\phi_{ij}, T_{ij}) = \phi_{ij} T_{ji} - [C_i(P_{gi} + T_{ij}) - C_i(P_{gi})] \tag{5.11}$$

R_{ij}^k is the payoff of DRA *i* (as a seller) after transmitting the power of T_{ij} to aggregator *j* (and receiving the power of T_{ji} by aggregator *j*) in contract *k*. The difference between T_{ij} and T_{ji} is due to transmission losses. With negligible losses $T_{ij} = T_{ji}$. Energy loss in distribution systems is considerable because of losses in connecting lines between aggregators and houses. These losses have been consided in this study. The parameter, ϕ_{ij}, is the transaction price and P_{gi} is the amount of the local loads of the aggregator *i* which is fed by the local storages before power transaction.

The first term in equation (5.11) is the gross revenue of the aggregator due to the transaction and the second bracketed term is the change in the aggregator's batteries discharging cost owing to the transaction. In the case of two aggregators shown in fig. 5.3 (aggregator 1 as seller and 2 as buyer), the payoff of the aggregators are:

$$R_{seller} = \phi_T T_{21} - [C_1(P_{g1} + T_{12}) - C_1(P_{g1})] \tag{5.12}$$

$$R_{buyer} = -\phi_T T_{21} - [C_2(P_{g2} - T_{21}) - C_2(P_{g2})] \tag{5.13}$$

ϕ_T is the tranction price and R_{seller} and R_{buyer} are the aggregators payoffs. In fig. 5.3, Bat_1 and Bat_2 are the aggregated residential batteries in aggreator 1 and 2, respectively. Each aggregator has a

constrained storage capacity, and payoffs are constrained by $R_{seller} \geq 0$, and $R_{buyer} \geq 0$, indicating that negative payoffs are excluded. When there are no transactions, the payoff is zero.

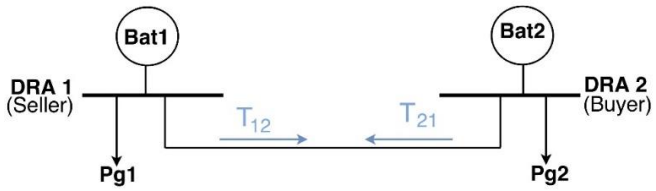

Figure 5.3: A system including two DRAs: one seller and one buyer

In real competition between aggregators, participants don't have information about the other participants such as cost function coefficients, availability of the batteries, and bidding prices. Next section shows the proposed game-theoretic market framework for competition between DRAs to sell energy stored in batteries in an *i*-game.

5.3 Proposed Game-Theoretic Market Framework for DRAs

The proposed methodology is explained in this section. Subsection 5.3.1 includes details about the game with incomplete information to make a market competition among DRAs. The proposed market framework based on game theory has been presented in subsection 5.3.2. All mathematical and probabilistic details for the developed market framework (including two different game types each with two demand scheduling programs) have been provided in 5.3.2.

Fig. 5.4 shows a visual schematic of the proposed market framework. The diagrams with blue background depict the non-cooperative games with no constraints and those with green background depict the non-cooperative Stackelberg games. Each DRA manages a number of houses with control signals sent through a wireless network. Each house contains various devices possibly including WHs, Batteries, ACs, and EVs. The DRAs decide how to bid for buying and selling power in the market.

A DP scheduler outputs signals for deciding when a WH should run-on/off setting as a function of time-to satisfy the conditions in the game (social welfare in all games, and price-sensitive DR WH scheduling in the games where it is implemented) given as inputs hot water usage data (in all games) and possibly electricity price signals from the utility (only for the games with price-sensitive WH scheduling). As fig. 5.4 shows, DP scheduler has two inputs including electricity price and hot water usage of end-users. Its output is price-based scheduling signals for thermostatic storage loads such as WHs. More details about the DP scheduling method have been provided in [137]. In [137], DR resources are considered agents in a stochastic/deterministic environment and models of demand resources (especially WHs) are explained and the required parameters are presented to formulate the optimization problem in DP framework.

The DRAs communicate through a wireless network with servers which communicate with the market directly to arrange transactions. In the Stackelberg games, the servers also mitigate size and price of transactions in accordance with utility policy constraints which are transmitted over the wireless network. As fig. 5.4 shows, communication devices are necessary for DRAs server to talk to aggregators in order to receive their bids (transaction powers and price) and also send them the control signal based on the limitations on transaction power, transaction price, availability of the connecting lines, etc. Also DRAs server needs to communicate with the utility to get information about the market constraints and policies.

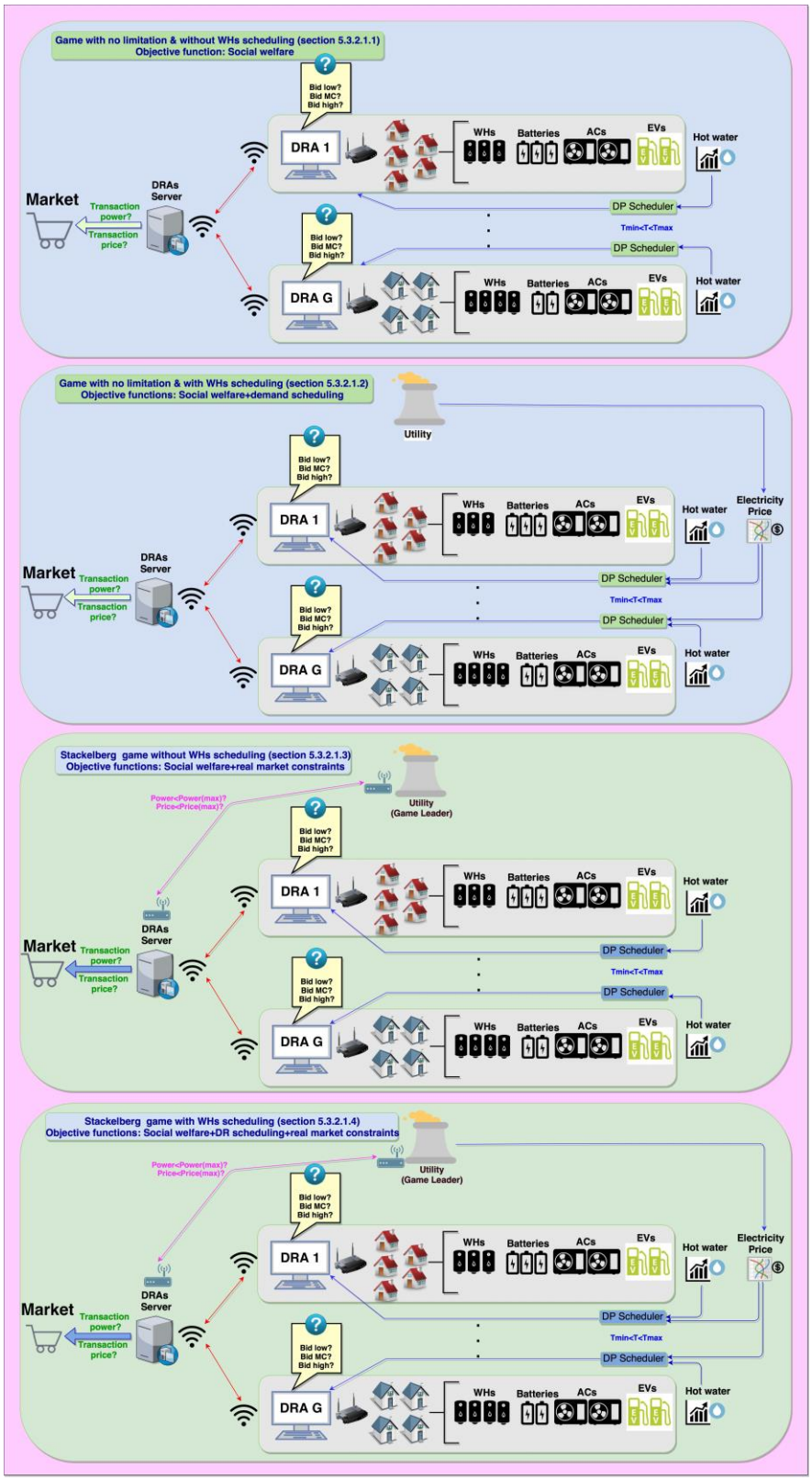

Figure 5.4: Schematic of the proposed market model in two types of games and two demand scheduling program

5.3.1 Market competition between DRAs with incomplete information

In this subsection, a market model is proposed to model competition among aggregators in an electricity market where participants have incomplete information. Based on equation (5.10), each aggregator's payoff is a function of storages discharging costs, power transactions, and the spot market price. Hence, an individual aggregator's payoff is a function of bids offered by other aggregators. Each participant estimates the other participants' bids in order to maximize its own payoff. Each aggregator has complete information concerning its own payoff but lacks information critical to predicting others actions precisely, this competition is known as an *i*-game.

Here, an aggregator's unknown characteristics are modeled by classification of participant's types. The aggregator's type contains information concerning: its own payoff function, other aggregators' payoff functions, electricity prices, availability of charged batteries, etc. An aggregator's type corresponds to its battery discharging cost, that is, coefficients a_i and B in equations (5.5) to (5.7). Each aggregator would have full knowledge of its own costs, but only an estimate of the remaining aggregators' costs. Each participant adjusts the slope of m in its bidding curve (fig. 5.2) in order to maximize its payoff, R_i, in equation (5.10). The choice of m corresponds with the bidding strategy (bid low, bid high, bid marginal cost) in the game. The main goal of the game is to determine the optimal bidding strategy which its process is to determine what value of m to choose in order to maximize payoff despite the unknown parameters of the other participants.

The aggregators use a Bayesian approach to deal with incomplete information. In this approach, a probability distribution, $\prod$, represents the unknown parameters. The expected value of the payoffs of the aggregators are maximized for $\prod$. In estimating the probability distribution, each aggregator uses only the information common to all aggregators.

Consider a scenario described from aggregator *B*'s perspective for competing with aggregator *A* to sell the stored energy of the batteries to aggregator *C* depicted in fig. 5.5. Let the participants' types be drawn at random from hypothetical populations Θ_A and Θ_B containing types t_A^m and t_B^n, respectively where $m = 1,...,M$ and $n = 1,...,N$ index the possible types of aggregators *A* and *B*, respectively. To model the uncertainty in *A*'s discharging cost, *B* would consider *M* possible types of *A*, t_A^m, each with its corresponding cost. Generally, aggregator *B* knows its own types completely but does not know the details of *A*'s types (i.e. it does not know *A*'s discharging costs).

Each aggregator estimates the probability distributions , $\prod$, for the random variable of the "type" of its competitors based on freely available published information such as electricity prices, demand curves, hot water usage (from WHs), availability of storages, and aggregators' parameters. Although the players don't know the details for the types and strategies of their opponents, but they might use some historical information about the opponents such as the number of types and strategies (which were previously used by the opponents) and also average of hot water consumption.

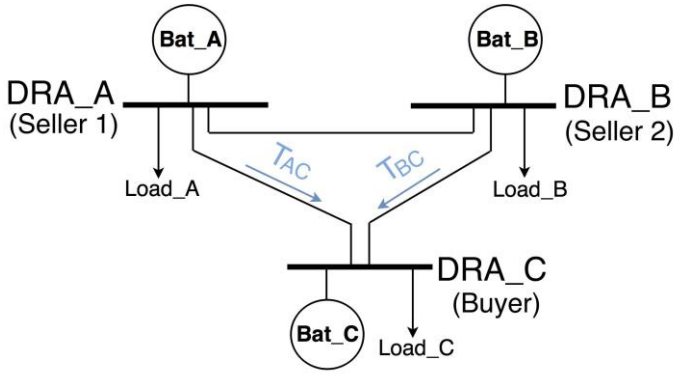

Figure 5.5: A grid including three aggregators: *A* and *B* as sellers and *C* as buyer

5.3.2 Game-theoretic market framework

For our purposes, the goal of the game is to calculate the expected payoffs for different strategies for aggregators *A* and *B* (in the mentioned scenario) to choose the strategy that maximizes payoff and to find the Nash equilibrium of strategies:

$$EP_A^m = \sum_{n=1}^{N} \eta_A^m(n).H_A^m(s_A^m, s_B^n, m, n) \tag{5.14}$$

where EP_A^m is the expected payoff function of aggregator *A* if it is of type $m \in M$. *n* is the type of opponent aggregator *B* ($n \in N$). Since this game has incomplete information the expected payoff function is used in place of the exact payoffs because the opponent's bidding strategy cannot be known precisely. The conditional probability $\eta_A^m(n)$ is the probability aggregator *A* is of type *m* for aggregator *B* of type *n*:

$$\eta_A^m(n) = prob(t_B^n \mid t_A^m) = \frac{\pi_{mn}}{\sum_{n=1}^{N} \pi_{mn}} \tag{5.15}$$

$prob$ shows the conditional probability function, and π_{mn} is the basic probability distribution $\prod$ corresponds to the probability that *A* is type *m* and *B* is type *n*. An aggregator's strategy (for bidding) is determined by its type. s_A^m is a vector of strategies for *A*'s type *m.* For example, a vector of strategies may be: bid high, bid at marginal cost, and bid low. H_A^m is the conditional payoff of aggregator *A* which depends on strategies of aggregator *A*, s_A^m, and aggregator *B*, s_B^n. Aggregator *A* needs to know the opponent's type to maximize H_A^m, and since the information is not available in an *i*-game, aggregator *A* maximizes its expected payoff EP_A^m. Similarly, for aggregator *B*, the expected payoff function is:

$$EP_B^n = \sum_{m=1}^{M} \eta_B^n(m).H_B^n(s_B^n, s_A^m, n, m) \tag{5.16}$$

where,

$$\eta_B^n(m) = prob(t_A^m \mid t_B^n) = \frac{\pi_{mn}}{\sum_{m=1}^{M} \pi_{mn}} \tag{5.17}$$

In equations (5.14) and (5.16), players would consider all types of opponents. Using the above equations and considering all possible types of participants convert the *i*-game to a *c*-game and Nash equilibrium is the solution.

5.3.2.1 Non-cooperative game

The previously considered *i*-game converts to a (*M* + *N*)-participant game as an imperfect information complete game, where *M* and *N* are the number of different types of aggregators *A* and *B*, respectively, in the case that each aggregator knows the others' payoff functions and, basic probability distributions involved in the game but does not know the details of opponent's type. In other words, each aggregator does not know which type and which strategy will be played by the other aggregators. The Nash equilibrium is the solution.

Two variants of non-cooperative *c*-game have been considered: one with no constraint and the other one with a leader (Stackelberg game), in a scenario involving two aggregators competing to sell energy stored in their batteries. In each game, the effect of price-sensitive demand scheduling (for WHs and other similar thermostatic storages) has been considered and the market model has been proposed with/without demand scheduling. Left side of the algorithm shown in fig. 5.6 depicts the procedure used to calculate the requisite parameters used in obtaining the Nash equilibrium and the right side shows the remaining process of the market clearing.

In the proposed game model, the players are the aggregators who sell the aggregated energy stored in the residential batteries [199, 200, 201]. Players' types are different sets of coefficients

in aggregators' cost functions which will be explained in step 1 of section 5.3.2.1.1 in detail. Players' strategies are different bidding slopes in fig. 5.2. Step 3 of section 5.3.2.1.1 includes more details about the strategies.

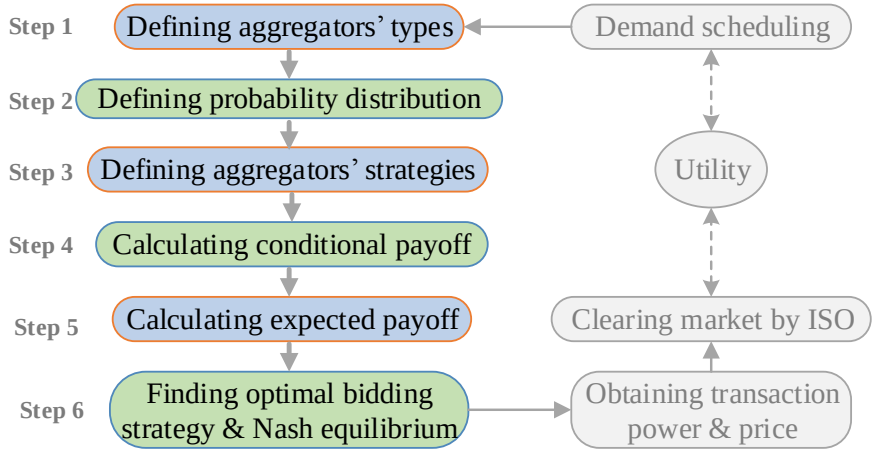

Figure 5.6: steps of calculating required parameters in the game-theoretic market

The following subsections explain how to determine the required parameters in the process of finding the optimal bidding strategy and Nash equilibrium of strategies for each game and each demand scheduling program.

5.3.2.1.1 Game with no limitation and without demand scheduling

In this case study, aggregators *A* and *B* compete to sell their stored energy to aggregator *C*: because the marginal cost is higher for aggregator *C* it is natural for him to wish to purchase energy. Aggregators *A* and *B* compete with each other for sale and may offer different bidding strategies (bidding high, low or marginal cost). The goal of the sellers is to make the best bidding decisions in order to maximize their own payoff. Both sellers know about the cost function of aggregator *C* because *C* does have different strategies as a buyer.

Step1: Define aggregators' types:

In the first step, a set of different possible discharging cost function's coefficients (a_i and B in equations (5.5) - (5.7)) is defined for each aggregator *A* and *B*. The number of defined types are *M* and *N* for aggregators *A* and *B*, respectively. The participant's type is determined largely by electricity price and availability of the batteries for discharging. The electricity price is significant because the batteries are charged directly from the grid.

Availability of the stored energy in the batteries may be estimated by considering usage patterns for high power consumption devices such as WHs and other thermostatic devices. For example, when the WHs are consuming power (based on the hot water usage and water temperature), most of the energy stored in the batteries is being consumed locally to power these devices. Considering these two factors, an aggregator's status can be classified into one of four scenarios: $\sigma_1 : \{elec_{\exp}, WH_{off}\}$, $\sigma_2 : \{elec_{\exp}, WH_{on}\}$, $\sigma_3 : \{elec_{ch}, WH_{off}\}$, $\sigma_4 : \{elec_{ch}, WH_{on}\}$.

For a non-cooperative game with no limitation and without price-sensitive demand response, scheduling depends entirely on water usage and is completely independent of the price of electricity since the thermostat functions only to maintain the social welfare demands of the customer without considering price (the objective is only to maintain the water temperature in a given range). When two events are independent, the probability of both events occurring is the product of the probabilities of each event. For aggregator scenarios σ_1, σ_2, σ_3, σ_4, we have:

$$P(\sigma_1) = P(elec_{\exp} \cap WH_{off}) = P(elec_{\exp}) * P(WH_{off})$$
$$P(\sigma_2) = P(elec_{\exp} \cap WH_{on}) = P(elec_{\exp}) * P(WH_{on})$$
$$P(\sigma_3) = P(elec_{ch} \cap WH_{off}) = P(elec_{ch}) * P(WH_{off})$$
$$P(\sigma_4) = P(elec_{ch} \cap WH_{on}) = P(elec_{ch}) * P(WH_{on})$$

$\sum_{f=1}^{4} P(\sigma_f) = 1$, and $P(\sigma)$ is the probability of event σ. The probability of the WHs' status ($P(WH_{off})$, $P(WH_{on})$) is obtained from the DP scheduler block described in fig. 5.4. In this case, the scheduling is determined by typical hot water consumption profile and the only objective function is to maintain social welfare- i.e. that the WH maintains temperatures in the required range by the customer to ensure sufficient hot water is available.

Let Ψ_A^f and Ψ_B^f be probability distributions modeling uncertainties in each aggregator's discharging cost:

$$\Psi_A^f = [\Psi_A^f(1), \Psi_A^f(2), ..., \Psi_A^f(M)] \tag{5.18}$$

$$\Psi_B^f = [\Psi_B^f(1), \Psi_B^f(2), ..., \Psi_B^f(N)] \tag{5.19}$$

$\Psi_A^f(m)$ is the probability that aggregator *A* is in type *m* ($m \in M$) in scenario *f* and $\Psi_B^f(n)$ is the probability that aggregator *B* is in type *n* ($n \in N$) in scenario *f.* For example the first element of Ψ_A^1 corresponds to the probability that *A* is in type 1 for the first scenario (*f=1*), and the second element of Ψ_A^1 corresponds to the probability that *A* is in type 2 for *f=1*. The same notation applies to other probability distributions. Choosing each pair of coefficients [*a, B*] by players and determining $\Psi_A^f(m)$ and $\Psi_B^f(n)$ depend on a few factors. These factors are: availability of the charged batteries and more important factor is the market conditions. For example, in equations (5.18) and (5.19), it is more probable that aggregators *A* and *B* will choose coefficients corresponding to the lower discharging cost when their storage devices have been charged with cheaper electricity.

Step2: Define the basic probability distribution of the game:

The probability that (*m*, *n*) would represent participants *A* and *B*'s types, respectively, would depend on electricity price and local demand (WHs' conditions). The expected probability that *A* is type *m* and *B* is type *n*, π_{mn}, is defined as:

$$\pi_{mn} = \sum_{f=1}^{4} (P(\sigma_f).\vartheta(\sigma_f).\Psi_A^f(m).\Psi_B^f(n)) \tag{5.20}$$

Where $\vartheta(\sigma_f)$ is a participation coefficient for scenario *f*: equal to 1 for participants selling energy in the market and 0 otherwise. For example, $\vartheta(\sigma_2) = 0$ because when the electricity is expensive and the water usage is high, energy stored in storage devices will be used preferably for powering local loads. $\vartheta(\sigma_1) = \vartheta(\sigma_3) = \vartheta(\sigma_4) = 1$ because if the price of electricity is cheap, the stored energy is available for sale as loads may be supplied directly from the grid at lower cost; whereas even if the price is high, absence of local demand leaves energy available for sale. Participation coefficient in eq. 20 shows the willingness of the battery owners to participate (or not participate) to sell the energy stored in their storage devices based on different conditions. Given this scheme for predicting π_{mn}, the original *i*-game may be treated as a *c*-game with imperfect information. In this step $\eta_A^m(n)$ and $\eta_B^n(m)$ are calculated using equations (5.15) and (5.17) $(n \in N, m \in M)$.

Step 3: Define aggregators' strategies:

An aggregator's type corresponds to a set of strategies defined by bidding slopes (fig. 5.2). In reality an aggregator may bid any amount, but in order to simplify our calculations for the sake of concise presentation we consider here only three characteristic bidding strategies: bidding above, below, or equal to marginal cost. Based on equation (5.9) and fig. 5.2, the slope of the bidding curve of aggregator *i* is $m_i = \varepsilon_S \times u_i$ where ε_S is set to $[\varepsilon_{S1}, \varepsilon_{S2}, \varepsilon_{S3}]$ for three different strategies.

These strategies are: $\varepsilon_{S1} < 2$ for bidding less than marginal cost, $\varepsilon_{S2} = 2$ for bidding at marginal cost, and $\varepsilon_{S3} > 2$ for bidding more than marginal cost. Coefficient u_i was defined in equation (5.7). In this step s_A^m and s_B^n are calculated $(n \in N, m \in M)$. Each element of the strategy vector (will be shown in section 5.4.1) represents a bidding slope for the combination of an aggregator's type and strategy.

Step 4: Define aggregators' conditional payoff:

The amount of power that each aggregator could trade is a function of spot market price. The higher the price, the lower will be the amount of sold power from aggregators *A* and *B* to *C*. In this step the following system of equations has been solved for a combination of the players' types and strategies:

$$\begin{cases} \lambda_A = \lambda_B = \phi_T \\ P_A + P_B = L_C \end{cases} \tag{5.21}$$

P_A and P_B are the power remaining in the storages cells of aggregator *A* and *B*, after feeding their local loads. This power is sold to aggregator *C* (L_C is the power purchased by aggregator *C*), and ϕ_T is the transaction price. After determining P_A, P_B, and ϕ_T, in equation (5.21), the conditional payoffs of aggregator *A* and *B* may be calculated. The conditional payoff matrices take the form:

$$H_A^m(n) = \begin{bmatrix} h_{A,11} & h_{A,12} & h_{A,13} \\ h_{A,21} & h_{A,22} & h_{A,23} \\ h_{A,31} & h_{A,32} & h_{A,33} \end{bmatrix} \tag{5.22}$$

$$H_B^n(m) = \begin{bmatrix} h_{B,11} & h_{B,12} & h_{B,13} \\ h_{B,21} & h_{B,22} & h_{B,23} \\ h_{B,31} & h_{B,32} & h_{B,33} \end{bmatrix} \tag{5.23}$$

In equations (5.22) and (5.23), combination of aggregators' types and strategies have been considered. In $H_A^m(n)$, each row corresponds to a strategy of *A* for type *m* and each column corresponds to a strategy of *B* for type *n*. For instance, $h_{A,23}$ in $H_A^2(1)$ corresponds to *A*'s type 2 payoff if *A* decides to bid marginal cost against a situation where *B* is type 1 and bids above marginal. $H_B^n(m)$ is defined similarly.

We use equations (5.11)-(5.13) to calculate conditional payoffs ($H_A^m(n), H_B^n(m)$) in equations (5.22) and (5.23). Finally, aggregators *A* and *B* (as sellers) need to maximize their own expected payoffs (next step). Players' types are the coefficients of the discharging cost function. Different possible sets of $[a_i, B]$ in equations (5.6) and (5.7) are different types of the players. But the strategies of the players are defined based on the bidding slopes in fig. 5.2. As mentioned in step 3, three strategies have been considered for each seller aggregator in this study.

Step 5: Define expected payoff matrices:

Expected values of the payoffs, EP_A^m and EP_B^n, are calculated using equations (5.14)-(5.17), (5.22), and (5.23). The final form of EP_A^m matrix is:

$$EP_A^m = \begin{bmatrix} \kappa_{11}^1 & \kappa_{12}^1 & \kappa_{13}^1 & \kappa_{21}^1 & \kappa_{22}^1 & \kappa_{23}^1 \\ \kappa_{11}^2 & \kappa_{12}^2 & \kappa_{13}^2 & \kappa_{21}^2 & \kappa_{22}^2 & \kappa_{23}^2 \\ \kappa_{11}^3 & \kappa_{12}^3 & \kappa_{13}^3 & \kappa_{21}^3 & \kappa_{22}^3 & \kappa_{23}^3 \end{bmatrix} \tag{5.24}$$

Each row corresponds to the strategy of participant *A*. Each column corresponds to the presumed strategy of participant *A*'s opponent e.g. the κ_{23}^1 in EP_A^1 is *A*'s type 1 payoff when *A* uses strategy 1 and *B* uses strategy 3 in its type 2. The same notation applies to EP_B^n.

Step 6: Obtain the optimal bidding strategy and Nash equilibrium of strategies:

Utilizing EP_A^m and EP_B^n, the best bidding strategy and Nash equilibrium pairs are obtained. We look for the collection of strategies in which each aggregator's strategy would be represented by the best response to other aggregator's strategies. The Nash equilibrium is a prediction of how the game will be played. An aggregator's optimal bid is derived for this equilibrium point. All aggregators predict that a particular Nash equilibrium will occur and there is no incentive to play differently. In the mentioned case with two seller aggregators *A* and *B*, first the dominant rows (strategies) should be found in EP_A^1 and EP_A^2. Then, the corresponding columns should be found in EP_B^1 and EP_B^2 to obtain the optimal bidding strategy and Nash equilibrium pairs. More details are explained in section 5.4.1.

System of equations (5.21) always has unique answer for transaction powers (P_A and P_B) and truncation price (ϕ_T) with a quadratic cost function (*C*). The cost function is quadratic and marginal cost (λ) is the first derivative of cost function which is a linear function of power (equation (5.8)). The system of equations (5.21) has unique solution because it is a non-homogeneous system of equations which its determinant is non-zero. It guarantees the uniqueness and existence of Nash equilibrium of strategies in the proposed method.

Also, the existence and uniqueness of Nash equilibrium has been proved in [202, 200]. In addition, it has been proven in [203] that a unique equilibrium always exists in unregulated competition and also always exists in Stackelberg game with spatially homogeneous cost function and unconstrained network (unconstraint network means connecting lines have enough capacity to transfer the power). Since in the proposed market model, the flowing power in grid's lines (between DRAs) are the stored energy in batteries (as a part of total load), all connecting lines

between the aggregators have much more than enough capacity to flow the mentioned power. In other words, the connecting lines of the grid have been designed in advance to be able to flow the power more than the peak demand which this number is much more than the capacity of aggregated storages. Also, the cost function is quadratic spatially homogeneous. Therefore, based on the mentioned reasons, the proposed market model guarantees the existence and uniqueness of Nash equilibrium of strategies.

5.3.2.1.2 Game with no limitation and with demand scheduling

In this game, price-sensitive scheduling of WHs is considered. The steps of this game are the same as game with no limitation and without demand scheduling (section 5.3.2.1.1) with a single exception in the first step. For a game without DR scheduling, WHs keep the water temperature in a given range to satisfy social welfare constraints, and situation of WHs (On/Off) is independent of the electricity price. In game with DR scheduling, the objectives are both social welfare and demand scheduling. The first step in finding the Nash equilibrium of the game with DR scheduling requires knowledge of conditional probabilities since the events are not independent.

Step1: Define aggregators' types:

As mentioned in section 5.3.2.1.1, a set of possible discharging cost function's coefficients (a_i and B in equations (5.6) and (5.7)) is defined for each aggregator acting as a seller (A and B). Similarly we define four scenarios ($\sigma_1,...,\sigma_4$) depending on the same two variables (electricity price and WHs' condition), but in this game these events are dependent due to price-sensitive demand scheduling. When two events are dependent, the probability of both occurring is defined using conditional probability:

$$P(\sigma_1) = P(elec_{\exp} \bigcap WH_{off}) = P(elec_{\exp}) * P(WH_{off} / elec_{\exp})$$
$$P(\sigma_1) = P(elec_{\exp} \bigcap WH_{on}) = P(elec_{\exp}) * P(WH_{on} / elec_{\exp})$$
$$P(\sigma_3) = P(elec_{ch} \bigcap WH_{off}) = P(elec_{ch}) * P(WH_{off} / elec_{ch})$$
$$P(\sigma_4) = P(elec_{ch} \bigcap WH_{on}) = P(elec_{ch}) * P(WH_{on} / elec_{ch})$$

The second part of each equation is the conditional probability. For instance $P(WH_{off} / elec_{\exp})$ is the probability that the WH is off given that electricity is expensive. These conditional probabilities are determined by the DP scheduler (mentioned in fig. 5.4) considering two objective functions: social welfare and DR scheduling. In this game more batteries are available to provide power because scheduling has disabled some loads, thus each aggregator stands to make a larger payoff then in the game without demand scheduling (5.3.2.1.1).

5.3.2.1.3 Stackelberg game without demand scheduling

In the previous subsections while considering non-cooperative games with no limitation, the transaction price (and transaction powers) depended only on the aggregators' bid prices (equation (5.21)), here we consider the effects of regulations on transaction size and price by modeling the regulatory action through the moves of an addition player, the market "leader". DRAs with storage capabilities will tend to charge their batteries when energy is less expensive during off-peak hours, in order to sell it to other DRAs during peak hours when the price is high thereby maximizing their gains per transaction.

When a large enough number of DRAs do this, a phenomenon termed "Reverse Peaks" becomes apparent where the shift of peak consumption is accompanied by a high tendency of aggregators to sell their stored energy back during high price hours. This undesirable effect can be resolved by allowing a market controlling center (i.e., utility or any other center empowered by the utility) to effect regulatory power over transaction deemed detrimental to the market. The

controller is allowed to enforce bounds on market transactions quantity and price thereby ameliorating the undesirable effects on the market associated with reverse peaks.

Competition including a market controller can be modeled as a non-cooperative Stackelberg game with an additional "leader" player who can move first and followed by all other players in such a manner to clear the market. The game leader announces the allowed ranges corresponding to transaction price and transaction powers based on the network constraints and then players (followers) have to take responses accordingly for avoiding undesirable transactions.

As the green parts of fig. 5.4 show, the game leader (ISO) has a server and communicates with the utility company to control the competition between the aggregators to ensure the transaction powers and price are in the allowed ranges according to the grid's constraint, limitations, and policies. The third part of fig. 5.4 show more details about the Stackelberg game without demand scheduling. This game is a regulated game since the game leader controls the transactions but the there is no price-based demand scheduling here. A Nash equilibrium exists for the Stackelberg game-i.e. each rational player will choose a particular predictable strategy which offers them no incentive to alter it despite the strategies chosen by the competitors.

Finding the Nash equilibrium for the Stackelberg game follows the procedure outlined in fig. 5.6, similar to the previous subsections with the exception that in calculating the conditional payoff (step 4), the transaction powers (P_A, P_B) and transaction price (ϕ_T) are observed and subject to limitation by the game's leader (acting as enforcer of the utility's policies). If these values, fall within the range permitted by policy, the transaction between the aggregators proceeds; but if the solutions of equation (5.21) are higher than the maximum allowable values $(P_{A_{\max}}, P_{B_{\max}}, \phi_{T_{\max}})$, the maximum values are used to clear the market instead. Enforcement of the utility's regulatory

policies in the market, which we model as a Stackelberg game, prevents individual players (aggregators) from having inordinately large effects in the market and also prevents reverse peaks.

5.3.2.1.4 Stackelberg game with demand scheduling

The analysis of the non-cooperative Stackelberg game with demand scheduling follows reasoning similar to one without scheduling (section 5.3.2.1.3) with the exception that electricity price and WH's status are dependent events since the DP scheduler determines hot water usage as a function dependent on price. Conditional probabilities are used in calculating the probabilities of the intersection of dependent events for the possible aggregator scenarios in step 1 analogous to what was done in section 5.3.2.1.2 when considering scheduling for a game with no limitation.

In the mentioned proposed method for all four games in section 5.3.2.1, competition between two aggregators has been modeled who sell the energy stored in the batteries to the third aggregator. Each player has two types (sets of coefficients in discharging cost functions) and three strategies (slopes of bidding curve). Clearly, with increasing the numbers of players, the size of the payoff matrices and complexity of the computations will be increased significantly but the model is the same. For example with 3 seller aggregators (each with 2 types and 3 strategies), there will be 6 expected payoff matrices for different players in different types and the size of each one will be 3 ×36. As a general formulation, the number of expected payoff matrices is: $(playes * types)$ and the size of each one is: (strategis) $\times (types * strategies)^{players-1}$.

5.4 Case Study, Discussion and Results

For illustration purposes, consider a system with three DRAs labeled *A*, *B*, and *C* as depicted in fig. 5.7. Load data for these three DRAs was taken from a real grid model on the island of Maui (Hawaii-United States) [204]. In order to make the case study much closer to a real-world model,

load behaviors and hot water consumption trend have been applied to the chosen case study. Also, real capacities of WHs (4.5kW) and batteries (3.3kW), and the number of houses have been considered in the mentioned case study. In Hawaii the high percentage of load include thermostatic storages (such as WHs and ACs) which this item has been considered as well.

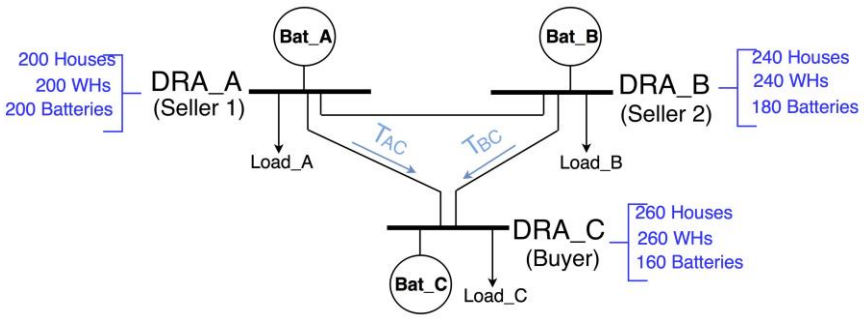

Figure 5.7: Case study including 3 aggregators: *A* and *B* as sellers and *C* as buyer

Aggregator *A* manages 200 houses, all of which contain storage devices. Aggregator *B* manages 240 house, but only 180 have storage devices and aggregator *C* manages 260 houses of which only 160 are equipped with storage devices. In the case study data, all houses have WHs whose average power consumption is 60% of the houses total load [204]. The nominal power of each residential storage device is 3.3kW. Thus, the maximum generation capacity of each aggregator is: $P_A^{gen} = 660kW,\ P_B^{gen} = 594kW,\ P_C^{gen} = 528\,kW$.

From the case study data, the nominal power of each WH is 4.5kW. Thus, the total power demand of aggregator *A* is: $P_A^{demand} = 200 * 4.5 * 10/6 + P_A^{gen} = 2{,}160kW$.

Similarly, for other aggregators: $P_B^{demand} = 2{,}394\,kW, P_C^{demand} = 2{,}478\,kW$.

Since the marginal cost of aggregator *C* is greater than other aggregators, *A* and *B* will compete to sell power to *C*. To limit the number of calculations, while clearly exhibiting the methodology used we let $M = 2$ and $N = 2$ and that the aggregators' discharging cost coefficients are:

$$\text{Seller\_A}\begin{Bmatrix} a_A = [4, 4.3] \\ B = [25, 23.5] \end{Bmatrix}, \text{Seller\_B}\begin{Bmatrix} a_B = [4.2, 4.5] \\ B = [24, 23.5] \end{Bmatrix}, \text{Buyer\_C}\begin{Bmatrix} a_C = 5 \\ B = 21.5 \end{Bmatrix}$$

Fig. 5.8 shows the normalized price of electricity (in Maui Island) over the course of a single day, price updates resolve every 15 minutes [63]. The normalized average hot water consumption for the houses of aggregators *A* and *B* is shown in fig. 5.9 for the same time intervals.

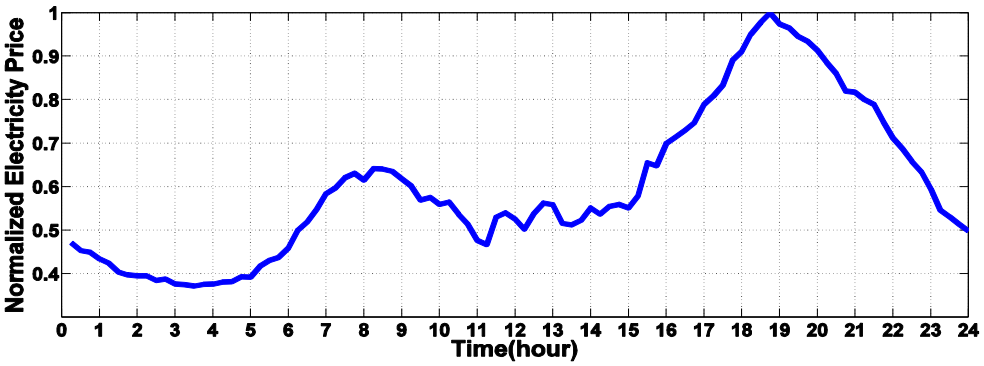

Figure 5.8: Normalized electricity price in one day of case study (for every 15 minutes) [63]

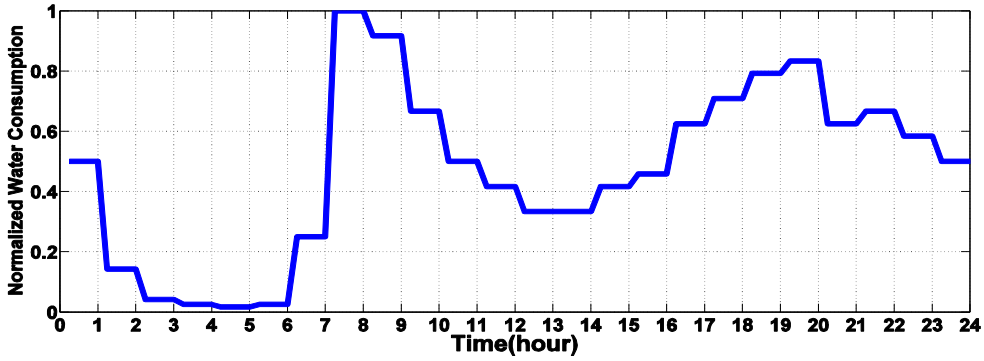

Figure 5.9: Normalized average of residential hot water consumption of seller aggregators (every 15 minutes)

Results for non-cooperative game with no limitation and non-cooperative Stackelberg game, with and without demand scheduling are presented in the following sections.

5.4.1 Results of game with no limitation and without demand scheduling

For our purposes, we take prices over half of the normalized price of electricity to be "expensive". From the normalized price data (fig. 5.8), $P(elec_{\exp}) = 0.7083, P(elec_{ch}) = 0.2917$. The status of the WHs (on/off) is determined from the hot water consumption data (fig. 5.9). In order to keep water temperatures in the range of 110-130°F, a typical WH runs (consumes power) for 18 of the 96 fifteen-minute intervals of the day. Fig. 5.10 is the output of DP scheduler and shows the status of the seller's WHs in this game (no constraint and without DR scheduling).

Figure 5.10: On/Off status of WHs in game with no limitation and without DR scheduling for the seller aggregators

The probabilities $P(WH_{on}) = 0.1875$ and $P(WH_{off}) = 0.8125$ follow immediately from the known ratio of on to off intervals. Using the equations from section 5.3.2.1.1, the probabilities of the four scenarios are: $P(\sigma_1) = 0.5755,\ P(\sigma_2) = 0.1328, P(\sigma_3) = 0.2370, P(\sigma_4) = 0.0547$.

Probability distributions for both aggregator *A* and *B* in the above mentioned scenarios are:

$$\Psi_A^1 = [0.16, 0.84], \Psi_B^1 = [0.21, 0.79], \Psi_A^2 = [0.11, 0.89], \Psi_B^2 = [0.18, 0.82],$$
$$\Psi_A^3 = [0.75, 0.25], \Psi_B^3 = [0.67, 0.33], \Psi_A^4 = [0.69, 0.31], \Psi_B^4 = [0.60, 0.40].$$

Using equation (5.20), the expected probabilities are:

$\pi_{11} = 0.0193,\ \pi_{12} = 0.0727, \pi_{21} = 0.1015, \pi_{22} = 0.3819$

Conditional probability vectors for aggregators *A* and *B* are calculated using equations (5.15) and (5.17): $\eta_A^1 = [0.21, 0.79], \eta_B^1 = [0.16, 0.84], \eta_A^2 = [0.21, 0.79], \eta_B^2 = [0.16, 0.84]$.

Each aggregator chooses one of the following strategies: bidding 80% of marginal cost $(\varepsilon_{S1} = 1.6)$, bidding marginal cost $(\varepsilon_{S2} = 2)$, and bidding 120% of marginal cost $(\varepsilon_{S3} = 2.4)$. Therefore, the strategies are:

$s_A^1 = [0.00064, 0.00080, 0.00096]$
$s_A^2 = [0.00078, 0.00097, 0.00117]$
$s_B^1 = [0.00073, 0.00091, 0.00109]$
$s_B^2 = [0.00081, 0.00102, 0.00122]$

Finally, from the equations in step 5 of section 5.3.2.1.1, the expected payoff matrices are:

$$EP_A^1 = \begin{bmatrix} 9.52 & 12.28 & 14.62 & 41.32 & 51.93 & 60.72 \\ 14.89 & 19.13 & 22.77 & 64.38 & 80.81 & 94.61 \\ 16.94 & 22.08 & 26.55 & 73.77 & 93.85 & 110.98 \end{bmatrix}$$

$$EP_A^2 = \begin{bmatrix} 7.42 & 10.10 & 12.42 & 33.17 & 43.63 & 52.53 \\ 11.87 & 15.89 & 19.43 & 52.47 & 68.31 & 81.97 \\ 13.23 & 17.97 & 22.22 & 58.93 & 77.80 & 94.30 \end{bmatrix}$$

$$EP_B^1 = \begin{bmatrix} 4.07 & 5.86 & 7.47 & 8.16 & 24.88 & 37.39 \\ 6.96 & 9.71 & 12.20 & -3.26 & 14.56 & 28.11 \\ 7.76 & 11.01 & 13.99 & -13.24 & 5.16 & 19.30 \end{bmatrix}$$

$$EP_B^2 = \begin{bmatrix} 16.85 & 25.70 & 33.83 & -9.28 & 87.52 & 160.13 \\ 30.21 & 43.73 & 56.20 & -75.56 & 26.48 & 104.09 \\ 33.18 & 48.93 & 63.70 & -132.01 & -27.46 & 52.85 \end{bmatrix}$$

Fig. 5.11 shows the expected payoffs graphically. Each different colored curve shows the expected payoff ($) for a bidding strategy as a function of the assumed strategy of the opponent. There are four graphs since we are considering aggregators *A* and *B*, each with two possible types.

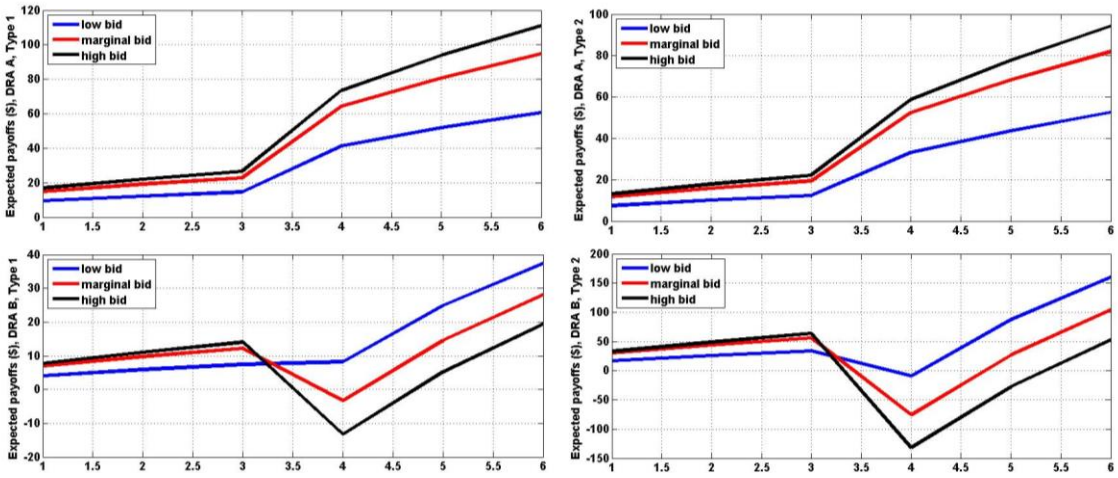

Figure 5.11: Expected payoffs of aggregators *A* and *B* in both types in game with no limitation and no scheduling

Inspecting the data, we see that *A* will choose strategy 3- "bidding above marginal cost" (row 3 is highlighted with gray color) for either of its types. *B* will also conclude that *A* will bid this way need only consider the best response to this strategy i.e. considering the 3rd and 6th columns of EP_B^1 and EP_B^2 which represents the payoffs for *B*'s possible strategies when competing against a player *A* who bids above marginal cost against any type of opponent: if *B* is type 1, it will receive the greatest payoff by bidding above marginal cost (blue array) in type 1 of *A* and bidding below marginal cost (red array) in type 2 of *A*; and if *B* is type 2, it will receive the greatest payoff by bidding above marginal cost (green array) in type 1 of *A* and bidding below marginal cost (purple array) in type 2 of *A*. Aggregator *A* knows that *B* will play this way, but has no incentive to change its strategy. Same colors show the corresponding payoffs for player *A*.

The colorful numbers are the payoffs corresponding to the optimal bidding strategy which leads to the Nash equilibrium pairs of the strategies. The Nash equilibrium is a "consistent" prediction of how the game will be played by rational players. All participants predict that a particular Nash equilibrium will occur and there is no incentive to play differently. The strategy

pairs in Nash equilibrium are the participants' strategies which maximize participants' conditional payoffs. That is, a participant could obtain at least the payoff at the equilibrium point (or it may obtain more depending on his opponent's strategy).

In this section, scheduling of WHs are based on only one objective function: social welfare. The situation of each WH is only based on hot water consumption (fig. 5.9) and is not effected by the electricity price (fig. 5.8).

5.4.2 Results of game with no limitation and with demand scheduling

In this section we wish to examine the effect of one player employing scheduling while its competitors do not, for comparison with the previous section where neither player scheduled their WHs. In this case, DP scheduler has been used to schedule the WHs of aggregator *A* only, based on the electricity price (fig. 5.8) with the joint objectives of social welfare (keeping water temperature in a given range 110-130°F as in fig. 5.9) and DR scheduling using DP. Similar to section 5.4.1, $P(elec_{\exp}) = 0.7083, P(elec_{ch}) = 0.2917$. Fig. 5.12 depicts scheduling of the WHs of aggregator *A* using DP (with inputs of data shown in figs. 5.8 and 5.9). The highlighted areas show the times when the electricity is expensive (prices higher than half of the maximum price).

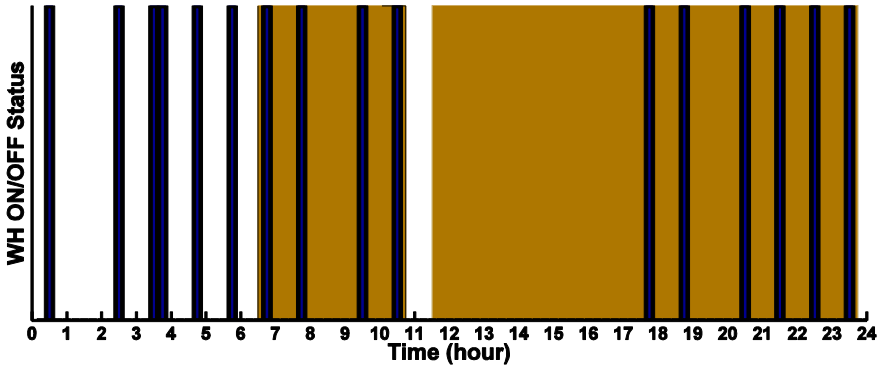

Figure 5.12: On/Off status of WHs in game with no limitation and with DR scheduling for the aggregator *A*

In this case, based on fig. 5.12 and equations of section 5.3.2.1.2:

$$P(\sigma_1) = P(elec_{\exp}) * P(WH_{off} / elec_{\exp}) = 0.7083 * 58/68 = 0.6041$$
$$P(\sigma_2) = P(elec_{\exp}) * P(WH_{on} / elec_{\exp}) = 0.7083 * 10/68 = 0.1042$$
$$P(\sigma_3) = P(elec_{ch}) * P(WH_{off} / elec_{ch}) = 0.2917 * 22/28 = 0.2292$$
$$P(\sigma_4) = P(elec_{ch}) * P(WH_{on} / elec_{ch}) = 0.2917 * 6/28 = 0.0625$$

In aggregator *A*, Comparison of fig. 5.10 with fig. 5.12 shows DR scheduling can curtail the load of WHs as much as 11.2%. Therefore the new demand of the aggregator *A* is: $P_A^{demand} = 0.888 * 200 * 4.5 * 10/6 + P_A^{gen} = 1{,}992kW$. Aggregators *B* and *C* do not schedule their WHs therefore, the demands of these aggregators are the same as in section 5.4.1: $P_B^{demand} = 2{,}394kW, P_C^{demand} = 2{,}478kW$. Because of the load curtailment, aggregator *A* has more power stored in its batteries to sell to the aggregator *C*. With the same probability distributions and same strategies as section 5.4.1 and following the same game process, the expected payoff matrices are:

$$EP_A^1 = \begin{bmatrix} 10.25 & 13.07 & 15.44 & 44.19 & 55.01 & 63.92 \\ 15.65 & 19.94 & 23.61 & 67.35 & 83.95 & 97.86 \\ 17.76 & 22.95 & 27.46 & 76.98 & 97.24 & 114.48 \end{bmatrix}$$

$$EP_A^2 = \begin{bmatrix} 8.18 & 10.94 & 13.33 & 36.22 & 46.95 & 56.06 \\ 12.67 & 16.77 & 20.37 & 55.66 & 71.77 & 85.60 \\ 14.10 & 18.93 & 23.24 & 62.38 & 81.53 & 98.23 \end{bmatrix}$$

$$EP_B^1 = \begin{bmatrix} 3.89 & 5.64 & 7.20 & 6.12 & 22.71 & 35.14 \\ 6.72 & 9.40 & 11.82 & -5.24 & 12.44 & 25.89 \\ 7.49 & 10.65 & 13.56 & -15.16 & 3.10 & 17.13 \end{bmatrix}$$

$$EP_B^2 = \begin{bmatrix} 16.05 & 24.64 & 32.54 & -20.56 & 75.59 & 147.74 \\ 29.08 & 42.22 & 54.36 & -86.46 & 14.85 & 91.92 \\ 31.94 & 47.26 & 61.64 & -142.50 & -38.73 & 41.01 \end{bmatrix}$$

Following the same reasoning used in section 5.4.1 for finding the optimal bidding strategy and Nash equilibrium, aggregator *A* obtains a higher payoff by bidding above its marginal cost (3rd rows). By inspecting the 3rd and 6th columns of EP_B^1 and EP_B^2, we learn that a rational participant *B* in type 1 would bid above its marginal cost for type 1 of *A* and would bid below its marginal

cost for type 2 of *A*. Same bidding strategy repeats for type 2 of *B*. The colorful numbers are the payoffs corresponding to the optimal bidding strategy which leads to the Nash equilibrium pairs of the strategies.

5.4.3 Results of Stackelberg game without demand scheduling

In the game with no constraint, there was no limitation for transacted powers and price for selling the stored energy between the aggregators. The transaction price and transaction powers are obtained from equation (5.21), but in real markets there will exist a controller who controls the transaction powers and transaction price. This independent controller is empowered by the utility and communicates with the utility to control the market. Communication devices are necessary for the game controller to talk to the aggregators in order to receive their bids (transaction powers and price) and also send them the control signal based on the limitations on transaction powers and transaction price.

Also the game controller needs to communicate with the utility to get information about the market constraints. In this case study, for the games with no limitation, the transaction prices (from equation (5.21)) varied between \$0.5063 and \$0.7522 in section 5.4.1 and between \$0.5017 and \$0.7452 in section 5.4.2. In this section, we consider the case where the controller limits the selling price of the stored energy; arbitrarily chosen for illustration purposes to be less than \$0.62 (a limit which will clearly effect the game). In the case of Stackelberg game without demand scheduling, the probabilities and strategies are the same as section 5.4.1, and the final expected payoffs are:

$$EP_A^1 = \begin{bmatrix} 9.52 & 12.28 & 14.62 & 41.32 & 51.93 & 60.72 \\ 14.89 & 19.13 & 21.75 & 64.38 & 80.81 & 81.41 \\ 16.94 & 20.82 & 21.42 & 73.77 & 79.94 & 81.42 \end{bmatrix}$$

$$EP_A^2 = \begin{bmatrix} 7.42 & 10.10 & 11.87 & 33.17 & 43.63 & 41.24 \\ 11.87 & 14.25 & 13.90 & 52.47 & 52.91 & 50.82 \\ 13.23 & 14.05 & 14.29 & 51.76 & 53.57 & 53.69 \end{bmatrix}$$

$$EP_B^1 = \begin{bmatrix} 4.07 & 5.86 & 7.47 & 8.16 & 24.88 & 37.39 \\ 6.96 & 9.71 & 11.23 & -3.26 & 13.25 & 23.91 \\ 7.76 & 10.56 & 11.03 & -13.24 & 1.85 & 12.96 \end{bmatrix}$$

$$EP_B^2 = \begin{bmatrix} 16.85 & 25.70 & 33.83 & -9.28 & 87.52 & 147.49 \\ 30.21 & 43.73 & 43.75 & -75.56 & 12.19 & 74.10 \\ 33.18 & 42.42 & 44.09 & -137.41 & -48.87 & 15.45 \end{bmatrix}$$

Because of limitations for transaction powers and price, the expected payoff values have been decreased in this game in comparison with the game with no limitation and unscheduled demand resources (section 5.4.1). The optimal bidding strategies and the Nash equilibrium of strategies are obtained using the same process mentioned in sections 5.4.1 and 5.4.2 which have been shown with colorful arrays in the above matrices.

5.4.4 Results of Stackelberg game with price-sensitive demand scheduling

In this case, aggregator *A* schedules its WHs based on the electricity price (fig. 5.8) and hot water consumption (fig. 5.9). Also, there are limitations in the market due to the constraints imposed by the controller which must be considered. This situation is the closest to reality in comparison with the other situations considered. The objective functions are both social welfare (keeping the water temperature of the houses in range of 110-130°F) and demand scheduling (based on electricity price and hot water consumption). Also, the real market policies (with real limitations) have been applied on this situation. In the game, the probabilities and strategies are the same as section 5.4.2 and the final expected payoff matrices are:

$$EP_A^1 = \begin{bmatrix} 10.25 & 13.07 & 15.44 & 44.19 & 55.01 & 63.92 \\ 15.65 & 19.94 & 23.22 & 67.35 & 83.95 & 87.07 \\ 17.76 & 22.17 & 22.81 & 76.98 & 85.10 & 86.73 \end{bmatrix}$$

$$EP_A^2 = \begin{bmatrix} 8.18 & 10.94 & 13.33 & 36.22 & 46.95 & 47.21 \\ 12.67 & 15.58 & 15.29 & 55.66 & 58.06 & 56.19 \\ 14.10 & 15.31 & 15.58 & 56.40 & 58.40 & 58.69 \end{bmatrix}$$

$$EP_B^1 = \begin{bmatrix} 3.89 & 5.64 & 7.20 & 6.12 & 22.71 & 35.14 \\ 6.72 & 9.40 & 11.24 & -5.24 & 11.53 & 22.20 \\ 7.49 & 10.49 & 10.98 & -15.16 & 0.18 & 11.29 \end{bmatrix}$$

$$EP_B^2 = \begin{bmatrix} 16.05 & 24.64 & 32.54 & -20.56 & 75.59 & 137.74 \\ 29.08 & 42.22 & 43.94 & -86.46 & 2.65 & 64.60 \\ 31.94 & 42.13 & 43.95 & -146.59 & -58.16 & 6.17 \end{bmatrix}$$

Because of the limitations in transaction price, the expected payoff values have been decreased in this game in comparison with the game with no limitation and without demand scheduling (section 5.4.2). The optimal bidding strategies and the Nash equilibrium of strategies have been shown with the colorful arrays in the above matrices. Because of the presence of a controller in the Stackelberg games enforcing more market restrictions in the game, payoffs of aggregator *A* and *B* have been decreased in section 5.4.3 in comparison with 5.4.1 and also in section 5.4.4 in comparison with 5.4.2.

5.5 Conclusions

In this work, game theory was applied to model the competition between DRAs for selling power which they had previously stored in residential storage devices, in a power market with other DRAs as buyers. The proposed method determines the optimal bidding strategy for each aggregator in order to maximize its own payoff. The situation naturally presents itself to competitors for market sales as a game with incomplete information -as any DRA is unable to precisely determine parameters associated with cost of operating other player's equipment and thus unaware of their prospective payoffs and bidding strategies.

In order to utilize the better developed theory of *c*-games with imperfect information we approximated local power demands using known hot water usage data (as WHs generally comprise the majority of energy expenditure) to approximate total loads and using public statistical data and a Bayesian approach to derive probability distributions for DRA types. We then examined and

applied our model to four variants in market conditions (construed as a determinant *c*-game through our procedure) to study the effects of pure competition (game with no limitation and without WH scheduling) and simple regulated competition (Stackelberg without WH scheduling).

We also considered both types of game with the addition of price-sensitive WH scheduling to examine the contrasting effect of adding DR to the games. Although the games with no limitation are admittedly quite idealized and would not be practical to implement for various reasons including, at least, those explained above, the Stackelberg games are relatively realistic and provide a possible beneficial alternative to currently popular market structures.

Application of our model to data compiled from the island of Maui served as a case study to analyze the results of our model under likely conditions, for the sake of clarity and concision of the presentations we considered a case of two competitors serving a single buyer; the procedure is fully scalable as it is essentially identical for larger numbers but quickly becomes cumbersome in presentation due to the large number of equations and the sizes of the matrices involved. Addition of DR in the form of price-sensitive WH scheduling increased payoffs to those DRAs which implemented it compared with those which did not. Payoffs were generally decreased in the regulated (Stackelberg) games compared with purer competition with no limitation.

Chapter 6

A Real-Time Demand Response Market through a Repeated Incomplete-Information Game

Abstract

In these days, DR programs have been developed to help traditional power market to meet the demand specially with increasing penetrations of renewable energies. This chapter focuses on application of a game-theoretic framework to model competition between DRAs to sell aggregated energy stored in storage devices directly to other aggregators in a market. Demand for power generated by the utility through combustion of fuel could be replaced, lowering emission of pollutants, when the energy used to charge the batteries is produced sustainably and traded on smaller scales. The proposed market is cleared in each time interval of a day using a repeated game-theoretic framework. Two non-cooperative games are studied: one without considering market's constraints in an unregulated competition and the other one is a Stackelberg game which includes a leader to control the transaction price and power in a regulated competition. Effect of DR scheduling has been shown in both games for increasing the efficiency of the market. In each time interval of a day, after clearing the market in an *i*-game, optimal bidding strategy has been determined for each aggregator in order to maximize the aggregators' payoffs. After finding the Nash equilibrium of strategies in each time interval, Dynamic Economic Dispatch (DED) is

performed in order to update the dispatch of the generators based on the updated demand. DED generates updated price signal for the next time interval. In other words, dynamic pricing has been considered in the proposed game-theoretic DR market framework in two forms: Real-Time Pricing (RTP) in each time interval of a day with updating demand and supply and TOU with demand price-based scheduling through DP.

The proposed method minimizes the emission, fuel, and operation costs and optimally schedules the generation in supply side. It also presents optimal prices during different periods i.e. valley, off-peak, and peak periods simultaneously. The customers in light of the utility's optimal price minimize theirs electricity costs and optimally schedule their power consumption in order to participate in the DR market and sell the energy stored in the storage devices. The presented model is applied to IEEE 24-bus model. DR scheduling (in the form of TOU) and RTP offer greater payoff for aggregators who implement it, compared with those who do not. Addition of transaction price and quantity regulations in Stackelberg game lowers payoffs for all aggregators participating in the market relative to unregulated competition. Obtained results indicate that the proposed DR market is mutually beneficial to utility and consumers alike and can bring about desired demand reduction in the power system.

6.1 Introduction

Development and implementation of smart grid technologies offers advantages over traditional electric utilities. Both parties (generation side and consumers) stand to benefit from proliferation of these technologies. End-users of electricity primarily wish to minimize the bill they pay to the utility for the energy they require to power their devices. Opposed to this, the utility company tries to maximize its own profit and is concerned with load scheduling as they must remain able to provide adequate supply. In this chapter, a repeated game-theoretic market model has been developed which DRAs compete with each other to sell aggregated energy stored in storage devices. The proposed model finds the optimal bidding decision for each aggregator to maximize

its own payoff in an *i*-game (as mentioned in chapter 5). In every time interval of a day, after finding the best bidding decision and Nash equilibrium of strategies through the game, a DED is performed to update the LMP based on the updated demand and updated generation supply.

Two types of non-cooperative games have been considered in this chapter: one is an unregulated game without limitation in transaction powers and price, and the other one is a Stackelberg game with a leader to control the transaction powers and price. Two different forms of dynamic pricing are considered in this chapter including TOU and RTP. TOU includes price-based scheduling of thermostatic storage loads such as WHs and ACs which DP has been used for this goal. RTP has been considered through updating LMP in each time interval using DED.

Dynamic pricing is a common method in attempts to influence the electrical energy consumption of residential end-users [205, 206, 207, 208, 209]. In [210], the interaction emerging among self-interested and foresighted consumers were modeled as a repeated energy scheduling game to prove that the stationary strategies are suboptimal in terms of long-term total billing and discomfort costs. In [157], a game theory based DR program was integrated into the dynamic economic emission dispatch problem to determine the optimal hourly incentive to be offered to customers who sign up for load curtailment. One of the main concerns in the TOU DR programs is the optimal pricing during different periods [211, 133, 212, 213, 214]. For solving this issue, DED has been used in literature. DED schedules generation units during the whole dispatch period in order to minimize the fuel costs [215] .

In this chapter, a repeated game-theoretic market model has been proposed where the game players are DRAs who compete with each other to sell aggregated energy stored in residential batteries. The proposed model finds the optimal bidding decision for each player to maximize its

own payoff in an *i*-game as mentioned in chapter 5. In each time interval of a day, best bidding strategy and Nash equilibrium of strategies are obtained through the proposed game model. After clearing the market in each time interval, LMPs are updated using DED based on the updated demand and generation. Two different games are considered. The first one is an unregulated non-cooperative game and there is no limitation in terms of transaction powers and price. The second one is a non-cooperative Stackelberg game which has a leader (managed by utility company) to control the transaction powers and price. The impacts of price-based demand scheduling (TOU) and RTP have been studied on the both games. DP has been used for price-based scheduling of thermostatic storage loads such as WHs. DED has been utilized for RTP and updating LMPs in each time interval. Fig. 6.1 shows a cycle which repeats in each time interval of a day based on the proposed game-theoretic model in this chapter. The initial price signal is updated in each time interval after clearing the market by the game and using DED. DED uses the updated demand to update generation supply in order to provide updated price signal [216, 217].

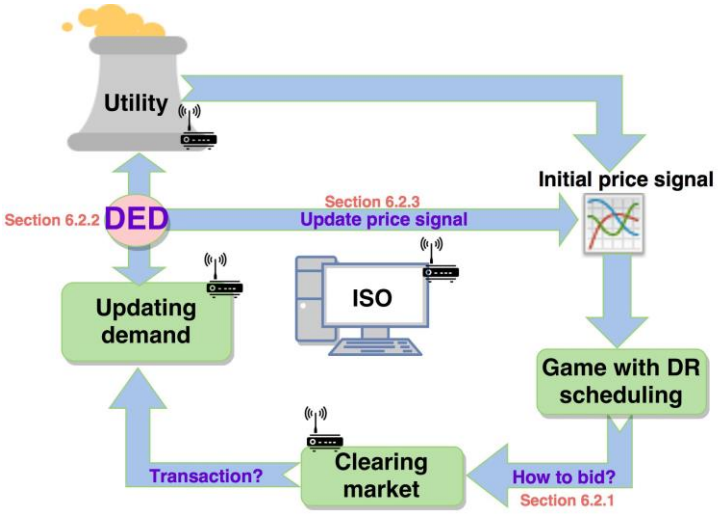

Figure 6.1: General schematic of the repeated game-theoretic DR market model

Section 6.2 of this chapter explains some principles for both mentioned games, DED, and the proposed repeated game-theorist model. The presented method has been applied on a case study (described in section 6.3) and its discussion and results have been provided in section 6.4. The summary of this research is available in section 6.5.

6.2 Repeated Game-Theoretic Market Method

This section contains the proposed market model based on the repeated game theory. The game-theoretic method to make competition between DRAs was described in sections 5.1 and 5.2 in detail which is used in each time interval of a day through an *i*-game. Section 6.2.1 includes a brief description of the used game-theoretic method in this chapter. Utilizing of DED and dynamic pricing have been explained in section 6.2.2. Section 6.2.3 includes the combination of game-theoretic model and DED as the proposed market model of this chapter.

6.2.1 Game theory algorithm

In this study, game theory has been used to model the competition between aggregators in order to maximize their own payoffs through selling aggregated energy stored in the residential storage devices. Based on the lack of information in an *i*-game, expected payoff values must be calculated using the probability theories because each DRA as a player does not have information about other players in terms of cost functions, strategies, payoffs, and etc. In each time interval of a day (one hour in this study), a game-theoretic market is cleared. This market model was explained in chapter 5 which its goals is to find the optimal bidding strategy by each DRA and obtain the Nash equilibrium of strategies.

In order to define the payoff function for each aggregator, cost function and bidding strategies of the aggregators are required which were explained in sections 5.1.2 and 5.1.3. Aggregator payoff function were defined in section 5.1.4. In this chapter the same game-theoretic market model as section 5.2 has been used for each time interval of a day. Two games are considered here in the following subsections. The first one is an unregulated game (as mentioned in section 5.2.2.1.2) and the second one is a Stackelberg game as a regulated game (as mentioned section 5.2.2.1.4). In both games, the effect of price-based demand scheduling has been considered. Since an *i*-game is used in this study, each aggregator as a player chooses a bidding strategy while other aggregators try to identify their best response to that strategy.

A general schematic of the unregulated game-theoretic market framework for each time internal has been represented in fig. 6.2. Seller DRAs compete to each other to sell the aggregated energy stored in their storage devices to other aggregators. The majority of the load in the case study of this chapter is thermostatic storages like WHs and ACs. Aggregators communication with a server (e.g. ISO) to submit their optimal bidding strategy (low, marginal cost, or high). Then, transaction price and transaction powers are obtained to clear the market in each time interval. In this type of game, there is no constraint for transaction powers and price. In order to price-based scheduling of demand, DP has been used as a block with two inputs (grid's electricity price and hot water usage of each aggregator) and one output (scheduling signal for WHs as TOU). The objective of the DP is to minimize the operation cost for generation side as well as end-users' cost considering the consumers' welfare.

Details of obtaining the optimal bidding strategy and Nash equilibrium of strategies were described in section 5.2.2.1.1. The Nash equilibrium is a prediction of how the game will be played.

The mentioned unregulated game (fig. 6.2) does not perfectly reflect a real world market model. Therefore, an regulated market has been explained here where an ISO controls the transaction powers based on the line capacities and controls the transaction price based on the market policies. This ISO might be utility company or any other center organized by the utility. This regulated game is called Stackelberg game which the ISO is the game leader and aggregators are the players.

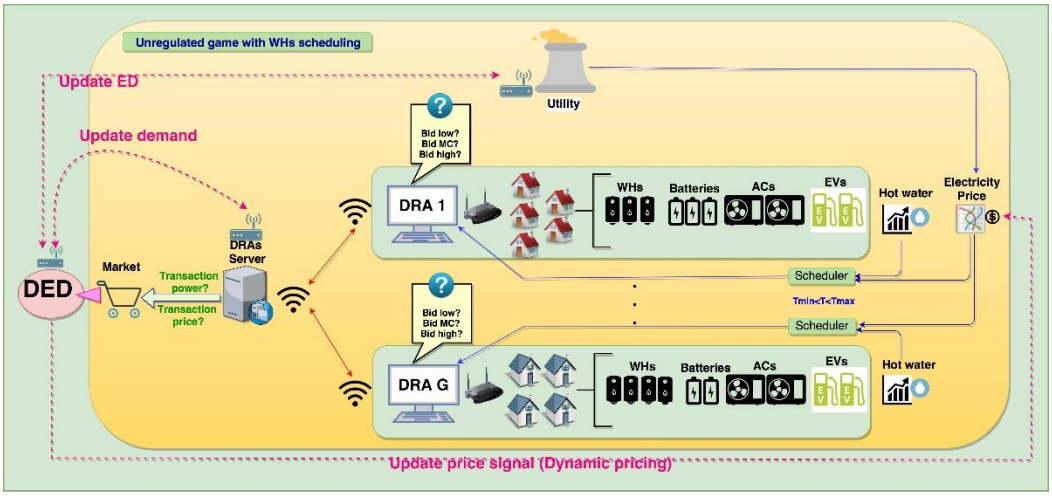

Figure 6.2: Schematic of the unregulated market with demand scheduling

The leader plays following the aggregators to control the market based on the constraints. In terms of finding the optimal bidding strategies and Nash equilibrium of the strategies, procedure of the regulated game (Stackelberg) is similar to what was explained earlier about the unregulated game with only one difference. The difference is that after calculating the transaction power (L_C) and the transaction price (ϕ_T) from system of equations (5.21), these values are controlled by the game leader to esnure they are in the allowed ranges. Fig. 6.3 shows the schematic of the regulated market model which demand scheduling has been considered.

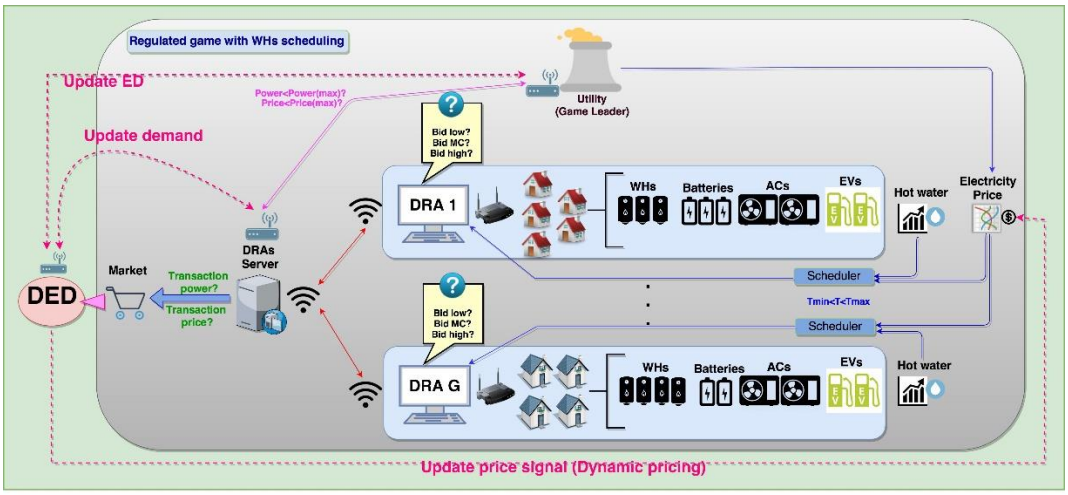

Figure 6.3: schematic of the regulated market with demand scheduling

6.2.2 Dynamic Economic Dispatch (DED)

After clearing the market in each time interval of a day through the explained game-theoretic market framework in section 6.2.1 and chapter 5, DED is utilized to determine the optimal scheduling of committed generating units' output whilst supplying the demand over a dispatch period at minimum operating cost and also satisfying ramp rate constraints among other constraints. Mathematical formulations of DED have been provided in this subsection. The objective function of the DED is to minimize the generation cost of N_G number of generators in each time interval $i \in I$:

$$\min \sum_{k=1}^{N_G} C_k^G(P_{k,i}), \qquad i \in I \tag{6.1}$$

with $$C_k^G(P_{k,i}) = \alpha_k + \beta_k . P_{k,i} + \gamma_k . {P_{k,i}}^2, \quad i \in I,\ k \in N_G \tag{6.2}$$

subject to the following network constraints:

$$\sum_{k=1}^{N_G} P_{k,i} = D_i + Loss_i, \quad i \in I \tag{6.3}$$

$$P_{k,min} \leq P_{k,i} \leq P_{k,max}, \quad k \in N_G \tag{6.4}$$

$$RR_k^L \leq (P_{k,i+1} - P_{k,i}) \leq RR_k^U, \quad i \in I, k \in N_G \tag{6.5}$$

$$P_{l,min} \leq P_{l,i} \leq P_{l,max},, \quad i \in I, l \in L \tag{6.6}$$

where C_k^G is operation cost of the k^{th} generator as a function of its power output in the i^{th} time interval ($P_{k,i}$). Coefficients of the quadratic cost function are: α_k, β_k, and γ_k. Equation (6.3) ensures that at any time i, total generated power equals the updated demand D_i after clearing the market by game-theoretic model, which transmission losses in the area during i^{th} time interval, $Loss_i$, has been considered. $P_{k,min}$ and $P_{k,max}$ are generation limits of the k^{th} generator. Constraint in equation (6.5) ensures that the generator ramp rate limits (RR_k^L, RR_k^U) are not violated and the final constraint is for the line flow limits of any transmission line $l \in L$. MATPOWER (as a package of MATLAB) has been used in this study for performing DED.

6.2.3 Repeated game theory using DED

In sections 6.2.1 and 6.2.2, the game-theoretic model and DED were described in details which both are used in each time interval of a day. The main proposed idea of this chapter is the combination of the game model and DED in order to consider dynamic pricing as described in fig. 6.1. More details are provided in fig 6.4.

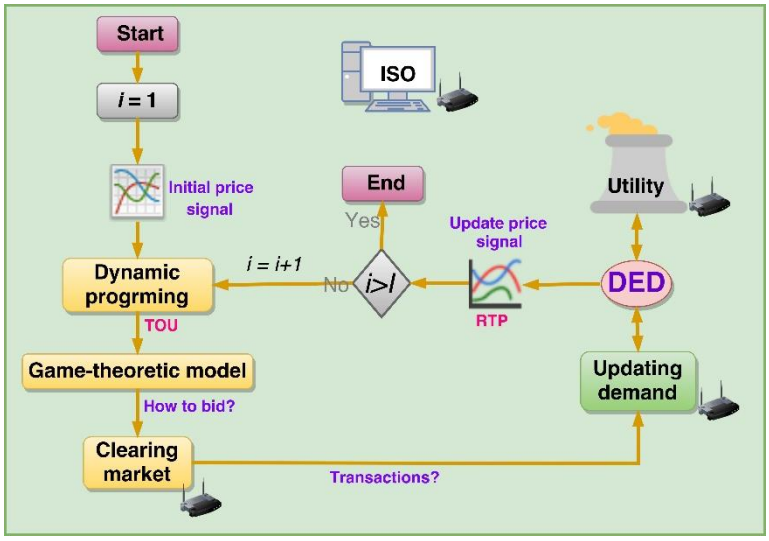

Figure 6.4: Repeated game-theoretic market model using DED for considering dynamic pricing

In each time interval i of a day ($i \in I$), aggregators compete to each other to trade the aggregated energy stored in the storage devices through an unregulated or regulated i-game as mentioned in section 6.2.1. DP has been used in order to price-based scheduling of thermostatic storage devices such as WHs. After clearing the market in each time interval i and obtaining the transaction powers and price through the game, demand is updated for the next time interval ($i + 1$). The updating is based on the change in the demand in the previous interval i because of demand scheduling and also trading the energy between the seller and buyer aggregates.

DED has been used to obtain the updated optimal dispatching of the committed generators whilst supplying the updated demand with satisfying all of the constraints. It leads to the updated price for each node of the grid. The updated price signal is different with the original price signal because the real-time demand and dispatch have been considered. For the next time interval, this updated price signal is used for demand price-based scheduling.

As fig. 6.3 shows, this loop repeats for the all *I* intervals of the day. In this repeated game-theoretic market model, two main types of dynamic pricing have been considered: TOU through the demand price-based scheduling and RTP through updating the generation dispatch based on the updated demand in each time interval of the day. Utilizing the dynamic pricing in this method, not only decreases the end-users' bills but also decreases the operation cost for utility company and decreases the pollution created by the generators.

6.3 Case Study

As a standard case study, IEEE 24-bus model (fig. 6.5) has been used and the purposed market model has been applied. Loads' data, lines' data, and generators' information are available in MATPOWER library [94]. MATPOWER software package (from MATLAB) has been used to perform DED in each time interval of a day.

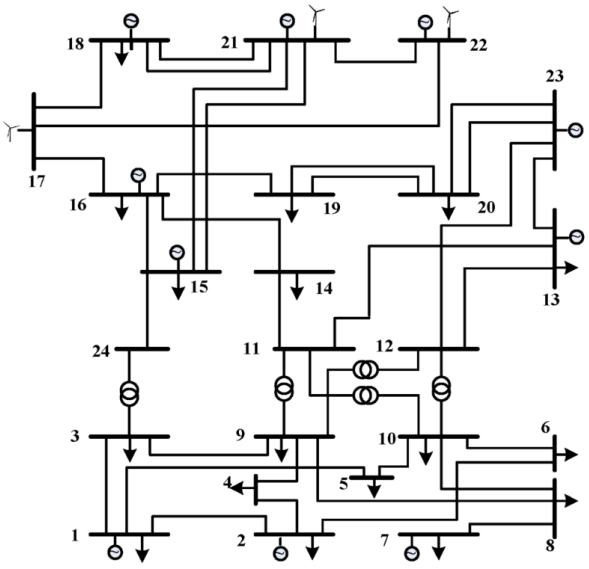

Figure 6.5: IEEE 24-bus model as a Case study

In the case study shown in fig. 6.5, there are three DRAs in buses 13, 15, and 18 as the largest loads. More details are illustrated in fig. 6.6 about these aggregators as game players in terms of number of houses, storage devices, and WHs. Aggregators *A, B,* and *C* show bus numbers 13, 15,

and 18, respectively. All houses of the mentioned aggregators participate in DR program based on the availability of their charged batteries. All houses have WHs assumed to draw the majority of the load (60%). For example aggregator *A* in bus 13 includes 25,305 houses which 90% of them are equipped to storage devices. Other similar information are available in fig. 6.6 (80% and 60% battery coverage in aggregator *B* and *C*).

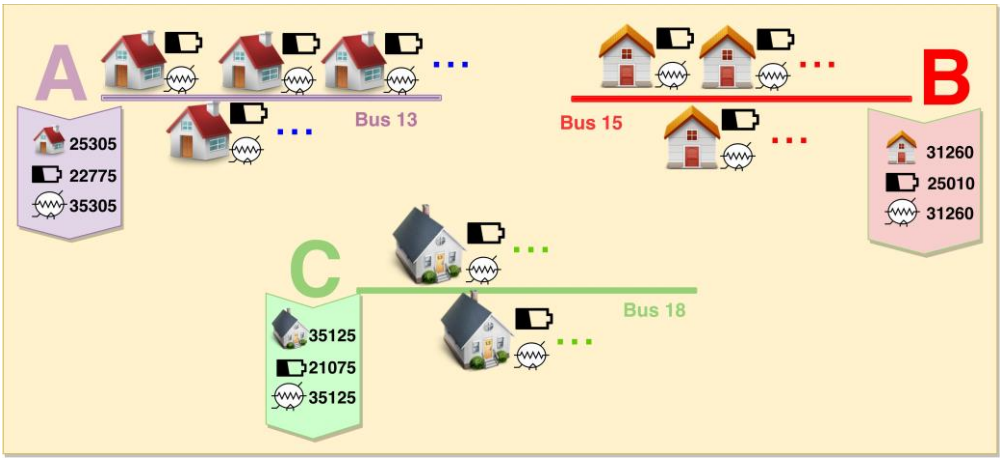

Figure 6.6: Load data of three aggregators in the case study

Nominal power of each residential battery is 3.3 *kW*. Therefore, the maximum generation capacity of each aggregator is: $P_A^{gen} = 75{,}158\text{kW}$, $P_B^{gen} = 82{,}533\text{kW}$, $P_C^{gen} = 69{,}548\,\text{kW}$.

In this case study, the nominal power of each WH is 4.5 *kW*. Thus, the total power demand of aggregator *A* in peak load time of the day (7-8 pm) is:

$$P_A^{demand} = 25{,}305 * 4.5 * 10/6 + P_A^{gen} = 264{,}945kW$$

Fig. 6.7 shows the peak load time of the day. Similarly, for other aggregators in peak load time:

$P_B^{demand} = 316{,}983kW, P_C^{demand} = 332{,}985kW$.

Since marginal cost of aggregator *C* is greater than other aggregators, *A* and *B* will compete to sell power to *C*. aggregators' discharging cost coefficients (players' types) are:

$$\text{Seller\_A}\begin{Bmatrix} a_A = [0.4, 0.43] \\ B = [200, 188] \end{Bmatrix},\quad \text{Seller\_B}\begin{Bmatrix} a_B = [0.42, 0.45] \\ B = [192, 188] \end{Bmatrix},\ \text{Buyer\_C}\begin{Bmatrix} a_C = 0.50 \\ B = 172 \end{Bmatrix}$$

Which shows $M = 2$ and $N = 2$ as the numbers of types. Both sellers, *A* and *B*, know the discharging cost coefficient of the buyer, *C*. As mentioned earlier, the Stackelberg game reflects the real world market better in comparison with the game without constraints. Therefore, the Stackelberg market model has been applied on the case study and the results have been obtained considering dynamic pricing.

6.4 Discussion and Results

The repeated game-theoretic market model has been applied to the previously mentioned case study in section 6.3. This section includes the results in two subsections: subsection 6.4.1 contains results of the game theory in order to obtain the optimal bidding strategy of the players and find the Nash equilibrium of strategies in one time interval of a day which is peak load time from 7pm to 8pm. Repeated game theory model has been used to clear the market every hour of the day. Since it is not possible to show the whole game's results for 24 hours based on the space limitation, only the results for the peak load hour has been demonstrated in this chapter. Subsection 6.4.2 includes the results of real time pricing after applying the repeated game theory model in every hour of the day.

6.4.1 Game results in peak load hour

Fig. 6.7 shows the normalized electricity price in one day of the mentioned case study which is available for every 15 minutes. This price signal (given in advanced by utility) is used to manage TOU in WHs. The normalized average hot water consumption for the houses of aggregators *A* and *B* is shown in Fig. 6.8.

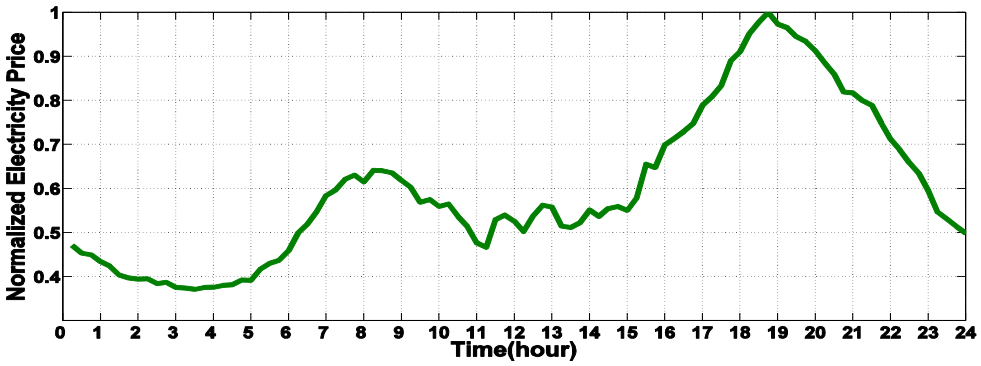

Figure 6.7: Normalized electricity price in one day of the case study (every 15minutes)

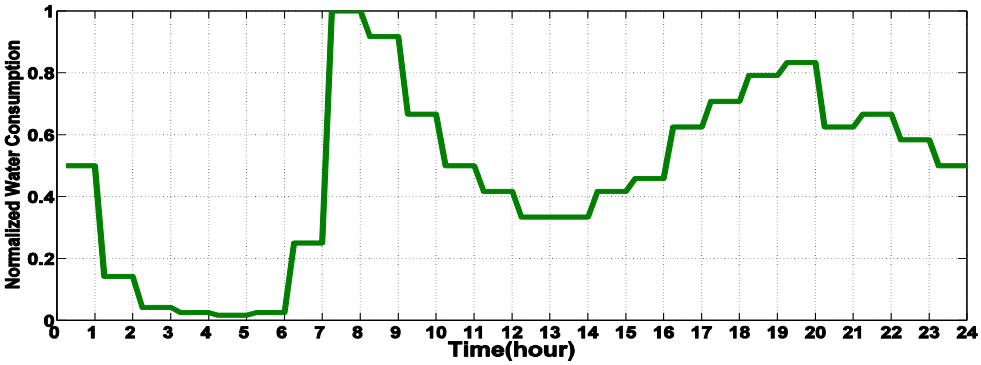

Figure 6.8: Normalized average water consumption for houses of seller aggregators of the case study

Results of the regulated game (Stackelberg) with demand scheduling for peak load time of the day are presented in this section. DP scheduler has been used to schedule the WHs of aggregators *A* and *B*, based on the electricity price (Fig. 6.7) to ensure the consumers' welfare for keeping the water temperature in a given range [110,130]°F using fig. 6.8. For our purpose, we take prices over half of the normalized price of electricity to be "expensive". From the normalized price data (Fig. 6.7), $P(elec_{ch}) = 0.2917, P(elec_{ex}) = 0.7083$. Fig. 6.9 shows status of the WHs in aggregators *A* and *B* without price-based scheduling. Fig. 6.10 depicts scheduling (TOU) of the WHs of aggregator *A* and *B* using DP with inputs of data shown in figs. 6.7 and 6.8. Highlighted

areas of fig. 6.10 show the times when the electricity is expensive which the electricity price is higher than half of the maximum price.

Figure 6.9: On/off status of WHS in aggregators *A* and *B* without demand scheduling

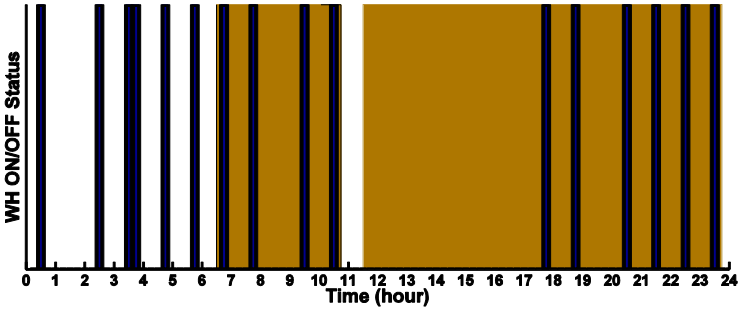

Figure 6.10: On/off status of WHS in aggregators *A* and *B* with demand scheduling through DP

Using the results shown in fig.13 and equations of section 2.1.1:

$$prob(\sigma_1) = prob(elec_{ex}) * prob\left(wh_{off}\middle|elec_{ex}\right) = 0.7083 * 58/68 = 0.6041$$
$$prob(\sigma_2) = prob(elec_{ex}) * prob(wh_{on}|elec_{ex}) = 0.7083 * 10/68 = 0.1042$$
$$prob(\sigma_3) = prob(elec_{ch}) * prob\left(wh_{off}\middle|elec_{ch}\right) = 0.2917 * 22/28 = 0.2292$$
$$prob(\sigma_4) = probP(elec_{ch}) * prob(wh_{on}|elec_{ch}) = 0.2917 * 6/28 = 0.0625$$

The number of 15-minute intervals corresponding to the expensive and cheap electricity are 68 and 28 out of 96, respectively. In aggregators *A* and *B*, Comparison of figs. 6.9 and 6.10 shows demand scheduling can curtail the load of WHs as much as 11.2%. Therefore the new demand of these aggregators are:

$P_A^{demand} = 0.888 * 25{,}305 * 4.5 * 10/6 + P_A^{gen} = 243{,}690kW$ and $P_B^{demand} = 290{,}720kW$.

Aggregator *C* as buyer does not schedule its WHs. Therefore, the demand of aggregator *C* is the same as the calculated number in section 6.3: $P_C^{demand} = 332{,}985kW$.

After scheduling the WHs and load curtailment, aggregators *A* and *B* have more power stored in the batteries to sell to the aggregator *C* to increase their payoff. Probability distributions for both players *A* and *B* in the previously mentioned scenarios are:

$$\Psi_A^1 = [0.16, 0.84], \Psi_B^1 = [0.21, 0.79], \Psi_A^2 = [0.11, 0.89], \Psi_B^2 = [0.18, 0.82],$$
$$\Psi_A^3 = [0.75, 0.25], \Psi_B^3 = [0.67, 0.33], \Psi_A^4 = [0.69, 0.31], \Psi_B^4 = [0.60, 0.40].$$

Using equation (5.20), the expected probabilities are:

$$\pi_{11} = 0.1613,\ \pi_{12} = 0.1503, \pi_{21} = 0.1566, \pi_{22} = 0.4275.$$

Conditional probabilities of players *A* and *B* are calculated using equations (5.15) and (5.17):

$$\eta_A^1 = [0.52, 0.48], \eta_B^1 = [0.51, 0.49], \eta_A^2 = [0.27, 0.73], \eta_B^2 = [0.26, 0.74].$$

Each player chooses one of the following strategies: bidding 80% of marginal cost ($\varepsilon_{S1} = 1.6$), bidding marginal cost ($\varepsilon_{S2} = 2$), or bidding 120% of marginal cost ($\varepsilon_{S3} = 2.4$). Therefore, the strategies are:

$$s_A^1 = [0.000016, 0.00002, 0.000024]$$
$$s_A^2 = [0.000019, 0.000024, 0.000029]$$
$$s_B^1 = [0.000018, 0.000023, 0.000027]$$
$$s_B^2 = [0.00002, 0.000025, 0.00003]$$

Transactions prices change between \$1.38 and \$2.11 per unit of power in the peak load time. In the regulated game (Stackelberg), the game leader controls the transaction price to be less than \$1.80 per unit of power. Finally, from the equations (5.14) and (5.16), the expected payoff values in the regulated game with price-based demand scheduling are:

$$EP_A^1 = \begin{bmatrix} 8{,}848 & 11{,}340 & 13{,}439 & 9{,}386 & 11{,}757 & 13{,}718 \\ 13{,}596 & 17{,}394 & 20{,}645 & 14{,}401 & 18{,}046 & 20{,}711 \\ 15{,}442 & 20{,}034 & 21{,}566 & 16{,}473 & 19{,}867 & 20{,}371 \end{bmatrix}$$

$$EP_A^2 = \begin{bmatrix} 3{,}729 & 4{,}993 & 6{,}089 & 11{,}866 & 15{,}447 & 18{,}487 \\ 5{,}803 & 7{,}690 & 7{,}942 & 18{,}349 & 21{,}791 & 21{,}404 \\ 6{,}459 & 7{,}716 & 7{,}928 & 20{,}501 & 21{,}472 & 21{,}803 \end{bmatrix}$$

$$EP_B^1 = \begin{bmatrix} 4{,}457 & 6{,}449 & 8{,}233 & 3{,}428 & 12{,}647 & 19{,}541 \\ 7{,}721 & 10{,}784 & 13{,}554 & -2{,}683 & 7{,}175 & 13{,}405 \\ 8{,}606 & 12{,}229 & 13{,}783 & -8{,}073 & 1{,}099 & 7{,}291 \end{bmatrix}$$

$$EP_B^2 = \begin{bmatrix} 3{,}480 & 5{,}307 & 6{,}984 & -5{,}008 & 23{,}870 & 45{,}385 \\ 6{,}301 & 9{,}099 & 10{,}794 & -24{,}374 & 4{,}511 & 23{,}136 \\ 6{,}917 & 10{,}001 & 10{,}537 & -40{,}999 & -14{,}042 & 5{,}339 \end{bmatrix}$$

According to the above matrices, we see that *A* will choose its 3rd strategy, ε_{S3}, and will bid above the marginal cost (row 3 is highlighted with gray) for either of its types. *B* will also conclude that *A* will bid this way need only consider the best response to this strategy i.e. considering the 3rd and 6th columns of EP_B^1 and EP_B^2 which represent the payoffs for *B*'s possible strategies when competing against a player *A* who bids above marginal cost against any type of opponent: if *B* is type 1, it will receive the highest payoff by bidding above marginal cost (blue color) in type 1 of *A* and bidding below marginal cost (red color) in type 2 of *A*; and if *B* is type 2, it will receive the highest payoff by bidding marginal cost (green color) in type 1 of *A* and bidding below marginal cost (purple color) in type 2 of *A*. Aggregator *A* knows that *B* will play this way, but has no incentive to change its strategy. Same colors show the corresponding payoffs for player *A*. The colorful numbers are the payoffs corresponding to the optimal bidding strategy which leads to the Nash equilibrium pairs of the strategies. The strategy pairs in Nash equilibrium are the participants' strategies which maximize participants' payoffs. That is, a participant could obtain at least the payoff at the equilibrium point (or it may obtain more depending on its opponent's strategy).

The above results are related to one time interval of day corresponding to peak load time through Stackelberg game with demand scheduling. After clearing the market and obtaining the Nash equilibrium in this interval, power of 114.68MW is sold to aggregator *C* from *A* and *B* which is about 4% of the peak demand in the mentioned case study. Because of the presence of a leader (controller) in the Stackelberg game enforcing more market restrictions in the game, payoffs of aggregator *A* and *B* have been decreased in comparison with the unregulated game.

6.4.2 RTP results

We use the repeated game theory to clear the market in each time interval of a day (every one hour). In section 6.4.1, we showed the game and Nash equilibrium results only in one time interval of the day corresponding to peak load time from 7pm to 8pm. After applying the same game-theoretic method to all time intervals of the day and clearing the market in each time interval, the initial daily price signal will be updated to a real-time one.

In the results below (figs. 6.11 and 6.12) three different situations have been considered. The first situation is the initial (traditional) condition for load and electricity prices. In this situation there is no DR program. In the second situation, price-based demand scheduling has been performed through DP. The scheduling program includes thermostatic loads such as WHs and uses two parameters for scheduling: given electricity price by utility in fig. 6.7 and given hot water usage in fig. 6.8. In figs. 6.11 and 6.12, updated demands and electricity prices in the second situation have been demonstrated with the green bars. The second situation includes TOU for the majority of the loads. In the third situation, the proposed repeated game-theoretic model has been used as well as price-based WH scheduling. In each time interval, updated demands and updated prices have been calculated through DED as explained in section 6.2.3. In the third situation, two

types of dynamic pricing have been considered including TOU and RTP. Fig. 6.11 shows the load of buses 13 and 15 (sellers) and 18 (buyer) of the case study in the mentioned situations.

The red bars of fig. 6.11 show the demand deduction after price-based scheduling based on the given electricity price by utility (fig. 6.7) and hot water consumption (fig. 6.8) through DP. After using the proposed repeated game method and considering TOU and RTP simultaneously, loads of buyers (bus 13 and 15) don't change from the second to the third situation because they need to keep their batteries charged and ready for sale to bus 18. But in bus 18, a part of the load is fed by the stored energy in busses 13 and 15 and this part of load does not need any power from the generation side of the grid. Therefore, the load of bus 18 is decreased in utility's point of view.

Fig. 6.12 shows the LMP of buses 13, 15 (sellers) and 18 (buyer) in the mentioned situations. Fig. 6.12 shows decreasing the LMP in the second situation because of shedding some WHs after using TOU. Another decreasing is observed in LMP after using the repeated game theory and applying TOU and RTP simultaneously.

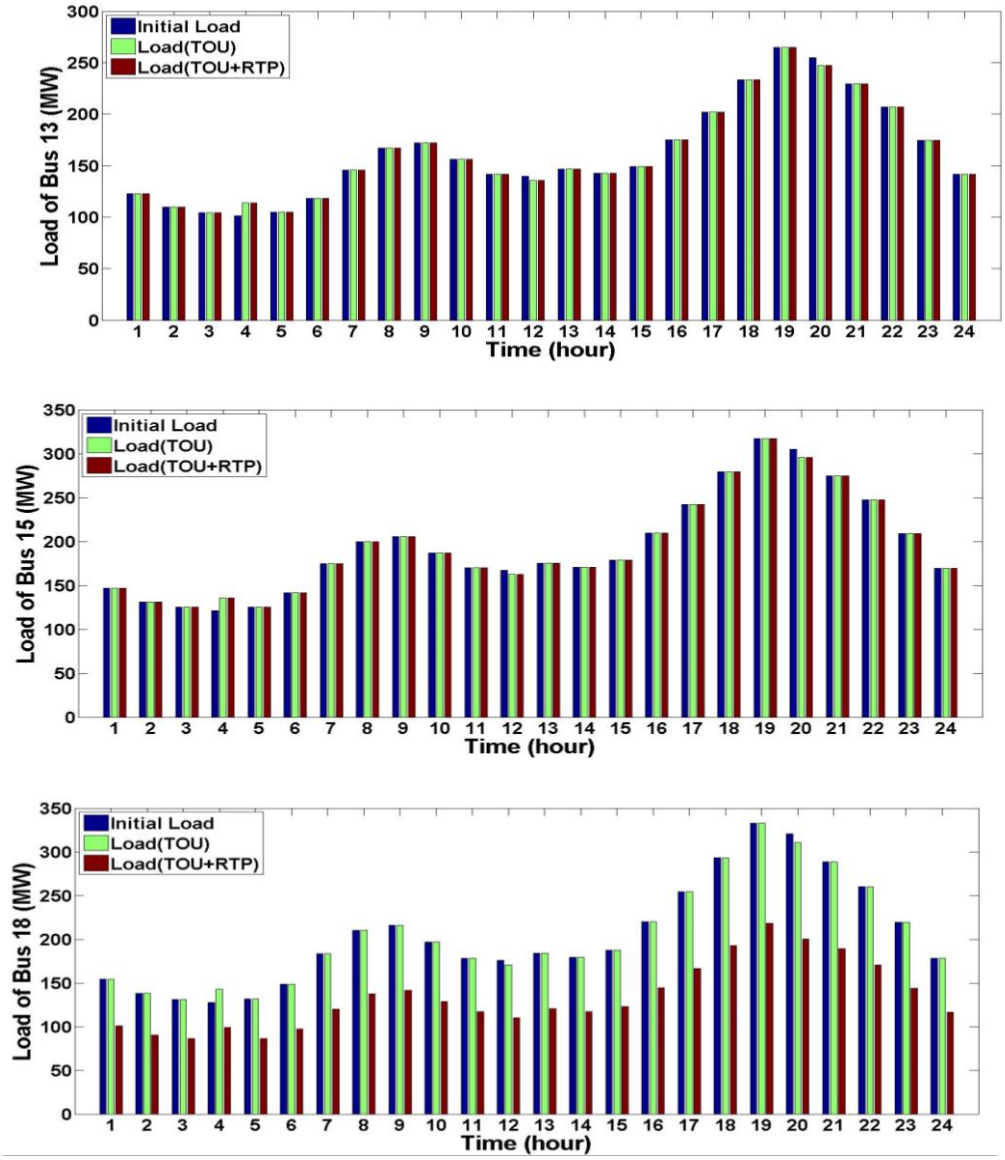

Figure 6.11: Updating demand in three mentioned situations: initial load, with TOU, with TOU and RTP

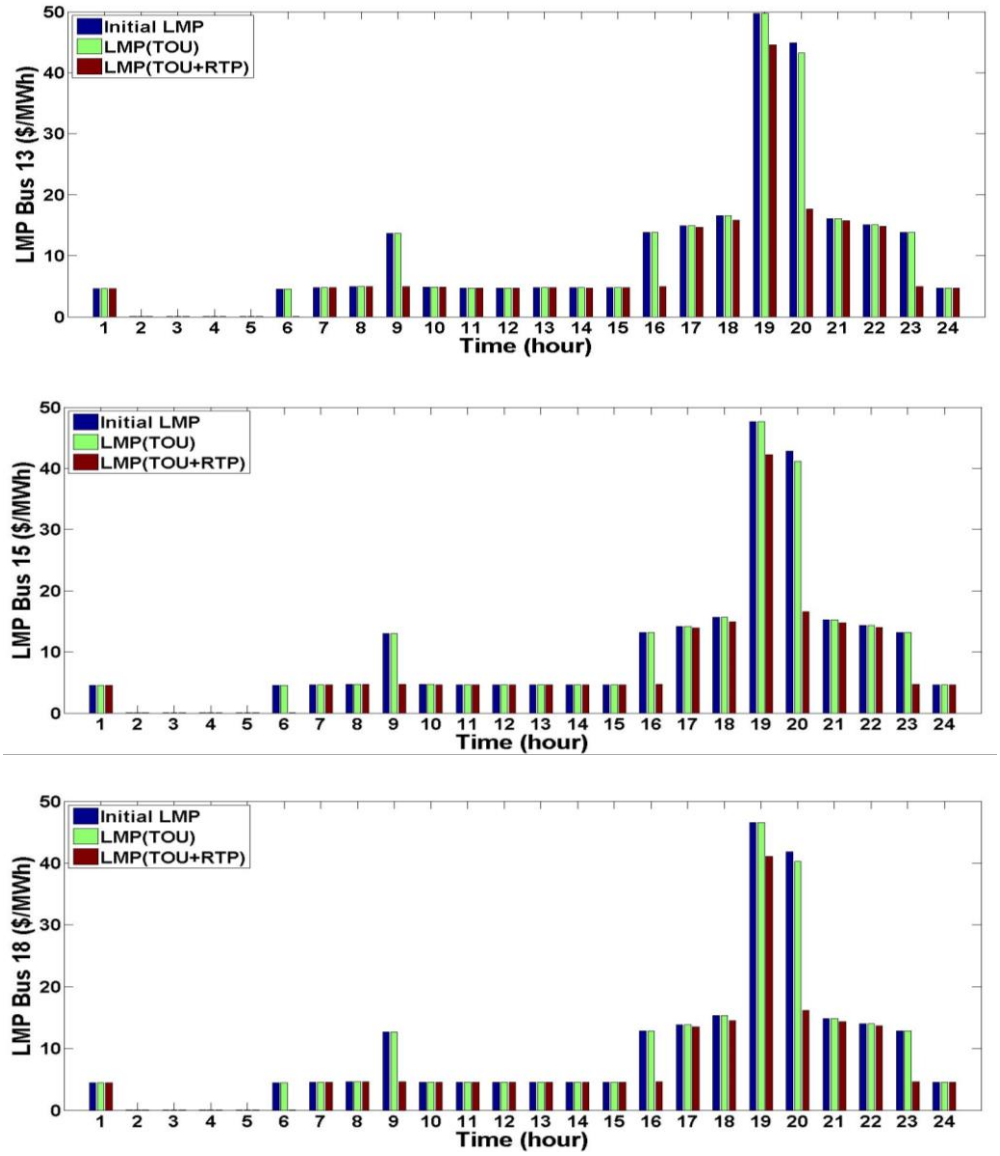

Figure 6.12: Updating LMP in three mentioned situations: initial LMP, with TOU, with TOU and RTP

6.5 Conclusions

In this chapter, a repeated game-theoretic market model has been developed to model the competition between DRAs for selling energy stored in electrochemical storage cells, in a power market with other DRAs as buyers. The proposed model finds the optimal bidding decision for each aggregator to maximize its own payoff in a game with incomplete information as any player is unable to determine parameters associated with cost of operating other player's equipment. In order to utilize the better developed theory of *c*-games with imperfect information we approximated local power demands using known water usage data by assuming that it was the major component of the local loads and using public statistical data and a Bayesian approach to derive probability distributions for DRA types.

In every time interval of a day, after finding the best bidding decision and Nash equilibrium of strategies through the game, DED was performed to update the LMP based on the updated demand and updated generation supply. Two types of non-cooperative games were considered in this chapter: an unregulated game without limitation in transaction powers and price, and a Stackelberg game (as a regulated game) with a leader to control the transaction powers and price. Stackelberg game is relatively realistic and provides a possible beneficial alternative to currently popular market structures.

Two different forms of dynamic pricing were considered in this work: one was TOU through price-based scheduling of thermostatic storage loads such as WHs and ACs which DP was used for this goal. The other one was RTP which includes updating LMP in each time interval of the day using DED. Results showed that the players' payoffs were decreased in the regulated (Stackelberg) game compared with the unregulated competition.

The game-theoretic based method is useful for energy management in distribution network since end-users can participate in a DR market to sell the energy stored in their batteries. This market also can help the utility company to decrease the amount of reserves through proving different types of AS which helps to reduce air pollution.

The University of Hawaii's Renewable Energy Design Lab (REDlab) is currently developing hardware systems capable of implementing the presented model. Further work will be forthcoming exploring the implications of our game-theoretic competition model utilizing an alternative market structure in the state of Hawaii where we currently face difficulties with integration of larger numbers of PV systems into the legacy grid. Much more work will be required if we are to reach the states 100% renewable energy goals.

Chapter 7

Networked Stackelberg Competition in a Demand Response Market

Abstract

In the classical Cournot competition model, each firm tries to maximize its own payoff by deciding an optimal strategy for determining the quantity of goods produced during each time period-–i.e. turn, of the game. In the typical application, all firms compete in the same market. In more recent economic models, firms compete across a number of markets simultaneously. In this situation, a Networked Cournot Competition (NCC) graph models the relationship between firms and markets. This chapter describes a model of competition among DRAs (as firms) to sell energy (as a homogenous good) stored in an aggregation of residential battery energy storage systems in a networked environment where market constraints are effected and trades are generally facilitated through the actions of a market maker who's turn is sequentially distinct from the other players. We call this game Networked Stackelberg Competition (NSC). The impact of strategic anticipative behavior in networked markets is of paramount importance in distinguishing NSC from other competition models. For each firm, the optimal bidding strategy and Nash equilibrium are obtained through analyses of in an *i*-game as mentioned in chapters 5 and 6. DRAs submit quantity bids and the market maker (system operator) controls the transaction power and transaction price over the network subject to transmission constraints and other market policies. Criteria required for existence of uniqueness of a Nash equilibrium are presented, and efficiency of the game is also studied in this chapter demonstrating DR scheduling improves market efficiency. The details are presented in the application of a NSC model to real world case study data taken from the island of Maui, Hawaii.

7.1 Introduction

With increasing availability and widespread penetration of renewable energy generation resources, DR has generally been acknowledged as a suitable resource for increasing flexibility in modern smart-grid power systems [218, 219, 220, 221, 222, 133]. Following consistently increasing total power demand and increasing associated energy prices propelling conservation efforts, energy management strategies are instrumental in any current consideration of further improving performance or economy of modernized smart homes integrating renewable energy and battery energy storage systems [223, 224, 225, 226]. DR in the residential sector plays a vital role in the smart-grid framework allowing lower demand from utilities during peak use periods while integrating ever increasing numbers of distributed renewable energy generation and energy storage resources [227, 228, 229, 230, 126]. In this chapter, a networked competition model has been proposed for DRAs to sell a part of DR in the form of aggregated energy stored in residential batteries to each other.

Various models for economic competition in energy and power markets have been proposed in the literature. The most common models used to investigate underlying market structure and predict/explain market outcomes have the structure of games where players (competitors) must decide on a fixed amount of energy to provide to the market or on a fixed price per unit of energy. Stackelberg game structures allow incorporation of market regulations through the action of a dominant player which acts before all other players decidedly influencing the market [231]. An unconventional Cournot model was examined in the European Union natural gas market with three major suppliers in [232]. In [233] a simple linear-quadratic model of homogeneous oligopoly was presented allowing a fully-fledged comparative analysis (supply function competition and Cournot

competition) of different market games. An extended Cournot model was developed from the classical Cournot model in [234] by including the consideration of demand elasticity to investigate impact on the electricity market.

A Stackelberg game was utilized in [235] to analyze the double dividend effect of an electricity tax under the consideration of a tax revenue neutrality when the government uses the electricity tax revenue to subsidize development of greenhouse gas emission-reducing technology. In a day-ahead electricity market, strategic behavior of wind power producers was modeled in [236] by a Stochastic Cournot model in which wind uncertainty, and imbalance costs were considered for evaluating the expected profit. A Cournot model of the natural gas market in the European Union was proposed in [237] involving mixed-motives delegation in a politicized environment.

A Stackelberg game approach was used in [161] to describe a DR model for electricity trading between one utility company and multiple users, which is aimed at balancing supply and demand, as well as smoothing the aggregated load in the system. In another work, a stochastic–multiobjective Nash–Cournot competition model was formulated in an uncertain energy market [238] to show that a DR program can reduce electricity generation, electricity price, and carbon dioxide emissions under uncertainty and in tradeoff scenarios. A dynamically consistent extraction equilibria was derived and analyzed in [182] through a two-period discrete-time "Truly" Stackelberg model of non-renewable resource extraction, where firms move sequentially within each period and where both the leader and follower have market power.

A Dynamic management framework for water transfer between two interconnected river basins was presented in [239] using a dynamic modeling approach, which relies on non-cooperative game theory, to compare solutions with different information structures (Nash, open-

loop, Nash feedback, and Stackelberg) with the social optimum. To examine how differences in pollution parameters between post- and pre-merger markets affect the attractiveness, the authors of [240] examined conditions under which the attractiveness of a merger deal increases in a Cournot market with product differentiation and environmental externality.

In the market models mentioned above, the firms compete with each other in a single market. In many settings, though, firms compete with one another across several different markets or segments which may be treated as such due to significant economic differences prevalent. In the last three years, the concept of networked competition has begun to be proposed in energy and power markets. Computation of Nash equilibria (existence and uniqueness), is necessarily more detailed and computationally difficult when a network of markets and their competing firms and concomitant cost and price function complexities are treated. An algorithm was proposed in [241] for finding pure Nash equilibria of NCC games under diverse conditions.

In [242, 196] possible mechanisms employed by the market maker to balance supply and demand were analyzed for NCC. Three candidate objective functions were considered that the market maker optimizes: social welfare, residual social welfare, and consumer surplus. A characterization of the unique equilibrium was provided in [243] that highlights the relationship between production quantities and supply paths in the underlying network structure. Its results illustrate that qualitative insights from the analysis of a single market do not generalize when firms compete with one another in multiple markets. In a recent work, the authors of [203], examined the impact of strategic anticipative behavior in a networked market by comparing the efficiency of a networked Stackelberg equilibrium, where generators anticipate the market clearing actions of the system operator, with a networked Cournot equilibrium, where generators are not anticipative.

In this chapter, we consider an upgraded form of networked competition which takes the form a Stackelberg, rather than Cournot game. One objective of this work proposes a market framework based on the networked Stackelberg model for competition between DRAs to sell aggregated stored energy in residential storage devices. We are not aware of any networked competition models in the literature using DRAs as market participants. The other objective of this work is to model competition as a more realistic *i*-game which means that each player does not have any information about other players in terms of cost functions, bidding strategies, etc.

Most of the related works in the literature are based on the more readily treated *c*-game requiring the assumption that all players have much information about each other which does not adequately reflect actual conditions. Also in the current work, the effect of scheduling DR resources on players' payoffs has been studied. In addition, aggregated energy stored in residential batteries can be gainfully employed to provide different types of required ancillary services within the grid. A portion of this provides information useful for regulating grid frequency in abnormal situations using DRA provided energy [244, 245].

Fig. 7.1 outlines the contents of the chapter diagrammatically. Section 7.2 describes the differences between classical networked competition models (primarily Cournot's) and that currently under consideration (NSC). The proposed market structure is presented in section 7.3 which also describes the mathematical model of competition as a Stackelberg game and defines the relevant game-theoretical concepts. Section 7.4 explains the decision-making process used to find the optimal bidding plan by each firm under the conditions of an *i*-game. Outputs of section 7.4 are quantities and prices of power to be traded by DRAs in the market. In a *c*-game, section 7.4 can be skipped since the transaction prices and quantities are given (there is no need to calculate

them in block of sec. 7.4 in fig. 7.1). Next, sets of strategies (transaction powers and prices) are formed in section 7.5 in a Stackelberg competition with a market maker as the game leader. The optimal sets of strategies (anticipating the action of the market maker), the existence of Nash equilibrium, and the model's efficiency are explained in section 7.6. A real-world case study application from the Hawaiian Island of Maui in the United States and its corresponding results are presented in section 7.7. Finally, the work is summarized in section 7.8.

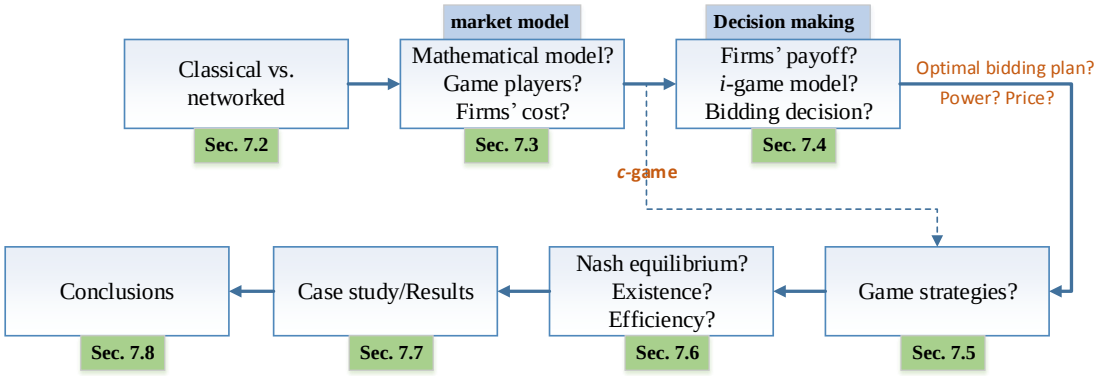

Figure 7.1. Outline of the chapter's contents

7.2 Classical Competition vs. Networked Competition

Classical competition models invariably have one market. A classical Cournot model is shown in fig. 7.2. J firms compete to sell power in the quantities $(q_1,...,q_J)$ in a single market. The commodity's price for aggregate quantity Q_J is a reverse function of demand: $p(Q_J)=x^{-1}(Q_J)$ which x is the demand function. A Nash equilibrium, Q_J^*, must satisfy:

$$p'(Q_J^*)(Q_J^*/J)+p'(Q_J^*)=c \tag{7.1}$$

where c is the production cost of firms (details may be found in [246]). If $J=1$, Q_J^* is the monopoly price and when $J\to\infty$, Q_J^* is the competitive price ($p(Q_J^*)\to c$).

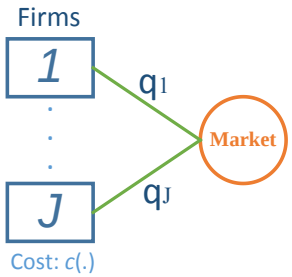

Figure 7.2. Diagram of classical Cournot competition (with one market)

In a networked competition model, there is more than one market. Fig. 7.3 shows the diagram for a networked competition Cournot model in which firms decide quantities to produce for each market. Consider a model with n firms $F = \{f_1, ..., f_n\}$ which produce an identical commodity and compete in m distinct markets, $M = \{m_1, ..., m_m\}$. Fig. 7.3 shows the graph of $G = (F \cup M, E)$, where E is a set of edges from the firms set (F) to the markets set (M) and represents the possible markets reachable. $F_i = \{m_k \in M \mid (f_i, m_k) \in E\}$ represents the set of markets f_i supplies to and $m_k = \{f_i \in F \mid (f_i, m_k) \in E\}$ represents the set of firms that supply to market m_k.

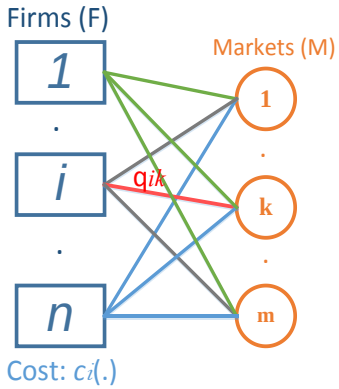

Figure 7.3. Diagram of networked Cournot competition (with more than one market)

In fig. 7.3, q_{ik} is the quantity firm f_i supplies to market m_k. In the Cournot model, firms compete by deciding quantities of a homogenous good to produce, meaning that they make

decisions to allocate their aggregate production among the markets in a particular way. Total aggregate supply determines sale price of marketable goods and cannont be arbitrarily chosen but is influenced by this decision. Cost of production for firm f_i is given by $c_i\left(\sum_{j\in F_i} q_{ij}\right)$. The price at market m_k is given by $p_k\left(\sum_{j\in M_k} q_{jk}\right)$. The goal is to maximize the profit of the i^{th} firm:

$$\max_{q_{ik}\geq 0} \quad \sum_{m_k\in F_i} q_{ik}.p_k\left(\sum_{j\in M_k} q_{jk}\right) - c_i\left(\sum_{j\in F_i} q_{ij}\right) \tag{7.2}$$

where the first term is total revenue and the second term is the cost of production of the i^{th} firm. Profit of firm i is not separable across markets unless c_i is linear [246, 243]. It has been shown in [243] that there exists a unique Nash equilibrium when p_k is twice differentiable, concave, and strictly decreasing, and c_i is twice differentiable, convex, and increasing.

Abolhassani et al. [241] described the computation of equilibrium given these conditions. It was shown that three possibilities exist: in the first case, the NCC with linear inverse demand functions forms an ordinal potential game. This algorithm has a time complexity equal to the time complexity of a convex optimization algorithm with e variables. The best such algorithm has a running time $(O(e^3))$. In the second case, with a strongly monotonic inverse demand function, a polynomial-time algorithm $(poly(e))$ finds the optimum of the potential function which describes the market clearance prices and the technique is reduction to a nonlinear complementarity problem. In the last case, with separable cost function and concave inverse demand function, supermodular optimization is used to design a nested binary search algorithm which finds the equilibrium quantity vector q when the price function is a decreasing function of Q and the cost functions of

the firms are convex. This algorithm runs in time $O(n \log^2 Q_{\max})$ where $Q_{\max}$ is an upper bound on total quantity produced at equilibrium and n is the number of firms [241]. It is hard to characterize the equilibrium in any general sense but the problem becomes tractable when the market can be characterized with quadratic costs c_i and linear inverse demand p_k. We will show how to define and characterize these functions in our proposed market model to check existence and uniqueness of the Nash equilibrium as well as determine market efficiency.

Our networked competition model employs a "market maker", **M** which is an ISO that determines quantity and price to charge each firm to meet the current demand considering network constraints. In a grid these constraints are mainly the maximum capacities of connecting lines and Kirchhof's laws constraints (these constraints will be shown in equation (7.3) later). In this chapter, competition is modeled as an *i*-game where each player of the game (DRA) doesn't not have any definite information about other players cost or bids accept that of rationality. Two different models of networked competition may be considered in such a game-theoretic market framework:

1) NCC: in this model all firms (players) and **M** engage in a simultaneous-move game.

2) NSC: in Stackelberg game, first, all firms participate in a simultaneous game and then market maker **M** follows by making a sequential-move based on relevant constrains.

The focus of this chapter is NSC between DRAs for selling aggregated stored energy in residential batteries through an *i*-game.

7.3 Structure of the Proposed Market Model

This study focuses on a networked electricity market in which the commodity is aggregated stored energy in residential storage devices. We model this electricity market competition as a

game between DRAs both facilitated and constrained through distinct actions of the market maker. This section describes the structure of the proposed market model. Subsection 7.3.1 describes the mathematical structure of the network model. Subsection 7.3.2 describes the players of the game as firms and markets.

7.3.1 Network model

In this model $\Re$ shows a set of real numbers and $\Re_+$ is a set with non-negative numbers. For two given vectors u and w, we define $u \geq w$ if the vector $u - w$ is element-wise non-negative (u and w are in the same size). w^T shows the transpose of given vector $w \in \Re^N$ and w_{-i} is a vector including all elements in w except the i^{th} one: $(w_1,...,w_{i-1},w_{i+1},...,w_N)^T$. We consider a power network with n DRAs $(1,2,...,n)$ and e edges. Each node has a power source (aggregated power of residential storages) and a load (demand). This load is a fraction of total load of the node which is not committed to be fed necessarily by GENCO and might be fed by local batteries. Based on the definition for the load used in this model, the load is less than or equal to the power that could be supplied by batteries in each DRA. In this model, nodes are connected through transmission lines (or just lines). Constraints on the lines are described by the set:

$$\mathrm{Y} \coloneqq \{y \in \Re^N \mid \ -l \leq Z_y \leq +l,\ 1^T y = 0\} \tag{7.3}$$

Where the matrix $Z_{e\times n}$ is a shift-factor matrix including the admittances of the connecting lines between nodes. The capacities of these lines are given by: $l \in \Re_+^e$.

7.3.2 Players of the networked model

In this chapter, the electricity market has two sets of participants: DRAs who buy, and compete to sell, power stored in batteries and a separate player called the "market maker" described below:

7.3.2.1 DRAs (as friendly energy companies)

DRAs are independent energy solution providers which assemble the electricity demand of their clients into larger blocks. Participation is voluntary and compensation is established per contract with the DRA which then negotiates with GENCOs at the wholesale level and with Distribution Companies (DISCOs) for local power delivery. DRAs may sell the aggregated stored energy in residential storages to each other in a power market. Let the DRAs be indexed by the variable *k.* Each DRA may be conceptualized as two separate effective functional parts:

-Aggregated charged batteries (as power providing aspect of a DRA): this part plays the role of power sellers in the game. The aggregated charged batteries' part of DRA_k is shown as DRA_k^B with the available power capacity of B_k. Since an *i*-game has been considered in this chapter, each DRA does not have any information about other DRAs. After a game-theoretic process and calculation of expected payoffs of DRAs (section 5.3.2.1.1, step 5), DRA_k^B submits a quantity offer $q_{km} \geq 0$ (and price p_k) and incurs a cost $c_k(.)$ (section 5.2.2). The map $c_k : \Re_+ \to \Re_+$ is assumed to be continuously differentiable, strictly increasing, and convex with $c_k(0) = 0$. In section 5.2.2, we discussed how we obtain a convex cost function for each DRA.

-Aggregated load of end-users (as the consumer aspect of a DRA): this part includes aggregated loads of residential houses based on the load definition given in section 7.3.1. The

aggregated load in node *k* is shown as DRA_k^L which acts as a buyer of power in the game. We model price-taking consumers at each node k (DRA_k) with an inverse demand function $p_k : \Re_+ \to \Re$ that shows how much consumer side of DRA_k is willing to pay to consume d_k units of power from stored energies in batteries. A Linear demand function widely accepted in the literature ($a_k - b_k.d_k$) has also been used in this. Based on the definition given in section 7.3.1, d_k is a part of total demand in DRA_k which is not committed to be fed by GENCO and also $d_k \le q_k$.

7.3.2.2 Market maker (**M**)

The market maker is an ISO which chooses the $n \times 1$ vector $r := (r_1, ..., r_n)$ to rebalance quantities, where $-r_k$ denotes to the net power injection into node *k*. The market maker decides on the rebalancing quantities based on market mechanism that allocates demands and prices across the network. The market mechanism balances the supply and demand through feasible flow direction optimization over the network. Since the market maker **M** only transports the power between DRAs (neither consumes nor produces power), we have $1^T r = 0$ where 1 is a vector of ones with dimension *n* [242, 203].

Fig. 7.4 shows the proposed networked market model in this chapter including firms (DRA^B), markets (DRA^L), and market maker (**M**). Based on fig. 7.4, there is no transaction power from each firm *i* (DRA_i^B) to its own market (DRA_i^L) because in the proposed model DRAs sell the excess stored energy of aggregated batteries after feeding local loads ($i \in n$). It means if local demand needs to be fed, local aggregated batteries feed them first (as first priority) and then participate in the market. All firms and markets are equipped with communication devices to transfer data with

market maker in order to submit bids, offers, power quantities, price, available charged batteries, demands, etc. More details about the communication devices are available in appendix B.

The cost function of a DRA as a firm for selling energy to the market has a quadratic form which was explained in section 5.2.2.

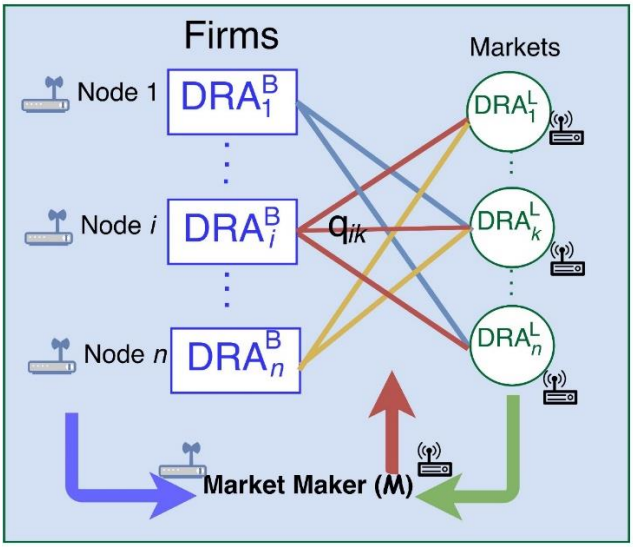

Figure 7.4. Diagram of the proposed networked competition model including DRAs and market maker

7.4 Decision Making Process in an *i*-game

In section 5.3.2.1, it was described the procedure employed by the DRAs to determine their optimal bids for quantity and price of a market transaction given incomplete information. Given complete information concerning competitor cost functions (a *c*-game which is currently unrealistic) section 7.4 can be skipped, because transaction price and power are completely determined.

A visual schematic of the proposed market framework is shown in fig. 7.5. Each aggregator manages a number of houses. The objective of the game formalization is to decide each DRA's optimal bidding plan which will maximize total payoff despite uncertainties associated with the

incomplete information available. As mentioned in section 4.2, price-based demand scheduling of the most significant loads (WHs) has been performed with a DP algorithm which schedules operational cycles of the devices considering GENCO price signal in a manner to minimize cost while satisfying adequate supplies of hot water as determined by average usage data. The DRAs communicate through a wireless network with a server (market maker, **M**) which controls the size and price of market transactions in agreement with constraints dictated by the utility such as necessary due to capacity of the connecting lines (equation (7.3)), etc.

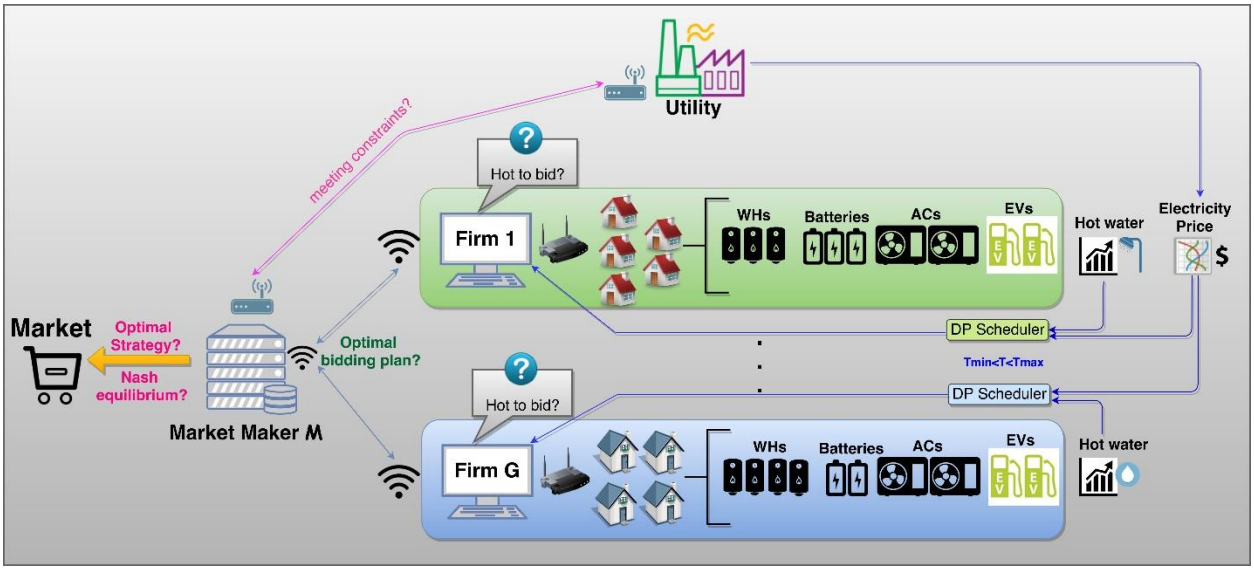

Figure 7.5: Diagram of the proposed market framework for competition between DRAs

Each player of the game wishes to maximize its own profit by choosing the appropriate bidding plan each turn and against any other player. In this work, we consider the conditions of an *i*-game to be the nearest approximation of reality. As mentioned in chapter 5, to determine the optimal bid plan, competitor cost and bid plan are estimated by a characterization into a finite number of "types" which cover the set of actual possibilities that may be encountered in the sense that we can define a mapping for any possibility to its nearest element in the set of types which is a proper

subset. As mentioned in chapter 5, the payoff corresponding to each bidding plan for each player of any type can then be calculated and compared directly to determine the optimal strategy each turn. Analysis of the conditions necessary for existence of the Nash equilibrium for the Stackelberg model and its efficiency are presented in section 7.6.

We consider an exemplary binary game between two aggregators, A and B, (as the firms in the networked model) to sell power to a third, C (as market in the model), who will buy the power. The same methods may be directly extended to an arbitrary number of competitors. For our purposes, the goal of the game is to calculate the expected payoff, EP_A^m, for the possible bidding plans for A (DRA_A^B) of type m (and similarly, EP_B^n, for firm B of type n) to choose the bidding plan for each turn of the game that maximizes expected payoff and determine the Nash equilibrium. 6 steps were described in section 5.3.2.1.1 in order to calculate the optimal bidding plan.

In applying our model, we assume that each firm has three possible bidding plans $\varepsilon_s = [\varepsilon_{s1}, \varepsilon_{s2}, \varepsilon_{s3}]$. The slope of the bidding curve is $m_i = \varepsilon_S \times u_i$ where $u_i$was defined in equation (5.9). The possible bidding plans are: bidding less than marginal cost ($\varepsilon_{s1} < 2$), bidding marginal cost ($\varepsilon_{s2} = 2$), and bidding more than marginal cost ($\varepsilon_{s3} > 2$).

From equations (5.14) and (5.16), the final form of expected payoff matrix of firm A of type m is:

$$EP_A^m = \begin{bmatrix} ep_{11}^1 & ep_{12}^1 & ep_{13}^1 & ep_{21}^1 & ep_{22}^1 & ep_{23}^1 \\ ep_{11}^2 & ep_{12}^2 & ep_{13}^2 & ep_{21}^2 & ep_{22}^2 & ep_{23}^2 \\ ep_{11}^3 & ep_{12}^3 & ep_{13}^3 & ep_{21}^3 & ep_{22}^3 & ep_{23}^3 \end{bmatrix} \quad (7.4)$$

The three rows of EP_A^m represent the three possible bidding plans that DRA A *(*of type *m)* must choose from. There are six possible strategies that A may encounter during a turn of competition

with *B*: *B* will be either type 1 or type 2, and in either case it may choose from three bidding plans as described in step 3 of section 5.3.2.1.1. Each column of EP_A^m corresponds to a bidding plan firm *A* may face in the market. For instance, ep_{12}^3 in EP_A^2 is *A*'s type 2 payoff when *A* uses bidding plan 3 and *B* is of type 1 playing bidding plan 2. EP_B^n is defined analogously. Each element of the expected payoff matrix has corresponding transaction price (p) and transaction power (q) which are obtained by solution of the system of equations shown in equation (5.21). The set of these pairs (p, q) form what are referred to as strategies matrices. A strategy matrix for firm *A* of type *m* is:

$$(P,Q)_A^m = \begin{bmatrix} (p,q)_{11}^1 & (p,q)_{12}^1 & (p,q)_{13}^1 & (p,q)_{21}^1 & (p,q)_{22}^1 & (p,q)_{23}^1 \\ (p,q)_{11}^2 & (p,q)_{12}^2 & (p,q)_{13}^2 & (p,q)_{21}^2 & (p,q)_{22}^2 & (p,q)_{23}^2 \\ (p,q)_{11}^3 & (p,q)_{12}^3 & (p,q)_{13}^3 & (p,q)_{21}^3 & (p,q)_{22}^3 & (p,q)_{23}^3 \end{bmatrix} \quad (7.5)$$

For instance, $(p, q)_{23}^1$ in $(P, Q)_A^1$ is strategy set of *A*'s type 1 (price, quantity) when *A* uses bidding plan 1 and *B* uses bidding plan 3 in its type 2. $(P, Q)_B^n$ is defined similarly. In a *c*-game game, sets of strategies are given and there is no need to make further calculations. The best strategy will be chosen consistently. But for the *i*-game, which is the focus of this study, strategy sets (and corresponding payoffs) must be calculated first using steps 1-5 of section 5.3.2.1.1 and then finally, in step 6 of section 5.3.2.1.1 a determination of the optimal bidding plan and strategy takes place. In step 6, the goal is to find the bidding plan (and corresponding strategy) that produces the highest payoff regardless of the other firms' type or bidding. In the following section 7.5, we will explain how optimal strategies are determined through comparison of the payoffs.

7.5 Payoff Functions and Strategy Sets

In section 7.4, after finding the optimal bidding plan for each firm *k*, DRA_k^B, the corresponding transaction price, p_k, and transaction quantity, q_k, are calculated by means of an *i*-game model of the competition between DRAs. As mentioned before, in a *c*-game (with given values of p_k and q_k) section 7.4 can be entirely skipped.

p_k is the price of power for node (or firm) *k* and q_k is the corresponding power quantity $(k \in n)$. According to "the supply and demand" economic model of price determination in a competitive market, we must have:

$$d_k := q_k + r_k \tag{7.6}$$

where r_k is an arbitrary constant that is used by the market maker to rebalance quantities at node *k*. Bidding price of each firm (DRA_k) is a direct function of demand as seen in equation (5.9). Therefore, $p_k(d_k) = p_k(q_k + r_k)$ which shows each firm at each node *k* has its own price p_k. Early it was explained that there are two sets of players which function very differently in the game: the aggregators $(DRA_1, ..., DRA_k, ..., DRA_n)$, and the market maker, **M**. The power source of DRA_k is paid as determined by the local nodal price $p_k(q_k + r_k)$. Thus, the profit (payoff) of the k^{th} firm is:

$$\prod_{DRA_k^B} = q_k . p_k(q_k + r_k) - c_k(q_k) \tag{7.7}$$

where $c_k(q_k)$ is the cost of producing power of q_k by the k^{th} firm. The objective function of the market maker **M** is:

$$\prod_M (p,q,r) = \sum_{k=1}^{n} \left(\int_0^{q_k + r_k} p_k(Q_k) dQ_k - c_k(q_k) \right) \tag{7.8}$$

As mentioned before, since this study focuses on an *i*-game, an action of DRA^B (following the procedure for bidding described in section 7.4 and chapter 5) affects the set of strategies for other $DRA^B s$. The set of strategies of DRA^B is shown as:

$$S := \{(p,q,r) \in \Re^n \times \Re^n \times \Re^n \mid \ q \geq 0, \ q + r \geq 0, \ r \in \mathrm{Y}\} \tag{7.9}$$

The values for transaction quantity (q) and price (p) are calculated following the steps of the *i*-game described in section 5.3.2.1 and solving the system of equations (5.21). In a *c*-game, set of strategies (p,q,r) is given but in an *i*-game, possible values of (p,q,r) are found following the procedure described in section 5.3.2. Each corresponding pair $(p,q,r) \in S$ is related to one strategy described in the bidding procedure. After finding the optimal bidding plan, the corresponding set (p,q,r).

The set of all possible strategies for the market maker, **M**, is given by:

$$S_M(q) := \{r \in \Re^n \mid \ (q,r) \in S\} \tag{7.10}$$

Since the fsocus of this chapter is on "regulated" market competition in an *i*-game (Stackelberg) anticipation of the market makers move plays a significant role. Each turn is divided roughly into two stages: first, all capable firms (DRAs) participate simultaneously in the game through bidding, this is followed sequentially by **M** (ISO or Utility) making its move [203]. The strategy set by Stackelberg game is then:

$$S_{G_k}(q_{-k}) := \{q_k \geq 0 \ \mid \ ((q_k, q_{-k}), r) \in S\} \tag{7.11}$$

when quantity offerings are allowed but anticipation of the market makers move is not, the Stackelberg competition reduces to Cournot competition.

7.6 Nash Equilibrium , Existence, and Efficiency

The computational process which determines the Nash equilibrium for competition modeled as a networked Stackelberg game has been demonstrated in [203]. We let $S^r := \{q \mid (p,q,r) \in S\}$ denotes the projection of the set S onto the coordinates in r where there exist a reaction function mapping $q \in S^r$ to $\rho(q) \in S(q)$. An action profile q^s and the corresponding map $\rho^s(.)$ determine a Stackelberg equilibrium, whenever:

$$\pi_m(q, \rho^s(q)) \geq \pi_m(q, \rho(q)) \tag{7.12}$$

For all $q \in S^r$ and all maps $\rho(.)$ from $q \in S^r$ to $\rho(q) \in S(q)$, and:

$$\pi_{G_k}\left(q_k^s, q_{-k}^s, \rho^s(q_k^s, q_{-k}^s)\right) \geq \pi_{G_k}\left(q_k, q_{-k}^s, \rho^s(q_k, q_{-k}^s)\right), \quad q_k \in S_{G_k}(q_{-k}^s) \tag{7.13}$$

In [203], it has been proven that an equilibrium always exists in networked Cournot competition but does not necessarily exist in networked Stackelberg competition even for the case of an unconstrained network ($l = \infty$ in equation (7.3)), but it exists provided that the price intercept of the inverse demand functions are spatially homogeneous (which means $p_j(0) = p_k(0)$, for all $0 \leq j,k \leq n$).

Since in the market model proposed in this chapter, the power flowing in transmission lines of the grid from one DRA to another originates from energy stored in batteries (as a fraction of total load), all connecting lines between firms have much more than enough capacity to flow the mentioned power between each other. In other words, the connecting lines of the grid have been

designed in advance to support much more than the maximum demand during peak times which exceeds the total aggregated storage capacity of the entire grid. Therefore, in our game, we can let $l = \infty$ in equation (7.3). Also, the price intercepts of the inverse demand functions are assumed to be spatially homogeneous as described above. Thus, using theorem 1 from [203], the Nash equilibrium must always exist in our proposed networked Stackelberg competition model.

In our case, given that the price intercepts of the inverse demand functions are spatially homogeneous, any equilibrium of the Stackelberg game is also an equilibrium of a classical non-networked Cournot game with an inverse demand curve aggregated from the individual nodal demand curves [203]. This allows us to apply well known existence results for classical Cournot games in our study. Proof of the existence of Nash equilibrium in a market where firm *k's* cost function, c_k, and inverse demand function D^{-1} in classical (non-networked) games may be found in [203, 247, 248].

There is an example in [203] which demonstrates that in the case of two firms in an unconstrained network $(n = 2,\ l = \infty)$, when the price intercepts of the inverse demand functions are not spatially homogenous, the aggregate demand function *D* may not be concave in which case existence of Nash equilibrium is not guaranteed. But in our work, as emphasized previously, the price intercepts of the inverse demand functions are spatially homogenous implying existence of Nash equilibrium.

In addition to the existence theorem, it has also been proven in [203] that the price of anarchy in networked Cournot competition can be unbounded (in the worst case) when firm are not anticipative of the following market maker moves, but in the case of unconstrained Stackelberg

competition we focus on, price of anarchy is bounded above by 3/2 whenever firms are anticipative. This result shows that our model is much more efficient than Cournot competition.

7.7 Case Study and Results in a 3-Node Network

Consider a system including three aggregators labeled A, B, and C ($DRA_A^B, DRA_B^B, DRA_C^B$ as firms and $DRA_A^L, DRA_B^L, DRA_C^L$ as markets); load data for these three was taken from a real grid model on the island of Maui (Hawaii-United States) [204]. A includes 200 houses, all of which contain battery energy storage systems. B manages 240 house, but only 180/240 are equipped with storage devices. C manages 260 houses of which only 160/260 are equipped with storage devices. All houses have WHs (or other similar thermostatic storages) that are assumed to draw the majority of the load (60%) [204]. Fig. 7.6 depicts graphically the most relevant relationships and data in the present case study.

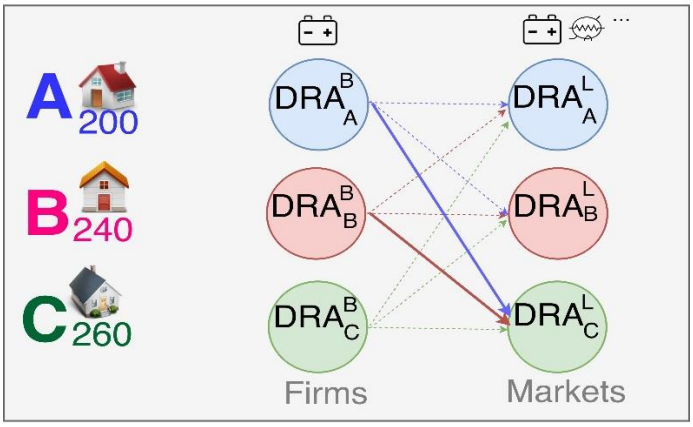

Figure 7.6: Networked graph of the Maui grid including DRAs and markets

The nominal power of each residential battery is 3.3 kW. Let P_k^B represent the maximum aggregated stored power available to the k^{th} aggregator: $P_A^B = 660kW, P_B^B = 594kW, P_C^B = 528kW$.With a nominal power of 4.5 kW for each WH and letting P_k^L represent the load of the k^{th}

aggregator. Loads of the aggregators (before price-based WH scheduling) are: $P_A^L = 200 * 4.5 * \frac{10}{6} + P_A^B = 2160kW$; $P_B^L = 2394kW$; $P_C^L = 2478kW$.

Since the marginal cost of aggregator C is greatest, A and B will compete to sell power to C. We assume $M = 2$ and, $N = 2$ are the number of types possible for *A* and *B,* respectively. It is assumed here that C (the buyer) has only a single definite type, and that both of the sellers fully know the buyers cost function's parameters, and the discharging cost coefficients. Let $\{[a_1, a_2], [b_1, b_2]\}$ be a set of discharging cost coefficients which are the coefficients a and b in equations (5.6) and (5.7) for each type:

DRA_A^B: {[4 , 4.3], [25 , 23.5]}; DRA_B^B: {[4.2 , 4.5], [24 , 23.5]}; DRA_C^B: {[5], [21.5]}.

We have already described a method to determine these parameters in section 5.2.2. A firm's selecting each pair of coefficients *a, b* ($\Psi_A^f(m)$ and $\Psi_B^f(n)$) depends on several factors on both availability of charged batteries (four scenarios were considered in step 1 of section 5.3.2.1) and prevalent market conditions. Energy stored in batteries can be sold for various purposes through the market such as energy, reserve, or other AS market provision. For example, in the normal energy market, a coefficient pair contrived to lower cost can be used. But in the case of provision for AS markets (like, for example, contingency reserve) where stored energy is used to recover grid frequency, the ramp rate of the battery is the primary factor determining applicability and utility. Many batteries with lower ramp-rates are not (or less) useful for these purposes so that energy stored in batteries with higher ramp-rates holds a higher value in the marketplace.

In the other words, the discharging cost function (equation (5.5)) indirectly depends on battery ramp rates (dP_i/dt). Aggregators naturally request higher prices for discharge of batteries with

higher ramp-rates such as during contingency events. Therefore, for the ancillary service markets, a coefficient pair representing higher cost is appropriate.

The normalized price of electricity and average hot water consumption for every 15 minutes of the Maui island case study were shown in figs 5.8 and 5.9. As mentioned in section 5.7, we take prices over half of the normalized price of electricity to be "expensive". From the normalized price data (fig. 5.8), $P(elec_{exp}) = 0.7083$, and $P(elec_{ch}) = 0.2917$. Typically, in the case without price-based WH scheduling where hot water consumption is independent of electricity price, a typical WH runs during 18 of the 96 fifteen minute intervals comprising one day to keep water temperatures in the range of $110 - 130$°F (fig. 5.10).

Under such conditions, The probabilities for WHs' status are: $P(WH_{on}) = 0.1875$ and $P(WH_{off}) = 0.8125$. But in our case study, price-based scheduling of WHs (or any similar thermostatic storage devices) is implemented to reduce energy expenditures and therefore increase payoffs. The DP scheduler considers both electricity price and normal water consumption patterns in determining efficient device scheduling. The output is shown in fig. 5.12 (the highlighted sections show 68/96 intervals when the electricity price is greater than the median). In the case with price-based scheduling of WHs, the probabilities of the scenarios are obtained from section 5.3.2.1.2: $P(\sigma_1) = 0.6041$, $P(\sigma_2) = 0.1042$, $P(\sigma_3) = 0.2292$, $P(\sigma_4) = 0.0625$.

In this case study, it has been assumed that the aggregated stored energy of batteries in firms *A* and *B* is sold to *C* for provision of AS such as regulating reserve market. In this case the discharging ramp-rate of batteries (dP_i/dt) is vitally important so that the probability of sellers using more

expensive coefficient pairs (a, b) is higher than the probability of sellers using less expensive coefficient pairs. Probability distributions of A and B are:

$\Psi_A^1 = [0.16,0.84]$, $\Psi_B^1 = [0.13,0.87]$,
$\Psi_A^2 = [0.11,0.89]$, $\Psi_B^2 = [0.09,0.91]$,
$\Psi_A^3 = [0.29,0.71]$, $\Psi_B^3 = [0.31,0.69]$,
$\Psi_A^4 = [0.22,0.78]$, $\Psi_A^4 = [0.21,0.79]$.

Probabilities, Ψ, depend on both the type of market and current scenario the DRAs are in during the current turn. In the case under consideration, the type effect manifest itself (in competition between DRAs to sell stored energy in the market for provision of AS) as the increase in probability of the more expensive coefficient pairs associated with Ψ. In terms of scenarios' type effect, scenario 2 has the highest and scenario 3 has the lowest probability of using the expensive coefficient pairs. Because in scenario 2 (expensive electricity and active WHs) firms choose the expensive coefficient pairs with higher probability in comparison with other scenarios and in in scenario 3 (cheap electricity and inactive WHs) firms choose the expensive coefficient pairs with lower probability in comparison with other scenarios.

The probabilities, π_{mn}, in equation (5.20) are: $\pi_{11} = 0.0361$, $\pi_{12} = 0.1408$, $\pi_{21} = 0.1267$, $\pi_{22} = 0.5923$. Conditional probability vectors for firms A and B are calculated using equations (5.15) and (5.17): $\eta_A^1 = [0.2039, 0.7961]$, $\eta_B^1 = [0.2216, 0.7784]$, $\eta_A^2 = [0.1762, 0.8238]$, $\eta_B^2 = [0.1921,0.8079]$.

We assume that each DRA choses one of the following strategies: bidding 85% of marginal cost ($\varepsilon_{S1} = 1.7$) , bidding marginal cost ($\varepsilon_{S2} = 2$) , and bidding 115% of marginal cost ($\varepsilon_{S3} = 2.3$), the strategies are then:

$s_A^1 = [0.00068, 0.00080, 0.00092], s_A^2 = [0.00083, 0.00097, 0.00111],$

$s_B^1 = [0.00077, 0.00091, 0.00104], s_B^2 = [0.00086, 0.00102, 0.00117].$

Comparison of fig. 5.10 with fig. 5.12 shows WHs scheduling curtails WHs load by 11.2% (18 time intervals have been decreased to 16 after scheduling). Therefore P_A^L and P_B^L are updated as:

$$P_A^L = 0.888 * 200 * 4.5 * \frac{10}{6} + P_A^B = 1992kW \ , P_B^L = 2192kW.$$

The expected payoff matrices may then be computed using equations (5.14) and (5.16):

$$EP_A^1: \begin{bmatrix} 3.03 & 4.32 & 5.53 & 15.48 & 20.87 & 25.79 \\ 5.66 & 7.57 & 9.35 & 27.46 & 35.40 & 42.64 \\ 6.57 & 8.87 & 11.04 & 32.11 & 41.75 & 50.60 \end{bmatrix}$$

$$EP_A^2: \begin{bmatrix} 1.10 & 1.99 & 2.88 & 8.10 & 12.77 & 17.26 \\ 2.82 & 4.17 & 5.50 & 17.67 & 24.68 & 31.34 \\ 3.17 & 4.78 & 6.37 & 20.16 & 28.56 & 36.59 \end{bmatrix}$$

$$EP_B^1: \begin{bmatrix} 3.60 & 5.16 & 6.66 & 18.66 & 32.25 & 43.21 \\ 5.96 & 8.15 & 10.24 & 8.61 & 22.81 & 34.35 \\ 6.68 & 9.24 & 11.70 & -0.55 & 14.01 & 25.92 \end{bmatrix}$$

$$EP_B^2: \begin{bmatrix} 8.54 & 13.43 & 18.26 & 35.92 & 98.61 & 149.20 \\ 15.62 & 22.49 & 29.23 & -10.58 & 54.35 & 107.15 \\ 17.24 & 25.20 & 33.07 & -52.14 & 14.01 & 68.12 \end{bmatrix}$$

As mentioned in section 5.4.1, we use the same text coloring of the respective matrix entries to identify pairs corresponding to the optimal bidding plans of the players. These optimal bidding plans lead to the maximum expected payoffs for each firm in an *i*-game. A rational player will consistently choose to play its optimal bidding plan.

For each entry of $EP_A^1, EP_A^2, EP_B^1, EP_B^2$, there is one corresponding strategy (p, q) taken from $(P, Q)_A^1, (P, Q)_A^2, (P, Q)_B^1, (P, Q)_B^2$ based on equation (7.5). The final significant consideration in determining expected payoff values in Stackelberg competition is a check of the market constraints performed by the market maker. After finding the optimal bidding plan for each fir, (colorful

number numbers in payoff matrices), corresponding strategies $(p, q) \in (P, Q)$ are checked against the established market bounds. As mentioned previously (section 7.6), the limitation on magnitude of power trades may be overlooked without error as the capacity of all the lines in the case study are guaranteed. Therefore, in this case, market maker **M** only needs to check consistency of transaction prices with limitations.

After solving equation (5.21) for all strategies, transaction prices are found to be in the range of \$0.54 and \$0.74 prior to enforcement of any regulatory policies by **M**. In the case study during the turn analyzed, **M** is responsible for enforcing a price cap of \$=0.65 dictated by the utility as maximum. This is implemented by treating any bids greater than \$=0.65 as equal instead. **M** makes its move in sequence directly following the moves of the DRAs to achieve this. The expected payoffs can then be updated:

$$EP_A^1: \begin{bmatrix} 3.03 & 4.32 & 5.53 & 15.48 & 20.87 & 25.79 \\ 5.66 & 7.57 & 9.35 & 27.46 & 35.40 & 42.21 \\ 6.57 & 8.87 & 10.23 & 32.11 & 39.68 & 41.17 \end{bmatrix}$$

$$EP_A^2: \begin{bmatrix} 1.10 & 1.99 & 2.88 & 8.10 & 12.77 & 13.55 \\ 2.82 & 4.17 & 4.16 & 17.67 & 19.57 & 18.53 \\ 3.17 & 3.97 & 4.18 & 18.07 & 19.49 & 19.84 \end{bmatrix}$$

$$EP_B^1: \begin{bmatrix} 3.60 & 5.16 & 6.66 & 18.66 & 32.25 & 43.21 \\ 5.96 & 8.15 & 10.24 & 8.61 & 22.81 & 32.40 \\ 6.68 & 9.24 & 10.88 & -0.55 & 12.40 & 22.18 \end{bmatrix}$$

$$EP_B^2: \begin{bmatrix} 8.54 & 13.43 & 18.26 & 35.92 & 98.61 & 144.13 \\ 15.62 & 22.49 & 27.24 & -10.58 & 48.56 & 92.42 \\ 17.24 & 24.99 & 26.50 & -54.20 & 3.55 & 48.73 \end{bmatrix}$$

In the above expected payoff matrices, the yellow highlighted arrays show those elements which have been changed by interposition of constraints. Except for the pair of bidding plans marked red (*A* of type 1 vs. *B* of type 2), the other pairs have the same optimal bidding plans as before the market maker made its move for the turn thereby effecting the market regulations. Note

that bidding above marginal cost (row 3) is associated with most these changes as would be expected. Each players' optimal strategy is determined directly from the corresponding optimal bidding plan; we have:

$$(P,Q)_A^1 = \begin{bmatrix} (0.54,331) & (0.57,263) & (0.60,207) & (0.56,362) & (0.59,293) & (0.62,236) \\ (0.56,373) & (0.60,304) & (0.63,246) & (0.58,403) & (0.62,333) & (0.65,274) \\ (0.59,408) & (0.63,338) & (0.65,280) & (0.61,436) & (0.65,365) & (0.65,306) \end{bmatrix}$$

$$(P,Q)_A^2 = \begin{bmatrix} (0.58,245) & (0.61,181) & (0.63,128) & (0.60,275) & (0.64,209) & (0.65,156) \\ (0.61,286) & (0.64,220) & (0.65,166) & (0.64,315) & (0.65,248) & (0.65,192) \\ (0.64,320) & (0.65,253) & (0.65,197) & (0.65,347) & (0.65,279) & (0.65,222) \end{bmatrix}$$

$$(P,Q)_B^1 = \begin{bmatrix} (0.54,306) & (0.57,349) & (0.60,385) & (0.56,259) & (0.59,301) & (0.62,336) \\ (0.56,242) & (0.60,284) & (0.63,318) & (0.58,198) & (0.62,238) & (0.65,271) \\ (0.59,190) & (0.63,230) & (0.65,263) & (0.61,148) & (0.65,186) & (0.65,218) \end{bmatrix}$$

$$(P,Q)_B^2 = \begin{bmatrix} (0.58,361) & (0.61,401) & (0.63,435) & (0.60,312) & (0.64,352) & (0.65,385) \\ (0.61,294) & (0.64,334) & (0.65,366) & (0.64,248) & (0.65,286) & (0.65,318) \\ (0.64,240) & (0.65,278) & (0.65,309) & (0.65,196) & (0.65,232) & (0.65,263) \end{bmatrix}$$

After finding the updated optimal bidding plans of the players with the effect of market maker **M**, the matrices of set of strategies are obtained as follow:

The colorful arrays in the above matrices show the sets of optimal bidding strategies (p, q) and Nash equilibrium in terms of transaction price p ($) and transaction power q (kW) after affecting the market maker **M** in the Stackelberg game. Obviously, the prices of $0.65 in these strategy sets, mainly are because of the role of market maker to control the prices to be less (or equal) than a specific number.

7.8 Conclusions

The most prevalent and well developed applications of price-determined competition models (as in Cournot) regard a single market that is shared by all participants neglecting much real variation especially in highly controlled power markets where differing grid regulation and

structure are prominent and inexorable legacies of the developing technology. This chapter presented a more realistic model of DRA competition for trading stored energy which takes place in multiple markets simultaneously (a networked power market). The model takes the form of an incomplete-information networked Stackelberg game mediated by a market maker. The impact of both network constraints and price-based demand scheduling are analyzed and presented alongside existence, uniqueness, and efficiency results, relevant to gainful utilization.

Chapter 8

Conclusions and Future Works

At the beginning of this thesis, a heuristic method was proposed in in order to find the optimal location(s) and capacity of a multi-purpose BESS in the power grid. One objective of the use of the BESS is related to the transmission side of the grid to cope with the contingencies and regulate the grid frequency under abnormal conditions. In the next objective, the BESS is used to manage the distribution system of the grid for peak shaving and load curve smoothing.

In the next section of this research, a market model was proposed to use DR resources to provide AS especially as CR. This method minimizes the cost of AS provided by DR, maximizes social welfare, and maintains grid stability by mitigating frequency transients to an operating range within industry standards especially in a grid with less inertia and higher penetration level of solar generation. The model included multiple aggregators competing for faster and slower DR programs. The simulations in this work clearly show that the proposed methods for providing AS through DR has a basis for being both economically viable and ensuring system security for credible contingencies.

As mentioned, using DR resources in contingencies helps the utility to turn off low efficiency generators to decrease pollution and save money. Since a high percentage of energy demands

include storages (such as batteries and WHs heaters) and also because of the nature of these devices (having delays), which are appropriate to use in lieu of reserves, a model was proposed in this thesis to schedule these devices by using DP in an effort to regulate the grid frequency under contingencies.

In the next step, the focus of this thesis was on the competing between DRAs in DR market. For this goal, game theory was applied to model the competition between DRAs for selling power which they had previously stored in residential storage devices, in a power market with other DRAs as buyers. The proposed method determines the optimal bidding strategy for each aggregator in order to maximize its own payoff through an *i*-game. In this research the effect of regulation and demand scheduling were considered.

Next, a repeated game-theoretic market model was developed to model the competition between DRAs for selling energy stored in electrochemical storage cells, in a power market with other DRAs as buyers. In every time interval of a day, after finding the best bidding decision and Nash equilibrium of strategies through the game, DED was performed to update the LMP based on the updated demand and updated generation supply. Two different forms of dynamic pricing were considered: one was TOU through price-based scheduling of thermostatic storage loads such as WHs and ACs which DP was used for this goal. The other one was RTP which includes updating LMP in each time interval of the day using DED. Results showed that the players' payoffs were decreased in the regulated (Stackelberg) game compared with the unregulated competition. Demand scheduling increased the DRA's payoff.

The mentioned game-theoretic based method is useful for energy management in distribution network since end-users can participate in a DR market to sell the energy stored in their batteries.

This market also can help the utility company to decrease the amount of reserves through proving different types of AS which helps to reduce air pollution.

The most prevalent and well developed applications of price-determined competition models regard a single market that is shared by all participants neglecting much real variation especially in highly controlled power markets where differing grid regulation and structure are prominent and inexorable legacies of the developing technology. This thesis presented a more realistic model of DRA competition for trading stored energy which takes place in multiple markets simultaneously (a networked power market). The model takes the form of an incomplete-information networked Stackelberg game mediated by a market maker. The impact of both network constraints and price-based demand scheduling were analyzed and presented alongside existence, uniqueness, and efficiency results, relevant to gainful utilization.

The University of Hawaii's REDlab is currently developing hardware systems capable of implementing the presented model. Further work will be forthcoming exploring the implications of our game-theoretic competition model utilizing an alternative market structure in the state of Hawaii where we currently face difficulties with integration of larger numbers of PV systems into the legacy grid. Much more work will be required if we are to reach the states 100% renewable energy goals.

Other possible future works can include: Analysis of security of the models against cyber attacks (e.g. Communication between houses, DRAs, and utility), focusing on industrial demand resources instated of residential (for DR market), Using other machine learning methods for having better estimation of consumption trends and availability of DR resources, analysis of arbitrage and risk analysis of DR market.

Appendix A

Complex-Valued Neural Networks (CVNN)

The major difference between ANN and CVNN is the nature of input parameters. Since real numbers are part of complex numbers, thus CVNN is counted as an extension of ANN. Fig. A.1 demonstrates CVNN's architecture including input, hidden, and output layers. The input layer (X_m) includes two parts: input data (v) and previous output data (y). If input vector, weights (i.e., $W_{n0}^1, W_{l0}^2, W_{nm}^1$, W_{ln}^2, etc.), and activations function (f_c) have real values, the network is normal ANN. Otherwise, the network is CVNN [40].

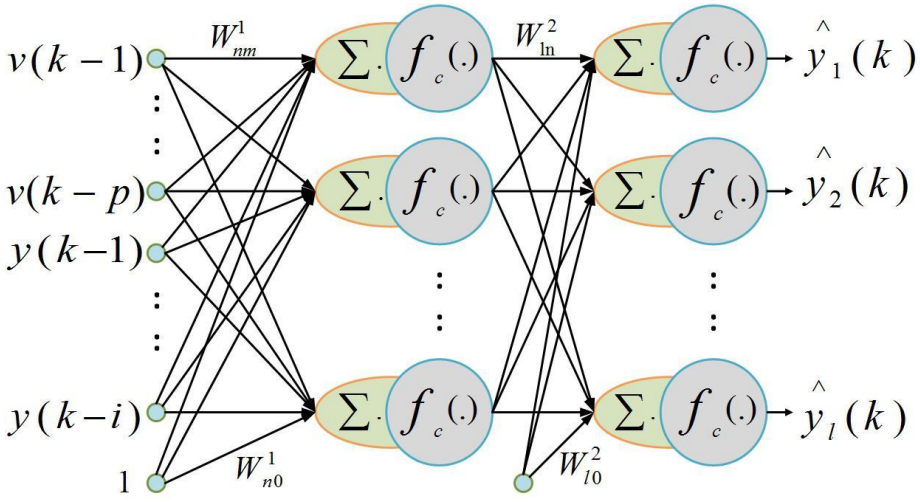

Figure A.1: Architecture of CVNN including the nodes, layers, and weights

Equation (A.1) shows the l^{th} output of the network (forecast value):

$$\hat{y}_l(k) = f_c(W_{l0}^2 + \sum_n W_{ln}^2 H_n) \tag{A.1}$$

The output of n^{th} hidden neuron is given as:

$$H_n = f_c(W_{n0}^1 + \sum_m W_{nm}^1 X_m) \tag{A.2}$$

where $X_m = [v(k-1), v(k-2), ..., v(k-p), y(k-1), y(k-2), ..., y(k-i)]$, which includes m complex valued inputs ($m = i + p$). The whole values of m, n, i, l and p are positive integers. In this thesis, the split sigmoid function is taken for the activation function as follows:

$$f_c(z) = \frac{1}{1+e^{-Re(z)}} + j\frac{1}{1+e^{-Im(z)}}, \tag{A.3}$$

where $z = x + jy$, with $j = \sqrt{-1}$. Using the split sigmoid function instead of non-split, avoids the problem of function's singularity. After applying complex back-propagation algorithm and calculation of the weight values (ΔW_{l0}^2, ΔW_{ln}^2, ΔW_{n0}^1, and ΔW_{nm}^1), the error is calculated using the following equation:

$$e_l(k) = y_l(k) - \hat{y}_l(k) \tag{A.4}$$

where $e_l(k)$ is the error between the l^{th} actual output $y_l(k)$ and forecast output $\hat{y}_l(k)$.

Appendix B

Developed IoT-based Devices and Testbed for Distributed DR Devices

This appendix presents integrated hardware design and software development tools to develop a DR simulation testbed for grid stabilization in a power grid with a high presence of intermittent renewable generation. These tools have been developed and tested in REDLab at the University of Hawaii at Manoa. The result is a comprehensive package for the internet of things hardware-in-the-loop simulation (iHILS) that was tested using DRA control to provide stability to a grid with high integration of distributed energy resources. A detailed description of the development of iHILS is discussed in [249, 250, 251]. The overall infrastructure of the DR testbed system is a Wireless Sensor and Actuator Network (WSAN), with a cluster topology that connects end devices through a Secure Smart Appliance Network (SSAN) gateway to a dedicated server in a bidirectional fashion.

Active smart end devices (i.e. a Smart Plug (SP)), receive forwarded control commands from the PSIM® controller (power system modeling software) [252] through the SSAN gateway, then report back power consumption of the dynamic loads, as shown in fig. B.1. The SSAN gateway connects to residential internet access points (modems/routers). The server writes the reported power consumption in processed and agglomerated packages to a relational SQL database. Lastly, the smart energy meter reports overall household power consumption at high sampling rates (~1Hz) to the database through the SSAN gateway.

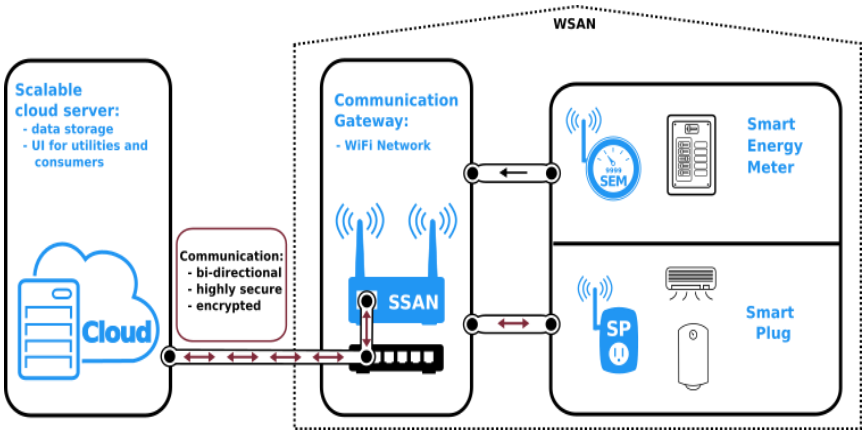

Figure B.1: WSAN system architecture overview

Several devices were developed, which were able to serve as distributed sensor and control systems operating through encrypted channels over an existing network infrastructure. These devices were designed to be able to monitor local power conditions and exert control over loads when a signal is received. A network database backend and web dashboard frontend were developed to handle the incoming sensor data and provide a simple interface for monitoring and controlling, respectively.

As a pilot implementation, several devices were installed in residential and commercial locations for testing and data collection. Two of such installations are shown in fig. B.2. In order to test the devices under variable grid conditions and provide scalability, iHILS was developed. iHILS utilized a modified version of the PSIM® power system modeling software [252] to provide a model and simulate power grids under various conditions and events. This simulation creates a space where control algorithms can be implemented as the simulation sends control signals to and receives sensor data from real and simulated devices. All simulated grid nodes can be monitored in the software, while hardware outputs can be tracked physically and through output to the network database.

Figure B.2: Network capable, distributed sensor and control devices installed on site

Figure B.3 shows the developed Smart Plug (SP), Smart Energy Meter (SEM), and sensor network gateway in REDLab. The SEM shown in Fig. B.3 (right) was designed to purely monitor and report overall household power consumption and power quality at 1 Hz intervals, which would be stored in the cloud server SQL database. A robust SEM design would need to be able to be

installed in both new and old residential buildings without interfering with existing utility energy meters; as such, the proposed testbed hardware can retrofit current electrical systems in addition to new installations. To accomplish this, current transducers are used to measure current in household wiring, shown in Fig. B.4.

Figure B.3: SP(left), SEM (right), and sensor network gateway (back) designed for testbed integration

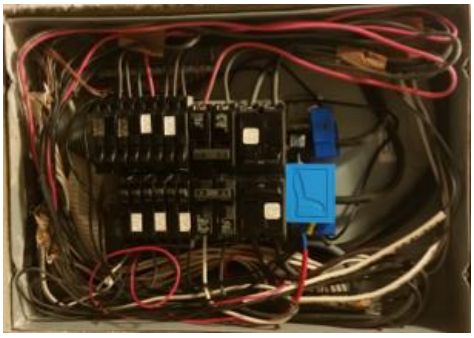

Figure B.4: Conventional household wiring retrofitted with non-intrusive high temporal resolution SEM

A microgrid test deployment station developed in REDlab is shown in Fig. B.5. This station contains a sensor suite with access to hundreds of points of telemetry data including solar power generation, battery state of charge, connected load data, frequency parameters, and grid feedthrough load. In addition to access to telemetry data, the microgrid controller allows access to control functions which include import/export of grid power, battery charge/discharge control, and

controllable relay positions. Network connectivity is provided by a single board computer with network access to MOD-BUS registers. The REDlab team has also developed various task specific control and sensor devices such as SEMs, relay-controlled SPs, switchable WHs, variable chilled water actuator overrides for commercial HVAC, and sensors for LEZETI hybrid AC/DC air conditioning systems which can be integrated into the simulation as a variety of DR resources.

Figure B.5: Network connected microgrid test station

REFERENCES

[1] H. Sangrody, M. Sarailoo, N. Zhou, N. Tran, M. Motalleb, E. Foruzan, "Weather Forecasting Error in Solar Energy Forecasting," *IET Renewable Power Generation* , vol. 11, no. 10, pp. 1274-1280, 2017.

[2] A. A. Akhil, G. Huff, A. B. Currier, B. C. Kaun, and D. M. Rastler, "DOE/EPRI 2013 Electricity Storage Handbook in Collaboration With NRECA," Sandia National Lab., Rep.SAND2013-513, Jul. 2013.

[3] S. V. Papaefthymiou, S. A. Papathanassiou, "Optimum sizing of wind-pumped-storage hybrid power stations in island systems," *Renewable Energy*, vol. 64, pp. 187-196, 2014.

[4] J. P. Fossati, A. Galarza, A. Martin-Villate, L. Fontan, "A method for optimal sizing energy storage systems for microgrids," *Renewable Energy*, vol. 77, pp. 539-549, 2015.

[5] A. K. Varkani, A. Daraeepour,and H. Monsef, "Anewself-scheduling strategy for integrated operation of wind and pumped-storage power plantsinpowermarkets," *Appl.Energy*, vol. 88, no. 12, p. 5002–5012, Dec. 2011.

[6] A. Sadeghi-Mobarakeh, M. Kohansal, E. E. Papalexakis, H. Mohsenian-Rad, "Data Mining based on Random Forest Model to Predict the California ISO Day-ahead Market Prices," in *Innovative Smart Grid Technologies (ISGT)*, 2017.

[7] J. Garcia-Gonzalez, R. M. R. delaMuela, L. M. Santos, and A. M. Gonzalez, "Stochastic joint optimization of wind generation and pumpedstorage units in an electricity market," *IEEE Trans. Power Syst.*, vol. 23, no. 2, p. 460–468, May 2008.

[8] H. Pandžić, I. Kuzle, and T. Capuder, "Virtual power plant mid-term dispatchoptimization," *Appl. Energy*, vol. 101, no. 1, p. 134–141, Jan. 2013.

[9] H. Pandžić, J. M. Morales, A. J. Conejo, and I. Kuzle, "Offering model for a virtual power plant based on stochastic programming," *Appl. Energy*, vol. 105, no. 5, p. 282–292, May 2013.

[10] M. Korpaas, A. T. Holen, and R. Hildrum, "Operation and sizing of energy storage for wind power plants in a market system," *Elect. Power Energy Syst.*, vol. 25, no. 8, p. 599–606, Oct. 2003.

[11] J. H. Kim and W. B. Powell, "Optimal energy commitments with storage and intermittent supply," *Oper. Res.*, vol. 59, no. 6, p. 1347–1360, Dec. 2011.

[12] Y. Zhou, A. Scheller-Wolf, N. Secomandi, and S. Smith, "Managing Wind-based Electricity Generation in the Presence of Storage and Transmission Capacity," Tepper School of Business, 2013. [Online]. Available: repository.cmu.edu/cgi/viewcontent.cgi?article=2469&context=tepper.

[13] K. M. Chandy, S. H. Low, U. Topcu, and H. Xu, "A simple optimal power flow model with energy storage," in *49th IEEE Conf. Decision and Control*, Atlanta, GA, USA, Dec. 2010.

[14] A. Faghih, M. Roozbehani, and M. Dahleh, "Optimal utilization of storage and the induced price elasticity of demand in the presence of rampconstraints," in *50th IEEE Conf. Decision and Control and Eur. Control Conf.*, Orlando, FL, USA, Dec. 2011.

[15] M. Nick, R. Cherkaoui, and M. Paolone, "Stochastic Day-ahead Optimal Scheduling of Active Distribution Networks with Dispersed Energy Storage and Renewable Resources," in *IEEE Conference on Technologies for Sustainability (SusTech)*, 2014.

[16] F. De Samaniego Steta, A. Ulbig, S. Koch, and G. Andersson, "A model-based optimal operation strategy for lossy energy storage systems: The case of compressed air energy storage plants," in *Power System Computation Conf.*, Stockholm, Sweden, Aug.2011.

[17] P. Harsha and M. Dahleh, "Optimal sizing of energy storage for efficient integration of renewable energy," in *50th IEEE Conf. Decision and Control and Eur. Control Conf.*, Orlando, FL, USA, Dec. 2011.

[18] P. Harsha and M. Dahleh, "Optimal Management and Sizing of Energy Storage Under Dynamic Pricing for the Efficient Integration of Renewable Energy," *IEEE Trans. Power Syst.*, vol. 30, no. 3, pp. 1164-1181, 2012.

[19] Y. Zhang, S. Zhu, and A. A. Chowdhury, "Reliability Modeling and Control Schemes of Composite Energy Storage and Wind Generation System With Adequate Transmission Upgrades," *IEEE Trans. Sustain. Energy*, vol. 2, no. 4, p. 520–526, Oct. 2011.

[20] K. Dvijotham, S. Backhaus, and M. Chertkov, "Operations-Based Planning for Placement and Sizing of Energy Storage in a Grid With a High Penetration of Renewables," arXiv:1107.1382v2, Jul. 2011.

[21] P. Denholm and R. Sioshansi, "The value of compressed air energy storage with wind in transmission-constrained electric power systems," *Energy Policy*, vol. 37, no. 8, p. 3149–3158, Aug. 2009.

[22] A. Arabali, M. Ghofrani, and M. Etezadi-Amoli, "Cost analysis of a power system using probabilistic optimal power flow with energy storage integration and wind generation," *Electrical Power & Energy Systems*, vol. 53, Dec. 2013.

[23] T. Kerdphol, Y. Qudaih, and Y. Mitani, "Battery Energy Storage System Size Optimization in Microgrid using Particle Swarm Optimization," in *5th IEEE PES Innovative Smart Grid Technologies Europe (ISGT Europe)*, Istanbul, Oct. 2014.

[24] X. Li, D. Hui, and X. Lai, "Battery Energy Storage Station (BESS)-Based Smoothing Control of Photovoltaic (PV) and Wind Power Generation Fluctuations," *IEEE Trans. Sustain. Energy*, vol. 4, no. 2, pp. 464-473, Apr. 2013.

[25] A. S. A. Awad, T. H. M. EL-Fouly, M. M. A. Salama, "Optimal ESS Allocation and Load Shedding for Improving Distribution System Reliability," *IEEE Trans. Smart Grid*, vol. 5, no. 5, pp. 2339-2349, Sept. 2014.

[26] M. Nick, R. Cherkaoui, and M. Paolone, "Optimal siting and sizing of distributed energy storage systems via alternating direction method of multipliers," *International Journal of Electrical Power & Energy Systems*, vol. 72, pp. 33-39, Nov. 2015.

[27] M. Nick, M. Hohmann, R. Cherkaoui, and M. Paolone, "On the Optimal Placement of Distributed Storage Systems for Voltage Control in Active Distribution Networks," in *3rd IEEE PES Innovative Smart Grid Technologies Europe (ISGT Europe)*, Berlin, 2012.

[28] M. Nick, R. Cherkaoui, and M. Paolon, "Optimal Allocation of Dispersed Energy Storage Systems in Active Distribution Networks for Energy Balance and Grid Support," *IEEE Trans. Power Syst.*, vol. 29, no. 5, pp. 2300-2310, Sep. 2014.

[29] S. Teleke, M. Baran, S. Bhattacharya, A. Huang, "Optimal control of battery energy storage for wind farm dispatching," *IEEE Trans. Energy Convers.*, vol. 25, no. 3, pp. 787-794, Sep. 2010.

[30] A. Keyhani, Design of Smart Power Grid Renewable Energy Systems, Wiley-IEEE Press, 2011.

[31] F. Milano, "Power System Analysis Toolbox, Documentation for PSAT," User's Manual, 2008.

[32] K. E. Brenan, S. L. Campbell, and L. R. Petzold, Numerical Solution of Initial-Value Problems in Differential-Algebraic Equations, Society for Industrial and Applied Mathematics, 1995.

[33] A. Abbaspour, M. Sanchez, A. Sargolzaei, K. Yen, N. Sornkhampan, "Adaptive Neural Network based Fault Detection Design for Unmanned Quadrotor under Faults and Cyber Attacks," in *25th International Conference on Systems Engineering (ICSEng)*, 2017.

[34] A. Abbaspour, A. Khalilnejad, Z. Chen, "Robust adaptive neural network control for PEM fuel cell," *International Journal of Hydrogen Energy*, vol. 41, no. 44, pp. 20385-20395, 2016.

[35] S. A. Kalogirou, "Applications of artificial neural-networks for energy systems," *Applied Energy*, vol. 67, pp. 17-35, 2000.

[36] S. A. Kalogirou, "Artificial neural networks in renewable energy systems applications: a review," *Renewable and Sustainable Energy Reviews* , vol. 5, pp. 373-401, 2001.

[37] A. Hirose, Complex-Valued Neural Networks: Advances and Applications, IEEE Press Series on Computational Intelligence, 2013.

[38] M. Motalleb, S. Sreedarsan, H. Sangrody, A. Eshraghi, R. Ghorbani, "Power Grid Reliability Improvement through Forecasting with Complex-Valued Neural Networks under System Contingency," *American Journal of Engineering Research (AJER)*, vol. 6, no. 7, pp. 106-122, 2017.

[39] N. Zagoras, "Battery Energy Storage System (BESS): A Cost/Benefit Analysis for a PV power station," Clemson University Restoration Institute, Sep. 2014.

[40] E. Reihani, M. Motalleb , R. Ghorbani, and L. S. Saoud, "Load Peak Shaving and Power Smoothing of a Distribution Grid with High Renewable Energy Penetration," *Renewable Energy,* vol. 86, p. 1372–1379, Feb. 2016.

[41] E. Reihani and R. Ghorbani, "Load Commitment of Distribution Grid with High Penetration of Photovoltaics (PV) Using Hybrid Series-Parallel Prediction Algorithm and Storage," *Electric Power Systems Research,* vol. 131, p. 224–230, Feb. 2015.

[42] M. H. Athari, Z. Wang, "Studying Cascading Overload Failures under High Penetration of Wind Generation," in *IEEE Power and Energy Society General Meeting (PESGM)*, 2017.

[43] E. Reihani, S. Sepasi, L. R. Roose,and M. Matsuura, "Energy management at the distribution grid using a Battery Energy Storage System (BESS)," *International Journal of Electrical Power & Energy Systems,* vol. 77, p. 337–344, 2016.

[44] "Hawaiian Electric Energy Cost Adjustment Factor for July 2015," K. Matsuura, Hawaiian Electric Company, Inc.

[45] D. Kirschen, and G. Strbac, Fundamentals of Power System Economics, John Wiley & Sons Ltd, 2004.

[46] D. D. Le, A. Berizzi, and C. Bovo, "A probabilistic security assessment approach to power systems with integrated wind resources," *Renewable Energy,* vol. 85, pp. 114-123, 2016.

[47] M. Gitizadeh, J. Aghaei, "Static and Dynamic Security-Augmented Market-Based Generation Scheduling Using Multi-Objective Artificial Bee Colony Algorithm," *International Review of Electrical Engineering (I.R.E.E.),* vol. 7, no. 1, pp. 3646-3656, 2012.

[48] J. Aghaei, H. A. Shayanfar, N. Amjady, "Joint market clearing in a stochastic framework considering power system security," *Applied Energy,* vol. 86, pp. 1675-1682, 2009.

[49] M. M. Esfahani, A. Sheikh, O. Mohammed, "Adaptive real-time congestion management in smart power systems using a real-time hybrid optimization algorithm," *Electric Power Systems Research,* vol. 150, pp. 118-128, 2017.

[50] Z. Ming, L. Ximei, and P. Lilin, "The ancillary services in China: An overview and key issues," *Renewable and Sustainable Energy Reviews,* vol. 36, pp. 83-90, 2014.

[51] M. H. Gomes, and J. T. Saraiva, "Allocation of reactive power support, active loss balancing and demand interruption ancillary services in MicroGrids," *Electric Power Systems Research,* vol. 80, pp. 1267-1276, 2010.

[52] S. Nistor, J. Wu, M. Sooriyabandara, J. Ekanayake, "Capability of smart appliances to provide reserve services," *Applied Energy,* vol. 138, pp. 590-597, 2015.

[53] I. Pavic, T. Capuder, and I. Kuzle, "Value of flexible electric vehicles in providing spinning reserve services," *Applied Energy,* vol. 157, pp. 60-74, 2015.

[54] A. Cagnano, F. Torelli, F. Alfonzetti, and E. D. Tuglie, "Can PV plants provide a reactive power ancillary service? A treat offered by an on-line controller," *Renewable Energy,* vol. 36, pp. 1047-1052, 2011.

[55] A. G. Madureira, J. A. Peças Lopes, "Ancillary services market framework for voltage control in distribution networks with microgrids," *Electric Power Systems Research,* vol. 86, pp. 1-7, May 2012.

[56] M. Scherer, M. Zima, and G. Andersson, "An integrated pan-European ancillary services market for frequency control," *Energy Policy,* vol. 62, pp. 292-300, 2013.

[57] N. Sasidharana, N. Madhu, J. G. Singh, and W. Ongsakula, "Real Time Active Power Ancillary Service using DC Community Grid with Electric vehicles and Demand Response," *Procedia Technology,* vol. 21, pp. 41-48, 2015.

[58] "Glossary of Transmission Grid Integration Terms," National Renewable Energy Laboratory (NREL), [Online]. Available: http: //www. nrel.gov /electricity/transmission/glossary.html.

[59] J. Wang, M. Shahidehpour, and Z. Li, "Contingency-Constrained Reserve Requirements in Joint Energy and Ancillary Services Auction," *IEEE Trans. Power Syst.,* vol. 24, no. 3, pp. 1457-1468, Aug. 2009.

[60] J. Aghaei, M. I. Alizadeh, "Robust n–k contingency constrained unit commitment with ancillary service demand response program," *IET Gener. Transm. Distrib.,* vol. 8, no. 12, p. 1928–1936, 2014.

[61] J. L. Bode, M. J. Sullivan, and D. Berghman, and J. H. Eto, "Incorporating residential AC load control into ancillary service markets: Measurement and settlement," *Energy Policy*, vol. 56, pp. 175-185, 2013.

[62] B. Biegel, M. Westenholz, L. H. Hansen, J. Stoustrup, P. Andersen, and S. Harbo, "Integration of flexible consumers in the ancillary service markets," *Energy*, vol. 67, pp. 479-489, 2014.

[63] M. Motalleb, E. Reihani, R. Ghorbani, "Optimal placement and sizing of the storage supporting transmission and distribution networks," *Renewable Energy*, vol. 94, pp. 651-659, 2016.

[64] J. Soares, M. A. F. Ghazvini, Z. Vale, P. B. de Moura Oliveira, "A multi-objective model for the day-ahead energy resource scheduling of a smart grid with high penetration of sensitive loads," *Applied Energy*, vol. 162, pp. 1074-1088, 2016.

[65] O. Ma, et al., "Demand Response for Ancillary Services," *IEEE Trans. Smart Grids*, vol. 4, no. 4, pp. 1988-1995, Dec. 2013.

[66] S. M. Nosratabadi, R. Hooshmand,and E. Gholipour, "Stochastic profit-based scheduling of industrial virtual power plant using the best demand response strategy," *Applied Energy*, vol. 164, pp. 590-606, 2016.

[67] J. L. Mathieu a,n, M. E. H. Dyson,and D. S. Callaway , "Resource and revenue potential of California residential load: participation in ancillary services," *Energy Policy*, vol. 80, pp. 76-87, 2015.

[68] P. Cappers, J. MacDonald, C. Goldman, and O. Ma, "An assessment of market and policy barriers for demand response providing ancillary services in U.S. electricity markets," *Energy Policy*, vol. 62, p. 1031–1039, Nov. 2013.

[69] E. Karfopoulos, L. Tena, A. Torres, P. Salas, J. G. Jorda, A. Dimeas, and N. Hatziargyriou, "A multi-agent system providing demand response services from residential consumers," *Electric Power Systems Research*, vol. 120, p. 163–176, Mar. 2015,.

[70] J. Aghaei, M. I. Alizadeh, "Demand response in smart electricity grids equipped with renewable energy sources: A review," *Renewable and Sustainable Energy Reviews*, vol. 18, pp. 64-72, 2013.

[71] P. Faria, T. Soares, Z. Vale, H. Morais , "Distributed generation and demand response dispatch for a virtual power player energy and reserve provision," *Renewable Energy*, vol. 66, pp. 686-695, 2014.

[72] J. Aghaei, M. Alizadeh, P. Siano, A. Heidari, "Contribution of emergency demand response programs in power system reliability," *Energy*, vol. 103, pp. 688-696, 2016.

[73] P. Siano, D. Sarno, "Assessing the benefits of residential demand response in a real time distribution energy market," *Applied Energy*, vol. 161, pp. 533-551, 2016.

[74] M. A. F. Ghazvini, J. Soares, N. Horta, R. Neves, R. Castro, Z. Vale, "A multi-objective model for scheduling of short-term incentive-based demand response programs offered by electricity retailers," *Applied Energy*, vol. 151, pp. 102-118, 2015.

[75] S. A. Pourmousavi, M.H. Nehrir, and C. Sastry, "Providing ancillary services through demand response with minimum load manipulation," in *North American Power Symposium (NAPS)*, Boston, 2011.

[76] S. Kiliccote, M. A. Piette, E. Koch, and D. Hennage , "Utilizing Automated Demand Response in Commercial Buildings as Non-Spinning Reserve Product for Ancillary Services Markets," in *50th IEEE Conference on Decision and Control and European Control Conference (CDC-ECC)*, Orlando, FL, USA, 2011 .

[77] M. Behrangrad, H. Sugihara, and T. Funaki, "Effect of optimal spinning reserve requirement on system pollution emission considering reserve supplying demand response in the electricity market," *Applied Energy*, vol. 88, pp. 2548-2558, 2011.

[78] G. Liu, and K. Tomsovic, "A full demand response model in co-optimized energy and reserve market," *Electric Power Systems Research*, vol. 111, pp. 62-70, 2014.

[79] E. Lakic, G. Artac, A. F. Gubina, "Agent-based modeling of the demand-side system reserve provision," *Electric Power Systems Research*, vol. 124, pp. 85-91, 2015.

[80] N. Rezaei, and M. Kalantar, "Smart microgrid hierarchical frequency control ancillary service provision based on virtual inertia concept: An integrated demand response and droop controlled distributed generation framework," *Energy Conversion and Management*, vol. 92, pp. 287-301, 2015.

[81] N. Rezaei, M. Kalantar, "Stochastic frequency-security constrained energy and reserve management of an inverter interfaced islanded microgrid considering demand response programs," *Electrical Power and Energy Systems*, vol. 69, pp. 273-286, 2015.

[82] Y. Chen, and J. Li, "Comparison of security constrained economic dispatch formulations to incorporate reliability standards on demand response resources into Midwest ISO co-optimized energy and ancillary service market," *Electric Power Systems Research*, vol. 81, p. 1786– 1795, 2011.

[83] M. Gitizadeh, J. Aghaei, "Dynamic security consideration in multiobjective electricity markets," *Applied Soft Computing*, vol. 16, pp. 1-9, 2014.

[84] J. Aghaei, E. Mahboubi-Moghaddam, K. M. Muttaqi, "Enhancing Corrected Transient Energy Margin in Electricity Energy Market Operation Using Stochastic Multiobjective Mathematical Programming," *IEEE Systems Journal*, vol. 9, no. 4, pp. 1419-1429, Dec. 2015.

[85] J. Aghaei, H. Shayanfar, N. Amjady , "Multi-objective market clearing of joint energy and reserves auctions ensuring power system security," *Energy Conversion and Management*, vol. 50, pp. 899-906, 2009.

[86] A. D. Banadaki, F. D. Mohammadi, A. Feliachi, "State Space Modeling of Inverter Based Microgrids Considering Distributed Secondary Voltage Control," in *North American Power Symposium (NAPS)*, Morgantown, WV, 2017.

[87] P. Kundur, Power System Stability and Control, McGraw-Hill Education (India), 1994.

[88] H. Saadat, Power system Analysis, McGraw-Hill Primis Custom Publishing, 2010.

[89] E. Reihani, A. Eshraghi, M. Motalleb, S. Jafarzadeh, "Frequency regulation of microgrid with droop control," in *IEEE PES T&D Conference & Exposition*, Denver, CO, 2018.

[90] "IEEE 1547 Standard for Interconnecting Distributed Resources," IEEE-SASB Coordinating Committees, 2003 .

[91] A. Eshraghi, R. Ghorbani, "Islanding detection and over voltage mitigation using controllable loads," *Sustainable Energy, Grids and Networks*, vol. 6, pp. 125-135, 2016.

[92] S. Sariri, V. Schwarzer, M. Angelo, D. Kalisch, R. Ghorbani, "Real-Time Data Collection and Processing of Utility Customer's Power Usage for Improved Demand Response Control," in *CompleXity: Technology for Complex Urban Systems*, Kauai, HI, Jan. 2016.

[93] A. Eshraghi, M. Motalleb, E. Reihani, R. Ghorbani, "Frequency Regulation in Islanded Microgrid Using Demand Response," in *North American Power Symposium (NAPS)*, Morgantown, WV, 2017.

[94] R. D. Zimmerman, C. E. Murillo-S´anchez, "Matpower 5.1, User's Manual," Power Systems Engineering Research Center (Pserc), 2015.

[95] M. Rashidinejad, Y. H. Song, M. H. Javidi Dasht-Bayaz, "Contingency reserve pricing via a joint energy and reserve dispatching approach," *Energy Conversion and Management*, vol. 43, pp. 537-548, 2002.

[96] A. Zakariazadeh, S. Jadid, P. Siano, "Smart microgrid energy and reserve scheduling with demand response using stochastic optimization," *Electrical Power and Energy Systems*, vol. 63, pp. 523-533, 2014.

[97] M. Motalleb, M. Thornton, E. Reihani, R. Ghorbani, "A Nascent Market for Contingency Reserve Services Using Demand Response," *Applied Energy*, vol. 179, pp. 985-995, 2016.

[98] K. Ma, T. Yao, J. Yang, X. Guan, "Residential power scheduling for demand response in smart grid," *Electrical Power and Energy Systems*, vol. 78, pp. 320-325, 2016.

[99] D. Setlhaolo, X. Xia, "Optimal scheduling of household appliances with a battery storage system and coordination," *Energy and Buildings*, vol. 94, no. 1, pp. 61-70, May 2015.

[100] A. N. Ghalelou, A. P. Fakhri, S. Nojavan, M. Majidi, H. Hatami, "A stochastic self-scheduling program for compressed air energy storage (CAES) of renewable energy sources (RESs) based on a demand response mechanism," *Energy Conversion and Management*, vol. 120, pp. 388-396, 2016.

[101] R. Menke, E. Abraham, P. Parpas, I. Stoianov, "Demonstrating demand response from water distribution system through pump scheduling," *Applied Energy*, vol. 170, pp. 377-387, 2016.

[102] J. Fleer, P. Stenzel, "Impact analysis of different operation strategies for battery energy storage systems providing primary control reserve," *Journal of Energy Storage*, In Press.

[103] A. Lucas, S. Chondrogiannis, "Smart grid energy storage controller for frequency regulation and peak shaving, using a vanadium redox flow battery," *Electrical Power and Energy Systems,* vol. 80, pp. 26-36, 2016.

[104] M. Aunedi, P. Kountouriotis, J. E. O. Calderon, D. Angeli, G. Strbac, "Economic and Environmental Benefits of Dynamic Demand in Providing Frequency Regulation," *IEEE Trans. Smart Grids,* vol. 4, no. 4, pp. 2036-2048, 2013.

[105] H. W. Qazi, D. Flynn, "Analysing the impact of large-scale decentralised demand side response on frequency stability," *Electrical Power and Energy Systems,* vol. 80, pp. 1-9, 2016.

[106] A. Zakariazadeh, S. Jadid, "Smart microgrid operational planning considering multiple demand response programs," *Journal of Renewable and Sustainable Energy,* vol. 6, no. 1, p. 013134 , 2014.

[107] O. Homaee, A. Zakariazadeh, S. Jadid, "Real time voltage control using emergency demand response in distribution system by integrating advanced metering infrastructure," *Journal of Renewable and Sustainable Energy*, vol. 6, p. 033145 , 2014.

[108] B. Kirby, M. Ally, "Spinning Reserve From Supervisory Thermostat Control," U.S. Department of Energy, Washington, DC, USA, 2002.

[109] E. Hirst, B. Kirby, "Load as a Resource in Providing Ancillary Services," Tech. Rep., Oak Ridge National Lab., Oak Ridge, TN, USA, 1999.

[110] D. Karl Critz, S. Busche, S. Connors, "Power systems balancing with high penetration renewables: The potential of demand response in Hawaii," *Energy Conversion and Management,* vol. 76, p. 76, 609-619.

[111] Hawaii Public Utilities Commission, "Demand Response as a Flexible Operating Resource," HDBaker & Company, Honolulu, HI, 2012.

[112] M. H. Athari, Z. Wang, "Modeling the uncertainties in renewable generation and smart grid loads for the study of the grid vulnerability," in *IEEE Power Energy Society Innovative Smart Grid Technologies Conference (ISGT)*, 2016.

[113] F. Rahimi, A. Ipakchi, "Demand response as a market resource under the smart grid paradigm," *IEEE Trans. Smart Grid,* vol. 1, no. 1, p. 82–88, Jun. 2010.

[114] M. Parvania, M. Fotuhi-Firuzabad, "Demand Response Scheduling by Stochastic SCUC," *IEEE Trans. Smart Grid,* vol. 1, no. 1, pp. 89-98, Jun. 2010.

[115] M. Song, K. Alvehag, J. Widen, A. Parisio, "Estimating the impacts of demand response by simulating household behaviors under price and CO2 signals," *Electric Power Systems Research,* vol. 111, pp. 103-114, Jun. 2014.

[116] US. Department of Energy, "Benefits of demand response in electricity markets and recommendations for achieving them," US. Department of Energy, 2006.

[117] ET. Mayhorn, SA. Parker, FS. Chassin, SH. Widder, RM. Pratt, "Evaluation of the Demand Response Performance of Capacity Electric Water Heaters," Pacific Northwest National Laboratory, Richland, Washington 99352, 2015.

[118] Y. F. B. Jiang, "Dynamic Residential Demand Response and Distributed Generation Management in Smart Microgrid with Hierarchical Agents," *Energy Procedia*, vol. 12, pp. 76-90, 2011.

[119] D. Zhang, S. Evangelisti, P. Lettieri, L. G. Papageorgiou, "Economic and environmental scheduling of smart homes with microgrid: DER operation and electrical tasks," *Energy Conversion and Management,* vol. 110, pp. 113-124, 2016.

[120] J . K. Kok, C. J. Warmer, I.G. Kamphuis, "Powermatcher: Multiagent control in the electricity infrastructure," in *Proc. AAMAS*, 2005.

[121] D. Setlhaoloa, X. Xiaa, J. Zhangb, "Optimal scheduling of household appliances for demand response," *Electric Power Systems Research,* vol. 116, pp. 24-28, 2014.

[122] M. Mazidi, A. Zakariazadeh, S. Jadid, P. Siano, "Integrated scheduling of renewable generation and demand response programs in a microgrid," *Energy Conversion and Management,* vol. 86, pp. 1118-1127, 2014.

[123] J. S. Vardakas, N. Zorba, C. V. Verikoukis, "Performance evaluation of power demand scheduling scenarios in a smart grid environment," *Applied Energy,* vol. 142, pp. 164-178, 2015.

[124] A. Zakariazadeh, S. Jadid, P. Siano, "Stochastic operational scheduling of smart distribution system considering wind generation and demand response programs," *Electrical Power and Energy Systems,* vol. 63, pp. 218-225, 2014.

[125] H. Falsafi, A. Zakariazadeh, S. Jadid, "The role of demand response in single and multi-objective wind-thermal generation scheduling: A stochastic programming," *Energy,* vol. 64, pp. 853-867, 2014.

[126] E. Heydarian-Forushani, M. E. H. Golshan, M. P. Moghaddam, M. Shafie-khah, J. P. S. Catalão, "Robust scheduling of variable wind generation by coordination of bulk energy storages and demand response," *Energy Conversion and Management,* vol. 106, pp. 941-950, 2015.

[127] M. Mazidi, H. Monsef, P. Siano, "Incorporating price-responsive customers in day-ahead scheduling of smart distribution networks," *Energy Conversion and Management,* vol. 115, pp. 103-116, 2016.

[128] Y. Xu, D. Liu, Q. Wei, "Action dependent heuristic dynamic programming based residential energy scheduling with home energy inter-exchange," *Energy Conversion and Management,* vol. 103, pp. 553-561, 2015.

[129] D. Eryilmaz, T. Smith, S. Dhople, E. Wilson, "Demand response for industrial-scale energy users in Midwest ISO: A dynamic programming approach for curtailing energy use," in *IEEE PES T&D Conference and Exposition*, 2014.

[130] S. S. Reka, V. Ramesh, "Demand side management scheme in smart grid with cloud computing approach using stochastic dynamic programming," *Perspectives in Science,* In Press.

[131] M. Rastegar, M. Fotuhi-Firuzabad, F. Aminifar, "Load commitment in a smart home," *Applied Energy,* vol. 96, pp. 45-54, 2012.

[132] A. Safdarian, M. Fotuhi-Firuzabad, M. Lehtonen, "A Distributed Algorithm for Managing Residential Demand Response in Smart Grids," *IEEE Trans. Ind. Informat.,* vol. 10, no. 4, pp. 2385-2393, 2014.

[133] G. R. Aghajani, H. A. Shayanfar, H. Shayeghi, "Presenting a multi-objective generation scheduling model for pricing demand response rate in micro-grid energy management," *Energy Conversion and Management,* vol. 106, pp. 308-321, 2015.

[134] C. Yan, X. Xue, S. Wang, B. Cui, "A novel air-conditioning system for proactive power demand response to smart grid," *Energy Conversion and Management,* vol. 102, pp. 239-246, 2015.

[135] B. Cui, S. Wang, C. Yan, X. Xue, "Evaluation of a fast power demand response strategy using active and passive building cold storages for smart grid applications q," *Energy Conversion and Management,* vol. 102, pp. 227-238, 2015.

[136] C. Goh, J. Apt, "Consumer strategies for controlling electric water heaters under dynamic pricing," in *Proc. Carnegie Mellon Elect. Ind. Center Working Paper CEIC-04* , 2004.

[137] M. Motalleb, M. Thornton, E. Reihani, R. Ghorbani, "Providing frequency regulation reserve services using demand response scheduling," *Energy Conversion and Management,* vol. 124, pp. 439-452, 2016.

[138] C. Wu, H. Mohsenian-Rad, J. Huang, "Vehicle-to-Aggregator Interaction Game," *IEEE Transactions on Smart Grid,* vol. 3, no. 1, pp. 434-442, 2012.

[139] N. Ruiz, I. Cobelo, J. Oyarzabal, "A direct load control model for virtual power plant management," *IEEE Transactions on Power Systems,* vol. 24, no. 2, p. 959–966, 2009.

[140] P. Finn, M. O'Connell, C. Fitzpatrick , "Demand side management of a domestic dishwasher: Wind energy gains, financial savings and peak-time load reduction," *Applied Energy,* vol. 101, p. 678–685, 2013.

[141] P. S. Moura, A. T. de Almeida , "The role of demand-side management in the grid integration of wind power," *Applied Energy,* vol. 87, no. 8, p. 2581–2588, 2010.

[142] C. Wu, H. Mohsenian-Rad, J. Huang, A. Y. Wang, "Demand side management for Wind Power Integration in microgrid using dynamic potential game theory," in *IEEE GLOBECOM Workshops (GC Wkshps)*, Houston, TX, 2011 .

[143] P. Samadi, H. Mohsenian-Rad, R. Schober, V. W. S. Wong, "Advanced Demand Side Management for the Future Smart Grid Using Mechanism Design," *IEEE Transactions on Smart Grid*, vol. 3, no. 3, pp. 1170-1180, 2012.

[144] A. H. Mohsenian-Rad, V. W. S. Wong, J. Jatskevich, R. Schober, A. Leon-Garcia, "Autonomous Demand-Side Management Based on Game-Theoretic Energy Consumption Scheduling for the Future Smart Grid," *IEEE Transactions on Smart Grid*, vol. 1, no. 3, pp. 320-331, 2010.

[145] A. Zeinalzadeh, "Learning in inventory competition games," PhD Thesis, University of Hawaii at Manoa, 2013.

[146] H. A. Shayanfar, A. Saliminia Lahiji, J. Aghaei, A. Rabiee, "Generation Expansion Planning in pool market: A hybrid modified game theory and improved genetic algorithm," *Energy Conversion and Management*, vol. 50, p. 1149–1156, 2009.

[147] S. M. Moghddas-Tafreshi, H. A. Shayanfar, A. Saliminia Lahiji, A. Rabiee, J. Aghaei, "Generation expansion planning in Pool market: A hybrid modified game theory and particle swarm optimization," *Energy Conversion and Management*, vol. 52, pp. 1512-1519, 2011.

[148] W. Lise, V. Linderhof, O. Kuik, C. Kemfert, R. Ostling, T. Heinzow, "A game theoretic model of the Northwestern European electricity market—market power and the environment," *Energy Policy*, vol. 34, p. 2123–2136, 2006.

[149] Z. Liu, X. Zhang, J. Lieu, "Design of the incentive mechanism in electricity auction market based on the signaling game theory," *Energy*, vol. 35, pp. 1813-1819, 2010.

[150] S. Kamalinia, M. Shahidehpour, L. Wu, "Sustainable resource planning in energy markets," *Applied Energy*, vol. 133, pp. 112-120, 2014.

[151] S. Bahrami, M. Parniani, "Game Theoretic Based Charging Strategy for Plug-in Hybrid Electric Vehicles," *IEEE Transactions on Smart Grid*, vol. 5, no. 5, pp. 2368-2375, 2014.

[152] S. Bahrami, V. W. S. Wong, "A potential game framework for charging PHEVs in smart grid," in *IEEE Pacific Rim Conference on Communications, Computers and Signal Processing (PACRIM)*, Victoria, BC, 2015.

[153] R. Tian, Q. Zhang, G. Wang, H. Li, S. Chen, Y. Li, Y. Tian, "Study on the promotion of natural gas-fired electricity with energy market reform in China using a dynamic game-theoretic model," *Applied Energy*, p. DOI: 10.1016/j.apenergy.2015.11.079, 2015.

[154] W. Su, A. Q. Huang, "A game theoretic framework for a next-generation retail electricity market with high penetration of distributed residential electricity suppliers," *Applied Energy*, vol. 119, pp. 341-350, 2014.

[155] N. Zhang, Y. Yan, W. Su, "A game-theoretic economic operation of residential distribution system with high participation of distributed electricity prosumers," *Applied Energy*, vol. 154, pp. 471-479, 2015.

[156] A. Sheikhi, M. Rayati, S. Bahrami, A. M. Ranjbar, S. Sattari, "A cloud computing framework on demand side management game in smart energy hubs," *Electrical Power and Energy Systems*, vol. 64, pp. 1007-1016, 2015.

[157] N. I. Nwulu, X. Xia, "Multi-objective dynamic economic emission dispatch of electric power generation integrated with game theory based demand response programs," *Energy Conversion and Management*, vol. 89, pp. 963-974, 2015.

[158] N. I. Nwulu, X. Xia, "Implementing a model predictive control strategy on the dynamic economic emission dispatch problem with game theory based demand response programs," *Energy*, pp. 404-419, 2015.

[159] S. Bahrami, A. Sheikhi, "From demand response in smart grid toward integrated demand response in smart energy hub," *IEEE Transactions on Smart Grid*, vol. 7, no. 2, pp. 650-658, 2016.

[160] A. Sheikhi, M. Rayati, S. Bahrami, A. M. Ranjbar, "Demand side management in a group of Smart Energy Hubs as price anticipators; the game theoretical approach," in *IEEE Power & Energy Society Innovative Smart Grid Technologies Conference (ISGT)*, Washington, DC, 2015 .

[161] M. Yu, S. H. Hong, "Supply–demand balancing for power management in smart grid: A Stackelberg game approach," *Applied Energy*, vol. 164, pp. 702-710, 2016.

[162] G. Wang, Q. Zhang, H. Li, B. C. McLellan, S. Chen, Y. Li, Y. Tian, "Study on the promotion impact of demand response on distributed PV penetration by using non-cooperative game theoretical analysis," *Applied Energy*, DOI: 10.1016/j.apenergy.2016.01.016.

[163] C. Gong, K. Tang, K. Zhu, A. Hailu, "An optimal time-of-use pricing for urban gas: A study with a multi-agent evolutionary game-theoretic perspective," *Applied Energy,* vol. 163, pp. 283-294, 2016.

[164] A. Sheikhi, M. Rayati, S. Bahrami, A. M. Ranjbar, "Integrated demand side management game in smart energy hubs," *IEEE Transactions on Smart Grid,* vol. 6, no. 2, pp. 675-683, 2015.

[165] L. Castillo, C. A. Dorao, "Consensual decision-making model based on game theory for LNG processes," *Energy Conversion and Management,* vol. 64, pp. 387-396, 2012.

[166] L. Castillo, C. A. Dorao, "Decision-making in the oil and gas projects based on game theory: Conceptual process design," *Energy Conversion and Management,* vol. 66, pp. 48-55, 2013.

[167] H. S. Aplak, M. Z. Sogut, "Game theory approach in decisional process of energy management for industrial sector," *Energy Conversion and Management,* vol. 74, pp. 70-80, 2013.

[168] V. Nanduri, N. Kazemzadeh, "Economic impact assessment and operational decision making in emission and transmission constrained electricity markets," *Applied Energy,* vol. 96, pp. 212-221, 2012.

[169] H. Khazaei, B. Vahidi, S. H. Hosseinian, H. Rastegar, "Two-level decision-making model for a distribution company in day-ahead market," *IET Generation, Transmission & Distribution,* vol. 9, no. 12, pp. 1308-1315, 2015.

[170] T. K. Das, P. Rocha, C. Babayigit, "A matrix game model for analyzing FTR bidding strategies in deregulated electric power markets," *Electrical Power and Energy Systems,* vol. 32, pp. 760-768, 2010.

[171] J. Wang, Z. Zhou, A. Botterud, "An evolutionary game approach to analyzing bidding strategies in electricity markets with elastic demand," *Energy,* vol. 36, pp. 3459-3467, 2011.

[172] M. A. F. Ghazvini, B. Canizes, Z. Vale, H. Morais, "Stochastic short-term maintenance scheduling of GENCOs in an oligopolistic electricity market," *Applied Energy,* vol. 101, pp. 667-677, 2013.

[173] S. Bahrami, V. W. S. Wong, J. Huang, "An online learning algorithm for demand response in smart grid," *IEEE Transactions on Smart Grid,* p. DOI: 10.1109/TSG.2017.2667599, 2017.

[174] Y. Maali, "A multiobjective approach for solving cooperative n-person games," *Electrical Power and Energy Systems,* vol. 31, pp. 608-610, 2009.

[175] C. L. Prete, B. F. Hobbs, "A cooperative game theoretic analysis of incentives for microgrids in regulated electricity markets," *Applied Energy,* vol. 169, pp. 524-541, 2016.

[176] H. Omrani, R. Gharizadeh Beiragh, S. Shafiei Kaleibari, "Performance assessment of Iranian electricity distribution companies by an integrated cooperative game data envelopment analysis principal component analysis approach," *Electrical Power and Energy Systems,* vol. 64, pp. 617-625, 2015.

[177] S. Rahmani Dabbagh, M. K. Sheikh-El-Eslami, "Risk-based profit allocation to DERs integrated with a virtual powerplant using cooperative Game theory," *Electric Power Systems Research,* vol. 121, pp. 368-378, 2015.

[178] D. J. Kang, B. H. Kim, D. Hur, "Supplier bidding strategy based on non-cooperative game theory concepts in single auction power pools," *Electric Power Systems Research,* vol. 77, pp. 630-636, 2007.

[179] I. Atzeni, L. G. Ordóñez, G. Scutari, D. P. Palomar, J. R. Fonollosa, "Noncooperative Day-Ahead Bidding Strategies for Demand-Side Expected Cost Minimization With Real-Time Adjustments: A GNEP Approach," *IEEE Transactions on Signal Processing,* vol. 62, no. 9, pp. 2397-2412, 2014.

[180] C. O. Adika, L. Wang, "Non-Cooperative Decentralized Charging of Homogeneous Households' Batteries in a Smart Grid," *IEEE Transactions on Smart Grid,* vol. 5, no. 4, pp. 1855-1863, 2014.

[181] S. Lorenczik, T. Panke, "Assessing market structures in resource markets — An empirical analysis of the market for metallurgical coal using various equilibrium models," *Energy Economics,* vol. 59, p. 179–187, 2016.

[182] R. Wan, J. R. Boyceb, "Non-renewable resource Stackelberg games," *Resource and Energy Economics,* vol. 37, pp. 102-121, 2014.

[183] C. Wu, H. Mohsenian-Rad, J. Huang, "PEV-based reactive power compensation for wind DG units: A stackelberg game approach," in *IEEE Third International Conference on Smart Grid Communications (SmartGridComm)*, Tainan, 2012 .

[184] E. Bompard, E. Carpaneto, G. Ciwei, R. Napoli, M. Benini, M. Gallanti, G. Migliavacca, "A game theory simulator for assessing the performances of competitive electricity markets," *Electric Power Systems Research*, vol. 78, p. 217–227, 2008.

[185] T. Wu, L. Ma, Z. Mao, X. Ou, "Setting up charging electric stations within residential communities in current China: Gaming of government agencies and property management companies," *Energy Policy*, vol. 77, pp. 216-226, 2015.

[186] A. Sheikhi, Sh. Bahrami, A. M. Ranjbar, H. Oraee, "Strategic charging method for plugged in hybrid electric vehicles in smart grids; a game theoretic approach," *Electrical Power and Energy Systems*, vol. 53, p. 499–506, 2013.

[187] M. X. Cheng, M. Crow, Q. Ye, "A game theory approach to vulnerability analysis: Integrating power flows with topological analysis," *Electrical Power and Energy Systems*, vol. 82, pp. 29-36, 2016.

[188] M. Jahangoshai Rezaee, A. Moini, A. Makui, "Operational and non-operational performance evaluation of thermal power plants in Iran: A game theory approach," *Energy*, vol. 38, pp. 96-103, 2012.

[189] A. Orlov, "Effects of higher domestic gas prices in Russia on the European gas market: A game theoretical Hotelling model q," *Applied Energy*, vol. 164, pp. 188-199, 2016.

[190] T. Lv, Q. Ai, "Interactive energy management of networked microgrids-based active distribution system considering large-scale integration of renewable energy resources," *Applied Energy*, vol. 163, pp. 408-422, 2016.

[191] Z. Wu, H. Tazvinga, X. Xia, "Demand side management of photovoltaic-battery hybrid system," *Applied Energy*, vol. 148, pp. 294-304, 2015.

[192] N. Yaagoubi, H. T. Mouftah, "A distributed game theoretic approach to energy trading in the smart grid," in *IEEE Electrical Power and Energy Conference (EPEC)*, London, ON, 2015 .

[193] M. Motalleb, J. Branigan, R. Ghorbani, "Demand Response Aggregator Stackelberg Competition for Selling Stored Energy," in *IEEE Power and Energy Society General Meeting*, Chicago, IL, 2017.

[194] A. Sadeghi-Mobarakeh, H. Mohsenian-Rad, "Optimal Bidding in Performance-Based Regulation Markets: An MPEC Analysis With System Dynamics," *IEEE Transactions on Power Systems*, vol. 32, no. 2, pp. 1282-1292, 2017.

[195] A. Sadeghi-Mobarakeh, H. Mohsenian-Rad, "Strategic selection of capacity and mileage bids in California ISO performance-based regulation market," in *IEEE Power and Energy Society General Meeting (PESGM)*, 2016.

[196] S. Bose, D. W. H. Cai, S. Low, A. Wierman, "The role of a market maker in networked cournot competition," in *53rd IEEE Conference on Decision and Control*, Los Angeles, CA, 2014.

[197] H. M. Soliman, A. Leon-Garcia, "Game-Theoretic Demand-Side Management With Storage Devicesforthe Future Smart Grid," *IEEE Trans. Smart Grids*, vol. 5, no. 3, pp. 1475-1485, 2014.

[198] E. Reihani, M. Motalleb, M. Thornton, R. Ghorbani, "A novel approach using flexible scheduling and aggregation to optimize demand response in the developing interactive grid market architecture," *Applied Energy*, vol. 183, pp. 445-455, 2016.

[199] M. Shahidehpour, H. Yamin, Z. Li , Market Operations in Electric Power Systems: Forecasting, Scheduling, and Risk Management, Wiley-IEEE Press, 2002.

[200] D. Fudenberg, J. Tirole, Game Theory, Cambridge, Massachusetts: The MIT Press, 1991.

[201] M. Motalleb, R. Ghorbani, "Non-cooperative game-theoretic model of demand response aggregator competition for selling stored energy in storage devices," *Applied Energy*, vol. 202, pp. 581-596, 2017.

[202] J. Aubin, Mathematical Methods of Game and Economic Theory, North-Holland, , Revised edition, 1982.

[203] Xu, Y., Cai, D., Bose, S., Wierman, A., "On the Efficiency of Networked Stackelberg Competition," *preprint available at http://boses.ece.illinois.edu/files/stackelberg.pdf*, 2016.

[204] GE Energy Consulting, "Hawaii Solar Integration Study: Final Technical Report for Maui," Hawai‘i Natural Energy Institute (HNEI), University of Hawai‘i, 2013.

[205] K. Vanthournout, B. Dupont, W. Foubert, C. Stuckens, S. Claessens , "An automated residential demand response pilot experiment, based on day-ahead dynamic pricing," *Applied Energy,* vol. 155, pp. 195-203, 2015.

[206] Z. Hu, J. Kim, J. Wang, J. Byrne, "Hu, Z., Kim, J. H., Wang, J., & Byrne, J. (2015). Review of dynamic pricing programs in the US and Europe: Status quo and policy recommendations," *Renewable and Sustainable Energy Reviews,* vol. 42, pp. 743-751, 2015.

[207] A. R. Khan, A. Mahmood, A. Safdar, Z. A. Khan, N. A. Khan, "Load forecasting, dynamic pricing and DSM in smart grid: A review," *Renewable and Sustainable Energy Reviews,* vol. 54, pp. 1311-1322, 2016.

[208] J. Katz, F. M. Andersen, P. E. Morthorst, " Load-shift incentives for household demand response: Evaluation of hourly dynamic pricing and rebate schemes in a wind-based electricity system," *Energy,* vol. 115, pp. 1602-1616, 2016.

[209] L. Shen, Z. Li, Y. Sun, "Performance evaluation of conventional demand response atbuilding-group-level under different electricity pricings," *Energy and Buildings,* vol. 128, pp. 143-154, 2016.

[210] L. Song, Y. Xiao, M. van der Schaar, "Demand Side Management in Smart Grids Using a Repeated Game Framework," *IEEE Journal on Selected Areas in Communications,* vol. 32, no. 7, pp. 1412-1424, 2014.

[211] F. Pallonetto, S. Oxizidis, F. Milano, D. Finn, "The effect of time-of-use tariffs on the demand response flexibility of an all-electric smart-grid-ready dwelling," *Energy and Buildings,* vol. 128, pp. 56-67, 2016.

[212] D. P. Chassin, D. Rondeau, "Aggregate modeling of fast-acting demand response and control under real-time pricing," *Applied Energy,* vol. 181, p. 288–298, 2016.

[213] F. Feijoo, W. Silva, T. K. Das, "A computationally efficient electricity price forecasting model for real time energy markets," *Energy Conversion and Management,* vol. 113, p. 27–35, 2016.

[214] Y. He, J. Zhang, "Real-time electricity pricing mechanism in China based on system dynamics," *Energy Conversion and Management,* vol. 94, p. 394–405, 2015.

[215] E. Dehnavi, H. Abdi, "Optimal pricing in time of use demand response by integrating with dynamic economic dispatch problem," *Energy,* vol. 109, pp. 1086-1094, 2016.

[216] M. Motalleb, J. Branigan, R. Ghorbani, "Demand response market considering dynamic pricing," *Computer Science-Research and Development,* pp. 1-2, 2017.

[217] M. Motalleb, A. Annaswamy, R. Ghorbani, "A Real-Time Demand Response Market through a Repeated Incomplete-Information Game," *Energy,* In Press.

[218] Tan, Z., Ju, L., Reed, B., Rao, R., Peng, D., Li, H., Pan, G., "The optimization model for multi-type customers assisting wind power consumptive considering uncertainty and demand response based on robust stochastic theory," *Energy Conversion and Management,* vol. 105, pp. 1070-1081, 2015.

[219] Zhang, N., Hu, Z., Springer, C., Li, Y., Shen, B., "A bi-level integrated generation-transmission planning model incorporating the impacts of demand response by operation simulation," *Energy Conversion and Management,* vol. 123, pp. 84-94, 2016.

[220] Ju, L., Li, H., Zhao, J., Chen, K., Tan, Q., Tan, Z. , "Multi-objective stochastic scheduling optimization model for connecting a virtual power plant to wind-photovoltaic-electric vehicles considering uncertainties and demand response," *Energy Conversion and Management,* vol. 128, pp. 160-177, 2016.

[221] Nwulu, N. I., Xia, X, "Optimal dispatch for a microgrid incorporating renewables and demand response," *Renewable Energy,* vol. 101, pp. 16-28, 2017.

[222] Jannati, J., Nazarpour, D, "Optimal energy management of the smart parking lot under demand response program in the presence of the electrolyser and fuel cell as hydrogen storage system," *Energy Conversion and Management,* vol. 138, pp. 659-669, 2017.

[223] Wu, X., Hu, X., Moura, S., Yin, X., Pickert, V. , "Stochastic control of smart home energy management with plug-in electric vehicle battery energy storage and photovoltaic array," *Journal of Power Sources,* vol. 333, pp. 203-212, 2016.

[224] Cui, B., Wang, S., Yan, C., Xue, X., "Evaluation of a fast power demand response strategy using active and passive building cold storages for smart grid applications," *Energy Conversion and Management,* vol. 102, pp. 227-238, 2015.

[225] Iwafune, Y., Ikegami, T., da Silva Fonseca, J. G., Oozeki, T., Ogimoto, K., "Cooperative home energy management using batteries for a photovoltaic system considering the diversity of households," *Energy Conversion and Management,* vol. 96, pp. 322-329, 2015.

[226] Zhang, X., Bao, J., Wang, R., Zheng, C., Skyllas-Kazacos, M., "Dissipativity based distributed economic model predictive control for residential microgrids with renewable energy generation and battery energy storage," *Renewable Energy,* vol. 100, pp. 18-34, 2017.

[227] Jabari, F., Nojavan, S., Ivatloo, B. M., Sharifian, M. B., "Optimal short-term scheduling of a novel tri-generation system in the presence of demand response programs and battery storage system," *Energy Conversion and Management,* vol. 122, pp. 95-108, 2016.

[228] Nojavan, S., Majidi, M., Najafi-Ghalelou, A., Ghahramani, M., Zare, K., "A cost-emission model for fuel cell/PV/battery hybrid energy system in the presence of demand response program: ε-constraint method and fuzzy satisfying approach," *Energy Conversion and Management,* vol. 138, pp. 383-392, 2017.

[229] Poudineh, R., Jamasb, T., "Distributed generation, storage, demand response and energy efficiency as alternatives to grid capacity enhancement," *Energy Policy,* vol. 67, pp. 222-231, 2014.

[230] Zhao, J., Kucuksari, S., Mazhari, E., Son, Y. J., "Integrated analysis of high-penetration PV and PHEV with energy storage and demand response," *Applied Energy,* vol. 112, pp. 35-51, 2013.

[231] Lorenczik, S., Panke, T. , "Assessing market structures in resource markets—An empirical analysis of the market for metallurgical coal using various equilibrium models," *Energy Economics,* vol. 59, pp. 179-187, 2016.

[232] Yang, Z., Zhang, R., Zhang, Z., "An exploration of a strategic competition model for the European Union natural gas market," *Energy Economics,* vol. 57, pp. 236-242, 2016.

[233] Delbono, F., Lambertini, L. , "Ranking Bertrand, Cournot and supply function equilibria in oligopoly," *Energy Economics,* vol. 60, pp. 73-78, 2016.

[234] Yan, J., Folly, K., "Investigation of the impact of demand elasticity on electricity market using extended Cournot approach," *International Journal of Electrical Power & Energy Systems,* vol. 60, pp. 347-356, 2014.

[235] Chang, M. C., "Electricity tax subsidizing the R&D of emission-reducing technology: The double dividend effect under FIT regime," *International Journal of Electrical Power & Energy Systems,* vol. 62, pp. 284-288, 2014.

[236] Sharma, K. C., Bhakar, R., Tiwari, H. P., "Strategic bidding for wind power producers in electricity markets," *Energy Conversion and Management,* vol. 86, pp. 259-267, 2014.

[237] Jansen, T., Van Lier, A., Van Witteloostuijn, A., von Ochssée, T. B., "A modified Cournot model of the natural gas market in the European Union: Mixed-motives delegation in a politicized environment," *Energy Policy,* vol. 41, pp. 280-285, 2012.

[238] Hu, M. C., Lu, S. Y., Chen, Y. H. , "Stochastic–multiobjective market equilibrium analysis of a demand response program in energy market under uncertainty," *Applied Energy,* vol. 182 , pp. 500-506, 2016.

[239] Cabo, F., Erdlenbruch, K., Tidball, M., "Dynamic management of water transfer between two interconnected river basins," *Resource and Energy Economics,* vol. 37, pp. 17-38, 2014.

[240] Fikru, M. G., & Gautier, L., "Mergers in Cournot markets with environmental externality and product differentiation," *Resource and Energy Economics,* vol. 45, pp. 65-79, 2016.

[241] Abolhassani, M., Bateni, M. H., Hajiaghayi, M. T., Mahini, H., Sawant, A., "Network Cournot Competition," *arXiv:1405.1794.*

[242] Cai, D., Bose, S., Wierman, A., "On the role of a market maker in networked Cournot competition," *Preprint available at http://boses.ece.illinois.edu/files/NwCournot.pdf,* 2016.

[243] Bimpikis, K., Ehsani, S., Ilkilic, R., "Cournot competition in networked markets," *EC* , p. 733, 2014.

[244] M. Motalleb, A. Eshraghi, E. Reihani, R. Ghorbani, "A Game-Theoretic Demand Response Market with Networked Competition Model," in *North American Power Symposium (NAPS)*, Morgantown, WV, 2017.

[245] M. Motalleb, R. Ghorbani, "Networked Stackelberg Competition in a Demand Response Market," under review.

[246] Wierman, A., Bose, S., Cai, D., Chen, N., Ruhi, N., Xu, Y., "Networked Markets: Market makers & market power," [Online]. Available: http://helper.ipam.ucla.edu/publications/gss2015/gss2015_12619.pdf.

[247] Mas-Colell, A., Whinston, M. D., Green, J. R. , Microeconomic theory, New York: Oxford university press, 1995.

[248] Novshek, W., "On the existence of cournot equilibrium," *Review of Economic Study*, vol. 52, no. 1, pp. 85-98, 1985.

[249] M. Thornton, H. Smidt, V. Schwarzer, M. Motalleb, R. Ghorbani, "Internet-of- Things Hardware-in- the-Loop Simulation Testbed for Demand Response Ancillary Services," in *TechConnect World Innovation Conference and Expo*, Washington DC, 2017.

[250] M. Motalleb, M. Thornton, H. Smidt, R. Ghorbani, "An IoT-based Market Framework for Demand Response in Smart Grids," in *DistribuTECH Transmission and Distribution Conference, San Diego*, San Diego, CA, 2017.

[251] M. Thornton, M. Motalleb, H. Smidt, J. Branigan, R. Ghorbani, "Demo abstract: testbed for distributed demand response devices—internet of things," *Computer Science-Research and Development*, pp. 1-2, 2017.

[252] "Powersim Simulation PSIM," [Online]. Available: https://powersimtech.com/products/psim/.